Durham E-Theses

Study on the expression of recombinant resistance proteins domains

DE-SAN-EUSTAQUIO-CAMPILLO, ALBA

How to cite:

DE-SAN-EUSTAQUIO-CAMPILLO, ALBA (2013) *Study on the expression of recombinant resistance proteins domains*, Durham theses, Durham University. Available at Durham E-Theses Online: http://etheses.dur.ac.uk/6964/

Studies on the expression of recombinant resistance proteins domains

Alba de San Eustaquio Campillo

THESIS SUBMITED TO

THE DEPARTMENT OF BIOLOGICAL AND BIOMEDICAL SCIENCES OF

THE UNIVERSITY OF DURHAM

FOR A MASTERS DEGREE BY RESEARCH

NOVEMBER 2012

Abstract

Towards a R protein crystal structure

Alba de San Eustaquio Campillo

Resistance (R) proteins are a key component of plant innate immunity. R proteins are cytoplasmic immune receptors in plants that recognize specific microbe-associated molecular patterns (MAMPs). This recognition activates the second layer of the immune system in plants, called effector-triggered immunity (ETI).

Most R proteins are multi-domain proteins with a C-terminal leucine-rich repeat (LRR) domain, a central nucleotide-binding (NB)-ARC domain and a variable N-terminal domain. The N-terminal domain can be a coiled-coil (CC) region or a homologue of the *Drosophila* Toll and mammalian Interleukin-1 Receptors (TIR) structure. R proteins are members of the NB-ARC family of proteins, together with the human Apaf-1 and *Caenorhabditis elegans* CED-4, apoptosis receptors. The proposed activity of the NB-ARC domain is that of an ATPase. Studies conducted on R proteins have proved them to be ATPases. Nevertheless, a study with a subset of three R proteins showed their main activity was nucleotide phosphatases, not strict ATPases.

In this project, expression, purification, and biochemistry experiments were conducted on Rx, R protein from potato that confers resistance against the potato virus X. Activity assays showed Rx-NBARC constructs to act as nucleotide phosphatases, not strict ATPases, supporting this newly found activity in R proteins.

Acknowledgments

Contents

Chapter 3. Results

Chapter 4. Conclusion and Future work

Chapter 5. References

Chapter 6. Appendices

List of Figures

Abbreviations

Ado: adenosine

ADP: adenosine diphosphate

AMP: adenosine monophosphate

ARC: human apoptotic protease-activating factor-1 (<u>A</u>paf-1), <u>R</u> proteins and *Caenorhabditis elegans* <u>C</u>ED-4

ATP: adenosine triphosphate

BSA: albumin from bovine serum

dsDNA: doble stranded DNA

DNA: deoxyribonucleic acid

DTT: dithiothreitol

dNTP: deoxyribonucleotide

E. coli: *Escherichia coli*

ECL: enhanced chemiluminescence

EDTA: ethylenediaminetetraacetic acid

Fig: figure

GSH: reduced glutathione

GSSH: oxidized glutathione

HRP: horseradish peroxidase

IPTG: isopropyl-beta-D-thiogalactopyranoside

LB: Luria broth

NB: nucleotide binding

OD$_{600}$: optical density at 600 nm

o/n: overnight

PCR: polymerase chain reaction

PEG: polyethylene glycol

PMSF: phenylmethanesulfonylfluoride

PVDF membrane: polyvinylidene fluoride membrane

SDS: sodium dodecyl sulfate

SDS-PAGE: sodium dodecyl sulfate polyacrylamide gel electrophoresis

TAE buffer: tris-acetate and EDTA buffer

TBST buffer: tris-buffered saline and Tween 20 buffer

TLC: thin layer chromatography

UV: ultraviolet

1. Introduction

1.1 Introduction to plant immunity

Vertebrates have both innate and acquired immune systems to defend themselves from potential infection. Innate immunity has developed over evolution and recognizes unchanged structures on microorganisms (Blach-Olszewska, 2005). Acquired or adaptive immunity is induced by infection, it recognizes and remembers specific pathogens and is able to mount stronger immune responses on pathogen reinfection (Alder *et* al., 2005). Plants posses only an innate immune system to activate a series of defence responses that will arrest pathogenic microbes. When a pathogen infects a non-resistant plant, disease might develop reducing the plant's fitness and even causing its death. The plants immune system recognizes the attack of organisms that cross physical barriers including the wax layers and rigid cell walls. Plant pathogens that activate plant innate immunity include viruses, bacteria, fungi, oomycetes and nematodes (Takken and Tameling, 2009). The immune responses they trigger protect the plant (Dangl and Jones, 2001, Zhang and Zhou, 2010, Zipfel, 2008).

Plants do not have specialized mobile immune cells, as animals. All plant cells have the innate ability to recognize and respond to pathogens autonomously. There are two receptor classes involved in pathogen recognition. The first immune receptor class is represented by the pattern recognition receptors (PRRs) that are, mainly, transmembrane receptors in the plasma membrane of the plant cell (Zipfel, 2008). PRRs detect pathogen- or microbe-associated molecular patterns (PAMPs or MAMPs, because non-pathogenic organisms also possess PAMPs, Ausubel *et* al., 2005). They are responsible for the inhibition of most pathogens, triggering an immune response that attenuates microbial growth and contributes to basal defence (Zhang and Zhou, 2010). Resistance or R proteins form the second layer of plant immunity. These are cytoplasmic immune receptors that detect, directly or indirectly, isolate-specific pathogen effectors, encoded by avirulence (*avr*) genes that are able to bypass PTI (Kim *et* al., 2008). R proteins evolved to

detect Avr effector proteins and trigger disease resistance.

Plants immunity evolution is described as a zigzag in Jones and Dangl, 2006. First, PAMPs are recognized by PRRs, causing PTI. Successful pathogens synthesize effectors that enhance pathogenic virulence and overcome PTI, causing effector-triggered susceptibility (ETS). R proteins can specifically recognize these effectors and activate ETI (effector-triggered immunity). PTI is considered a basal defence response while ETI is an amplified reaction and, normally, induces a hypersensitive response (HR) at the infection site. HR is a rapid host cell suicide induced by pathogen infection detection by R proteins (Fig. 1; Heath, 2000).
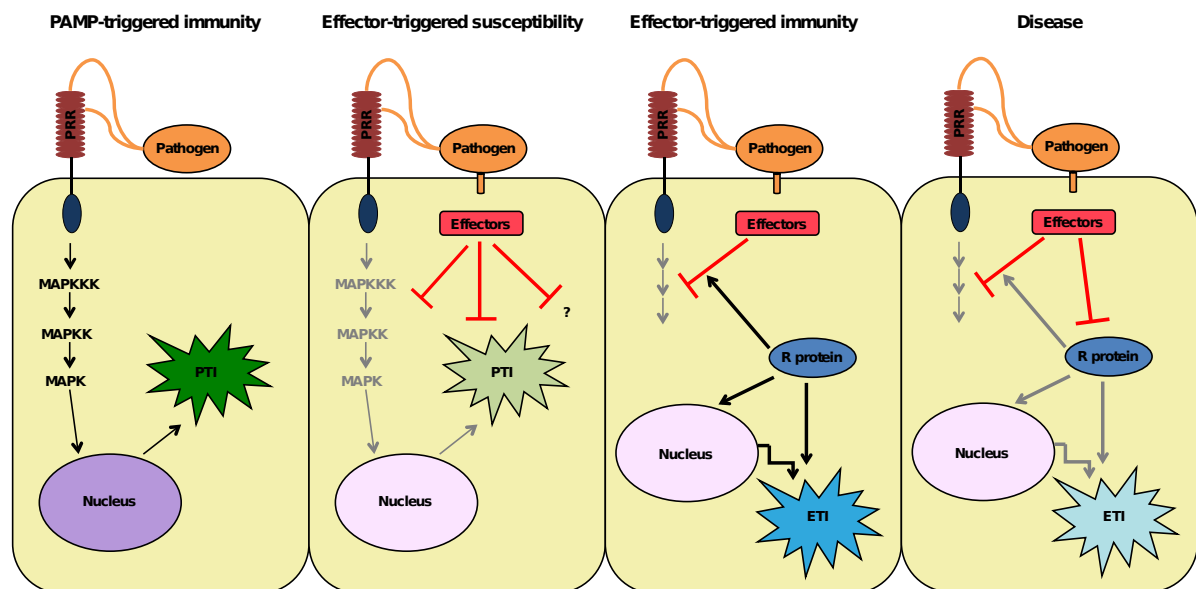
Figure 1 Diagram of plant innate immune system. Based on Figure 3 from Pieterse *et* al., 2009.

Understanding the function of the components of plant innate immunity is of great relevance. It will provide important knowledge of possible methods for pest control. Identifying the proteins involved in plants immunity and how they function will permit the manipulation of those proteins towards obtaining multiresistant crops (Baker *et* al., 1997).

1.1.1 PAMP-triggered immunity (PTI)

Pattern recognition receptors (PRRs) recognize specific conserved epitopes in MAMPs at subnanomolar concentrations (Boller and He, 2009). These are essential molecules that are difficult for the microorganism to mutate or delete without negatively affecting the fitness of the microbe. Flagellin, lipopolysaccharides, bacterial elongation factor-Tu (EF-Tu) and peptidoglycans are examples of MAMPs/PAMPs that activate a PAMP-triggered immunity or PTI (Jones and Dangl, 2006).

PRRs are multidomain transmembrane proteins that cross the plasma membrane only once (Zipfel, 2008). They present an extracellular leucine-rich repeat (LRR) region outside the cell, a transmembrane domain and an intracellular Ser/Thr protein kinase domain (Figure 2). There are at least 200 LRR-kinases in the *Arabidopsis* genome (Meyers *et* al., 2003). An extra 56 genes might be added if transmembrane proteins with LRR ectodomains but no intracellular kinases are included (Jones and Dangl, 2006). Most of the studies on PRRs have been conducted on the flagellin receptor FLS2 and EF-Tu receptor EFR from *Arabidopsis* (Boller and Felix, 2009).
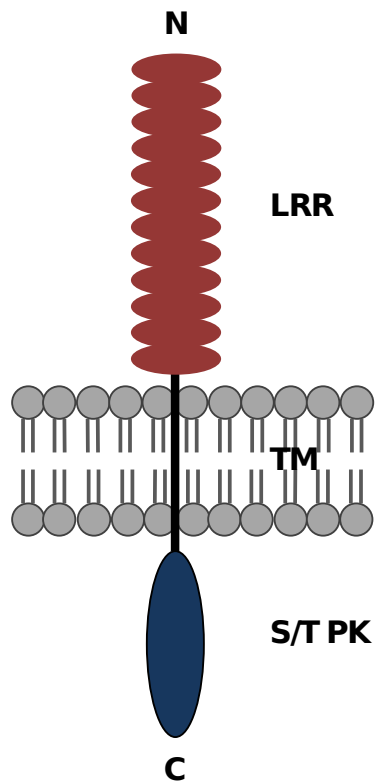
Figure 2 Diagram of a general PRR with leucine-rich repeats (LRR) at the N-terminus, a transmembrane (TM) domain and a C-terminus serine/threonine protein kinase (S/T PK) domain.

Once MAMPs are recognized, the activation pathway or pathways of PTI converge to a common response: rapid ion fluxes across the membrane, mitogen-activated kinase (MAPK) signalling, localized callose deposition in the cell wall, accumulation of reactive oxygen species (ROS), and activation of defence-related genes involving WRKY transcription factors after the activation of MAPK pathways (Kim *et* al., 2008, Zhang and Zhou, 2010, Zipfel, 2008). Although PTI prevents most infections, the disease resistance that it triggers can be suppressed by avirulence effectors encoded by *avr* genes in the pathogen (Boller and He, 2009, Pan *et* al., 2000). R proteins recognize Avr effectors. Though mutations in R proteins do not affect PTI (Jones and Dangl, 2006), MAPK pathways are convergence points for both ETI and PTI (Kim *et* al., 2008). Tao *et* al., 2003 show that PTI overlaps R protein mediated immunity, but is temporally delayed and of lower amplitude.

1.1.2 Avr effector proteins

Some pathogens express avirulence (*avr*) genes, whose products are called Avr proteins or effectors (Pan *et* al., 2000). These effectors enhance the pathogen's virulence and, many, enable it to overcome PTI, causing diseases in plants (Bent *et* al., 1994). Most Avr effectors are secreted by the pathogen through the type III secretion system (TTSS, Boller and He, 2009). The C-terminal domain of AvrPtoB for example, a *Pseudomonas* type III effector, initiates degradation of PRRs, inhibiting PRR signalling and PTI (Boller and He, 2009).

1.1.3 Effector-triggered immunity (ETI)

Specific R proteins recognise specific Avr proteins in the so called gene-for-gene recognition model (Staskawicz *et* al., 1995). R proteins in plants have co-evolved with these effectors to create a second layer of immunity called effector triggered immunity or ETI (Jones and Dangl, 2006, Zipfel, 2008). ETI induces the production of ROS, modification of ion fluxes, protein phosphorylation, reinforcement of the cell wall, and transcriptional reprogramming at the infection site and at close proximities (Belkhadir *et* al., 2004, Bent *et* al., 1994). ETI effects are similar to those of PTI, but they differentiate quantitatively and kinetically, ETI being faster and stronger (Shen *et* al., 2007). ETI immune responses normally lead to a host cell suicide at the invasion site known as the hypersensitive response or HR (Shirasu and Schulze-Lefert, 2000). Nevertheless, disease resistance can happen in the absence of HR (Heath, 2000, Jones and Dangl, 2006). This has been reported in potato, where Rx (R protein conferring resistance against potato virus X) does not cause a HR while activating a resistance response (Bendahmane *et* al., 1999). This has also been shown in the case of Rsv-1 (Hajimorad and Hill, 2001), which confers resistance against Soybean mosaic virus-N without inducing HR.

The vast majority of R proteins are multi-domain proteins, so called NB-LRR proteins, with a central nucleotide binding site (NB) and a C-terminal leucine rich repeat (LRR) region (Kim *et* al., 2008). There are other smaller

groups of R proteins that lack a NB-LRR structure, but those are not going to be studied in this thesis. The NB domain of R proteins has similarity with that of CED-4 (*Caenorhabditis elegans*) and Apaf-1 (human), regulators of apoptosis (Bendahmane *et* al., 2002, van der Biezen and Jones, 1998). Common sequences include the P-loop and other ATPase motifs found in both eukaryotes and prokaryotes (Aravind *et* al., 1999). NB-LRR R proteins can be divided into two subfamilies that differ in their N-terminus. They can present a coiled-coil (CC) motif (CC-NB-LRR proteins), or a TIR (homologue to the *Drosophila* Toll and mammalian Interleukin-1 Receptors) domain (TIR-NB-LRR proteins) (Kim *et* al., 2008).

1.2 P-loop proteins, Apaf-1, and CED-4

The NB domain is, actually, a sub-domain that is part of a bigger domain, the NB-ARC domain. The NB-ARC domain is the most conserved region in R proteins (Lukasik-Shreepaathy *et* al., 2012). R proteins, together with Apaf-1 (human apoptotic protease-activating factor 1) and CED-4 (apoptosis regulator from *Caenorhabditis elegans*), form the NB-ARC protein family, which is member of the P-loop NTPases superfamily (Figure 3, van Ooijen *et* al., 2008). P-loop NTPase conserved domains are present in 5-10% of the predicted gene products of sequenced prokaryotic and eukaryotic genomes. This makes P-loop NTPases the most common NTP-binding proteins in the proteome (Gueguen-Chaigon *et* al., 2007). P-loop containing proteins are involved in various cellular processes including signalling, metabolism, and regulation (Gueguen-Chaigon *et* al., 2007). The most common reaction catalysed by this domain is the hydrolysis of the β-γ phosphate bond of a bound nucleotide triphosphate to generate the diphosphate (Leipe *et* al., 2004).
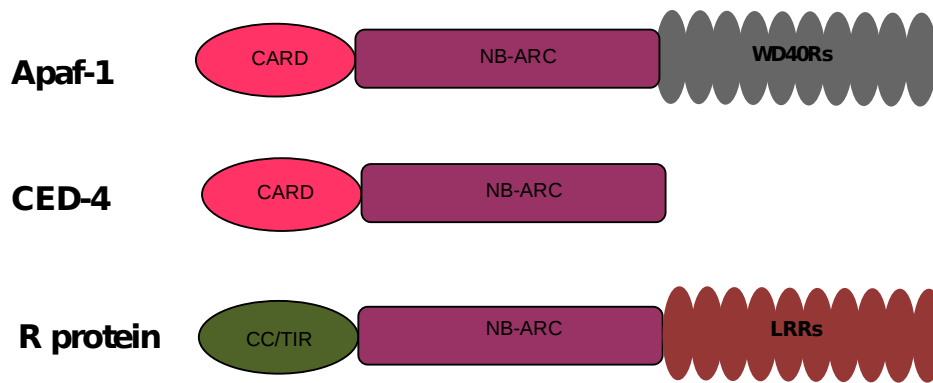
Figure 3 Diagram of Apaf-1, CED-4 and a general R proteins. They all share a central NB-ARC domain. Apaf-1 and CED-4 have a N-terminus CARD domain, while most R proteins have a CC/TIR domain. Apaf-1 presents C-terminal WD 40 repeats, while R proteins have leucine-rich repeats.

Both Apaf-1 and CED-4 have been crystallized and their structures solved (Riedl *et* al., 2005, Qi *et* al., 2010). Comparison of their sequence with that of resistance proteins allows a better understanding of R proteins structure and function as they share sequence similarities (Takken and Goverse, 2012).

Apaf-1, in the presence of cytochrome *c* and ATP/dATP, undergoes a conformational change and forms the apoptosome, recruiting caspases and activating programmed cell death (Riedl *et* al., 2005). Four sub-domains can be identified in the NB-ARC domain of Apaf-1 (Riedl *et* al., 2005): a nucleotide-binding sub-domain and three ARC sub-domains (ARC1, ARC2 and ARC3). The NB sub-domain is a classical NTPase fold and, therefore, is part of the P-loop NTPase superfamily (Takken *et* al., 2006). The structure of the P-loop is that of a three layered α/β sandwich with central parallel β-sheets surrounded by α-helices at both sides (Leipe *et* al., 2004). There are two distinct motifs in the sequence of the P-loop: Walker A (or kinase 1a) and Walker B (or kinase 2 motif) (Gueguen-Chaigon *et* al., 2007, Takken *et* al., 2006). These motifs bind the β and γ phosphates of the bound NTP and a Mg^{+2} cation respectively (Leipe *et* al., 2004). ARC1 is a four-helix bundle, ARC2 a winged-helix fold, and ARC3 is another helical bundle (Leipe *et* al., 2004, Riedl *et* al., 2005, Yan *et* al., 2005). The nucleotide binds at the interface between the NB, ARC1, and ARC2 sub-domains. Depending on the nucleotide that is bound to the NB domain, ATP or ADP, the conformation

adopted by Apaf-1 undergoes a change. Thus Apaf-1 perfectly suited to activate signalling pathways through conformational change (Takken *et* al., 2006). The ADP molecule is buried between the NB sub-domain and the three ARC sub-domains, maintaining the protein in its inactive conformation (Riedl *et* al., 2005).

In the case of CED-4, its inactive conformation corresponds to an asymmetric homodimer sequestered by CED-9 (anti-death protein) and with a molecule of ATP buried and bound at the NB domain (Yan *et* al., 2005). Upon activation, CED-4 is liberated from CED-9 and forms a tetramer of asymmetric dimers (Qi *et* al., 2010), the apoptosome. This homooligomer interacts with two CED-3 (a caspase) molecules, activating programmed cell death in a similar manner to that of Apaf-1. CED-4, as Apaf-1, when forming the apoptosome, is bound to an ATP molecule and a Mg^{+2} cation (Qi *et* al., 2010), which are deeply buried. Nevertheless, no H_2O molecule is found in the NB-ARC domain of CED-4, its catalytic site, so it is doubtful that it hydrolysis ATP. CED-4 might function by nucleotide exchange and not as an ATPase. CED-4 molecules present an NB sub-domain, ARC1 and ARC2 sub-domains. However, the ARC3 sub-domain found in Apaf-1 is missing in this NB-ARC protein and is substituted by a short linker of unknown structure (Qi *et* al., 2010, Yan *et* al., 2005). R proteins posses an NB sub-domain, an ARC1 sub-domain and an ARC2 sub-domain, but lack ARC3, as CED-4 (Qi *et* al., 2010).

1.3 R proteins

R proteins are intracellular innate immune receptors that trigger ETI. Most of them have a central nucleotide-binding (NB) domain and a C-terminus leucine-rich (LRR) region of 20-30 amino acids (Figure 4, van Ooijen *et* al., 2008). The majority of these NB-LRR proteins have a conserved N-terminus with a TIR (Toll/Interleukin-1 Receptor) domain. Other NB-LRR proteins exhibit a coiled-coil (CC) region in the N-terminus. These two NB-LRR protein groups are called TNL and CNL respectively (Meyers *et* al., 1999). The are other NB-LRR proteins that do not have a conserved N-terminus domain

(Dodds and Rathjen, 2010). R proteins are thought to function as molecular switches (Takken and Tameling, 2009) where their conformation varies with the nucleotide bound to the NB domain.
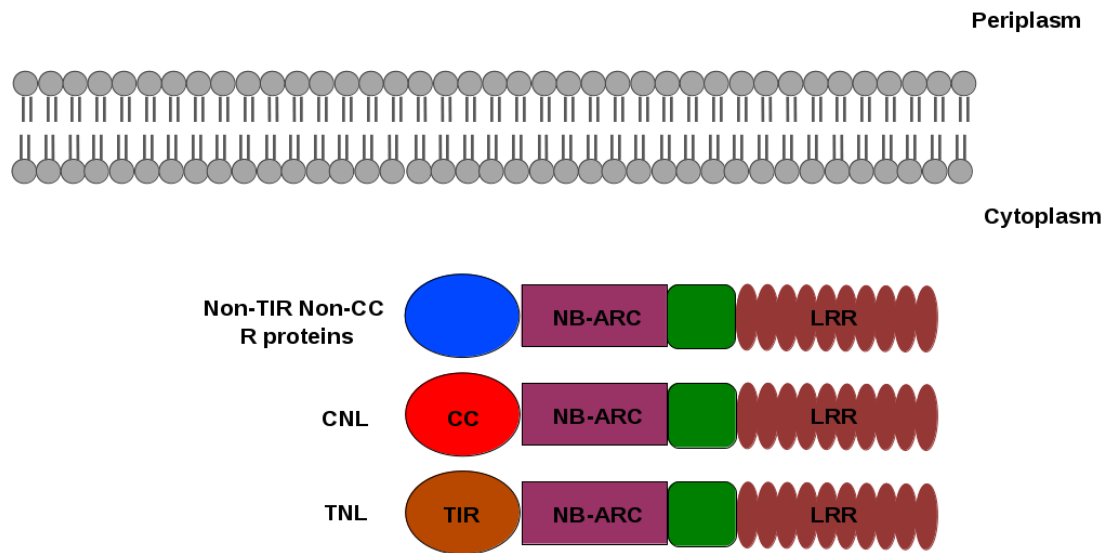
Figure 4 Diagram of R proteins classification. Most R proteins can be divided into two subgroups: CNL and TNL proteins. They have a central NB-ARC domain and N-terminal LRRs. They differentiate in the C-terminus: CNLs have a CC region while TNLs have a TIR structure. There are some other R proteins that do not have a conserved C-terminus, although they do have a conserved NB-LRR structure.

1.3.1 R proteins genes and their evolution

R gene (dominant or semidominant alleles) products specifically identify pathogen avirulence gene products in a gene-for-gene recognition manner (Pan *et* al., 2000). Modelling suggests that indirect recognition can lead to a stable, durable resistance, while direct recognition can, most likely, lead to relatively rapid evolution of new virulence phenotypes in the pathogen and resistance in the plant (Dodds *et* al., 2006). Examples of indirect Avr receptors in *Arabidopsis* are Rpm1, Rps2 and Rps5. The corresponding loci of these R proteins show low levels of genetic diversity. An evolutionary arms race occurs in direct R-Avr protein recognition, as happens with L, an R protein from flux, and AvrL567, from *Melampsora lini* (Dodds *et* al., 2006).

Most R genes have evolved by gene duplication followed by diversifying selection (Dodds *et* al., 2006, Pan *et* al., 2000). Unequal crossing-over is the most common mechanism of gene duplication observed for the production of R gene homologues. It has been demonstrated in a number of *R* loci including the *Rp1* locus of maize (Bent, 1996) and the *L* locus of flux (Ellis *et* al., 1999). Alternative splicing and interallelic recombination has also been demonstrated (Michelmore and Meyers, 1998, Pan *et* al., 2000, Staskawicz *et* al., 1995).

Variation of R gene sequences is concentrated over predicted binding surfaces within the LRR region (Allen *et* al., 2004, Dodds *et* al., 2006, Michelmore and Meyers, 1998, Seeholzer *et* al., 2010). Both the NB-ARC domain and the N-terminus of R proteins are highly conserved (Allen *et* al., 2004), suggesting the conservation of their function.

Different plant species have various numbers of R genes. The Columbia (Col0) ecotype of *Arabidopsis* has 149 genes that encode for NB-LRR proteins. This number increases to ~200 if the genes coding for truncated versions of R proteins are added (Meyers *et* al., 2003). In rice, this number goes up to more than 600 NB-LRR genes (Bai *et* al., 2002). Some genome sequencing studies (Bai *et* al., 2002, Meyers *et* al., 1999, Meyers *et* al., 2003) have demonstrated that the majority of NB-LRR protein encoding genes are arranged in clusters, both in *Arabidopsis* and rice (Meyers *et* al., 2003). This supports the hypothesis of generating novel resistance specificities through recombination. There are differences in R genes, depending on the type of NB-LRR R proteins they encode. It has been shown in *Arabidopsis* (Meyers *et* al., 2003) that its CNL proteins are generally encoded by single exons with the exception of two subclasses, which present introns in unique positions. On the other hand, TNL proteins are encoded by modular exons where protein domains are separated by introns in a conserved manner (Meyers *et* al., 2003).

<u>1.3.2 R protein structure-function</u>

Most plant R proteins are formed by a central NB domain and a C-terminal LRR (Shen *et* al., 2007). The N-terminus can be formed by a CC structure, a TIR domain or not have a conserved N-terminus domain (Dodds and Rathjen, 2010, Goff *et* al., 2002, Meyers *et* al., 1999, Pan *et* al., 2000, Shen *et* al., 2007). These NB-LRR R proteins are subject to a more detailed description below.

R protein C-terminus

The C-terminus of R proteins presents a series of leucine-rich repeats. The repeated motif comprises ~24 amino acids where leucines and other hydrophobic residues are found at regular intervals (Figure 5, Kobe and Deisenhofer, 1995). LRR domains are found in many other proteins and normally function as protein-protein interaction regions or as peptide-ligand binding sites (Bai *et* al., 2002). The LRR domain in plant R proteins can be involved in the recognition of ligands produced by the activity of Avr effectors or it may provide the platform for the interaction of R proteins with other proteins involved in the recognition of these effectors (Bent, 1996).
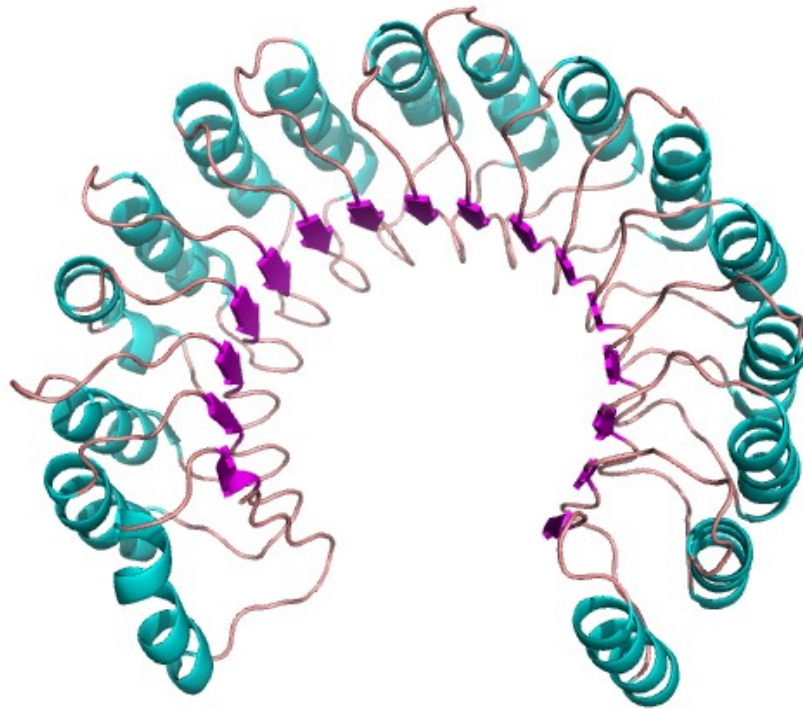
Figure 5 Structure of ribonuclease inhibitor (Kobe and Deisenhofer, 1995). Generated by Pymol (pdb = 2BNH).

The crystal structure of porcine RNase inhibitor (protein with an LRR region) was solved in Kobe and Deisenhofer, 1995. Its tertiary structure was that of a fist with each of the curled fingers representing a single LRR. It is likely that exposed amino acids are the ones presenting specificity for the ligand (Avr effector or partner protein), while the conserved hydrophobic amino acids are oriented internally and have a structural role (Bent, 1996). Modelling of the LRR domain of Lr10, a R protein from wheat, shows similarities in its structure with that of the RNase inhibitor (Sela *et* al., 2012). The region is divided into N- and C-terminal parts. The N-terminal part contains a high number of positively charged residues and might be involved in the modulation of NB-ARC domain activation, while the C-terminal part accumulates aromatic residues and might have a role in the interaction with upstream activators as Avr effectors or other proteins involved in the recognition of those effectors (Belkhadir *et* la., 2004).

R protein NB domain

The central domain of R proteins is identified as a nucleotide binding site (NB). This NB sub-domain is part of a bigger domain called NB-ARC. It is formed by three sub-domains: NB, ARC1 and ARC2 (van Ooijen *et* al., 2008). These sub-domains are highly conserved in various eukaryotic proteins where they form a nucleotide-binding pocket required for ATP- and GTP-binding (Bent, 1996, Meyers *et* al., 1999, Traut, 1994).

The conserved NB domain is formed by five parallel β sheets with seven α-helices surrounding it, ARC1 is formed by a bundle of four helices and ARC2 forms a winged-helix (Takken and Goverse, 2012). To date, no crystal structure of a R protein NB-ARC domain has been obtained. Models created using crystal structures of related proteins, as Apaf-1 and CED-4, show the NB-ARC domain as a compact globular structure (Riedl *et* al., 2005, Takken and Goverse, 2012, Yan *et* al., 2005).

Studies with Rx show that ARC1 is necessary for the intramolecular interaction between the N-terminus and the LRR domain (Rairdan and Moffet, 2006). Mutations in the LRR domain support the hypothesis of the interaction between LRR and NB-ARC domains being due to various contact points (Rairdan and Moffet, 2006). This would explain how the interaction between these domains is maintained despite the high degree of variability seen in NB-LRR proteins. ARC2 contains a MHDV motif. In Bendahmane *et* al., 2002 and de la Fuente van Bentem *et* al., 2005 mutations of the conserved Asp in this motif are studied and shown to cause a constitutive gain-of-function where the R protein cannot be autoinhibited. Rairdan and Moffet, 2006 propose it communicates the recognition of an effector, eliciting the activation of the NB-ARC protein.

R proteins N-terminus

Plants NB-LRR R proteins are divide into two subgroups depending on the domain present in their N-terminus. This could be a homologue of the TIR domain or a CC structure (Bent, 1996).

-Toll/Interleukin-1 Receptor (TIR) domain

Examples of TNL R proteins are N, from tobacco, L6, from flax, and RPP5, from *Arabidopsis* (Bent, 1996). The crystal structure of L6TIR was solved in Bernoux *et* al., 2011. It shows that L6TIR forms an asymmetric unit with two monomers. This domain is necessary and sufficient for the activation of HR. Mutations at the interface do not permit dimerization, and correspond with a loss-of-function *in planta*, suggesting a correlation between these two events (Bernoux *et* al., 2011). In Chan *et* al., 2010 AtTIR (TIR domain from *Arabidopsis thaliana*), was crystallized and it's structure studied. This molecule is a monomer in solution, but shows dimer interfaces in the crystallographic cell. This crystal structure revealed the existence of an αD-helix, which is present in all TIR plant proteins, but absent in bacteria and mammalian TIR domains (Chan *et* al., 2010). Mutations in this area in other R proteins have been shown an impact on function, suggesting a dual role of TIR domains in R proteins: transmission of the resistance signal and the death signal through protein-protein interactions (Chan *et* al., 2010, Weaver *et* al., 2006).

-Coiled-coil (CC) structure

The crystal structure of MLA10CC, a CNL R protein from barley, was recently solved (Maekawa *et* al., 2011). It shows that CC structures form homodimers. This data supports structural models for RPM1, a CNL R protein from *Arabidopsis* (Takken and Goverse, 2012).

It has been demonstrated (Hwang *et* al., 2000) for Mi-1, a CNL R protein from tomato that confers resistance against root-knot nematodes, that the N-terminus represses the ability of the LRR region to transmit the signal for ETI activation. In the presence of the nematode, an Avr effector produced by the nematode interacts directly or indirectly with the N-terminus or the LRR region, preventing repression of cell death.

An EDVID conserved motif is found in the CC domain (Rairdan *et* al., 2008). This motif appears to be involved in the intramolecular NB-ARC-LRR-

CC interaction. Mutations in NB-ARC-LRR inhibit the interaction of these domains with the CC, suggesting that a correct tertiary structure is needed for the correct intramolecular interactions to take place (Rairdan *et* al., 2008).

1.3.3 Effectors recognition and cell compartmentalization

Pathogen effectors are detected specifically by R proteins. This interaction can be direct or indirect (Kim *et* al., 2008). The interaction between the AvrM effector from flax rust and the M R protein, a TNL R protein, is studied in Catanzariti *et* al., 2010. This is an example of direct interaction between a R protein and its effector. M recognises AvrM via its LRR. This is necessary and sufficient to elicit HR (Catanzariti *et* al., 2010). In other studies, indirect effector-R protein relations are studied (Bhattacharjee *et* al., 2011, Dodds, 2010). Pathogen effectors from *Peronospora*, *Erysiphe*, and *Pseudomonas* interact with *Arabidopsis* EDS1 or RIN4. These proteins form a guard complex with TNL and CNL R proteins respectively. EDS1 is essential for ETI to happen with all TNL R proteins studied to date (Wiermer *et* al., 2005). The recognition of the correct effector by EDS1 or RIN4 causes the activation of the R protein and starts ETI (Bhattacharjee *et* al., 2011). Heidrich *et* al., 2011 and Wirthmueller *et* al., 2007 demonstrate that *Arabidopsis* EDS1 interacts with the *P. syringae* Avr effector AvrRsp4 and the R protein RSP4 (TNL R protein). For a fully activated immune response, the three molecules have to be localized in the nucleus (Heidrich *et* al., 2011 and Wirthmueller *et* al., 2007). It is likely that a nuclear mobilizing signal is produced once the interaction with the effector takes place.

R proteins have also been proposed to work in a "bait and switch" model (Collier and Moffet, 2009). This model unites the direct and indirect recognition of pathogen effectors. The presence of other host proteins as decoys does not inhibit the possibility of a direct interaction between the effector and the R protein. The "bait and switch" model proposes a two-step recognition process where the effector interacts with the LRR R protein domain and with other proteins that act as cofactors. Once the effector is

recognized, the NB site is hypothesized activate a single or reduced number of signalling pathways resulting in the activation of ETI.

1.3.4 Current activation model of R proteins

Activation of R proteins triggers a localized cell death known as the HR (Monaghan and Li, 2008). R protein activation should therefore be tightly regulated. When HR occurs, pathogens are confined in dead cells with no nutrients. This is usually sufficient to prevent the spread of the infection in the plant.

In order to avoid inappropriate activation, intramolecular interactions between the multiple domains autoinhibit the protein (Takken *et* al., 2006, Takken and Tameling, 2009). The current hypothesis for how R proteins are activated is that of an "on-off" switch (Figure 6). The "off" or resting state is represented by an ADP molecule bound to the NB-ARC domain in absence of pathogens (Monaghan and Li, 2008). ADP interacts with the NB-ARC domain, maintaining the protein in a very stable conformation. In addition, both the N-terminal and LRR domains interact with the NB-ARC domain (Ade *et* al., 2007).
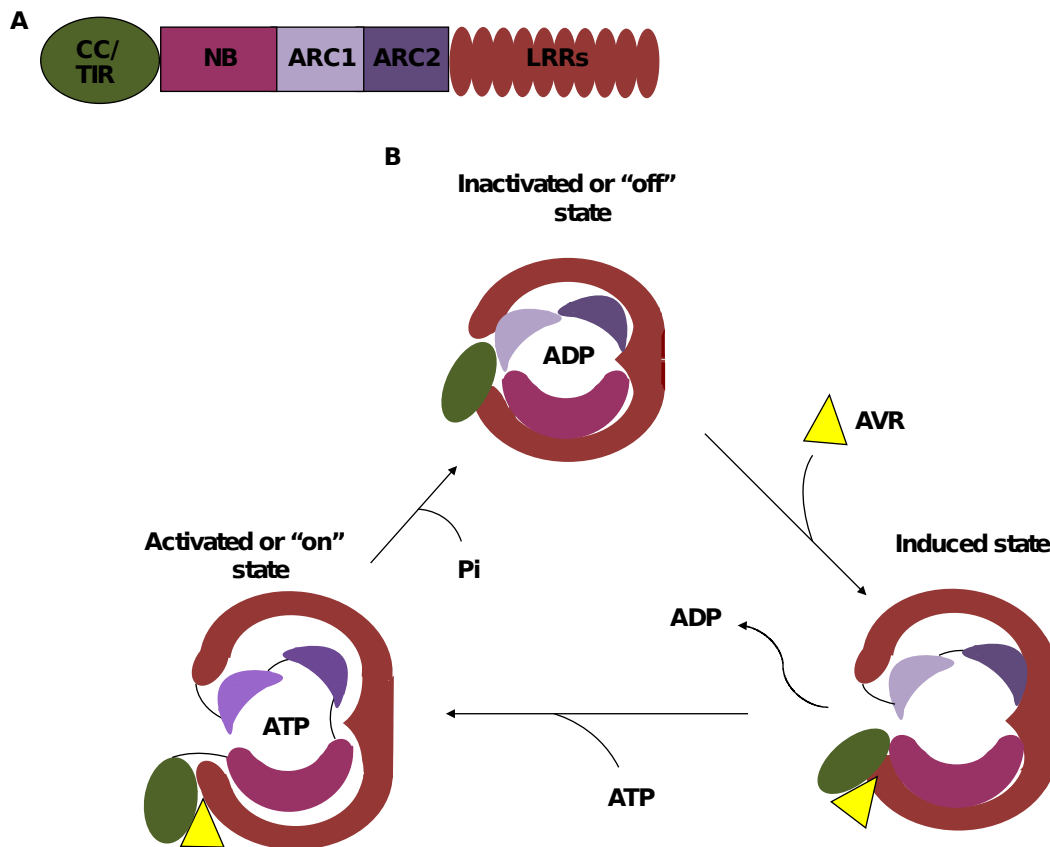
Figure 6 A Diagram of a general R protein. **B** Diagram of the "on-off" switch activation model for R proteins.

Effector recognition is hypothesized to cause a conformational change in the protein where the N-terminal part of the LRR domain stops interacting with the NB-ARC domain enabling the exchange of ADP for ATP and eliciting the protein to enter its "on" or activated state (Ade *et* al., 2007, Lukasik and Takken, 2009). Nucleotide exchange causes an additional conformational change that stops the C-terminal domain from interacting with the NB-ARC-LRR domains (Lukasik and Takken, 2009). This permits the establishment of interactions between the R protein and other proteins involved in the signalling process, mainly through the N-terminus (Ade *et* al., 2007). ATP hydrolysis returns the protein to its "off" state, forming ADP. This ATPase activity of R proteins has been demonstrated by the identification of loss-of-function mutations (Tameling *et* al., 2002) in the NB-ARC domain of I-2, a resistance protein from tomato where ATPase defective mutants are non-functional *in planta*. This data supports the hypothesis that R proteins work as

strict ATPases in a switch activation model.

This model is further consistent with data from nucleotide binding, oligomerization (NOD)-like receptors, intracellular animal immune receptors, which are also members of the P-loop family of proteins (Austin *et* al., 2002). Various gain-of-function mutations have been studied on Nod2 (Danot *et* al., 2009, Rairdan and Moffett, 2006). These mutations abolish the capability of the NB domain in Nod2 to hydrolyse ATP, forcing the protein to remain in a constitutively activated state.

Though there is not much information about the downstream molecular events that occur after effector recognition, stable R protein complexes are formed. These complexes involve different co-chaperones like HSP90, RAR1, Suppressor of G2 allele of SKP1 (SGT1), heat shock cognate 70 kDa (HSC70) and protein phosphatase 5 or PP5 (Monaghan and Li, 2008). The role of co-chaperones may be that of stabilizing activated R proteins or modifying them. Experiments where some of these co-chaperones were suppressed show that they are necessary for HR activation (Lukasik and Takken, 2009). Transcriptional factors and nucleo-cytoplasmic transporters have been identified to bind to the N-terminal part of NB-ARC proteins in plants (Lukasik and Takken, 2009).

A study in *Arabidopsis* (Aarts *et* al., 1998) showed that some R proteins signal through the EDS1 (enhanced disease susceptibility) lipase-like protein (RPP2, RPP4, RPP5, RPP21 and RPS4), while RPS2 and RPS5 require NDR1 (nonrace-specific disease resistance). This study also demonstrated that RPM1 and RPP8 do not depend on any of these molecules to activate their immune responses in *Arabidopsis*. It is thought that the preference of one pathway or the other is dependent on the R protein structure rather than the pathogen type. Some studies have shown that activated NB-LRR R proteins (MLA10 in barley, N in tobacco and RPS4 in *Arabidopsis*) accumulate in the nucleus where they might derepress inhibitory transcription factors to activate defence gene expression (Shen *et* al., 2007). The truth is that the pathway or pathways leading R proteins to activate host defence against pathogen invasion are not yet known.

1.4 The biochemistry of the NB domain

The accepted hypothesis for R proteins activation model supports them as strict ATPases (Tameling *et* al., 2006). However, recent evidence found by Fenyk *et* al., 2012 demonstrated this biochemistry is not true for a series of NB-LRR proteins. NB domains of R1 (an orphan R protein from rice), Rpm1 (R protein from *A. thaliana*), and PSiP (an orphan R protein from maize) proved to have a nucleotide phosphatase activity. R1 was used to fully characterize this protein's biochemistry. Terminal phosphates are sequentially cleaved leading to the formation of adenosine as the final product when adenosine nucleotides are used as substrate. This is in contrast to previous work with other R proteins (I-2 and Mi-1) that showed they act as ATPases (Tameling *et* al., 2002). R proteins NB domains might therefore exhibit different enzyme activities.

1.5 Recombinant R proteins

R proteins have been studied *in planta* in many cases. Some examples are Azevedo *et* al., 2006, Baures *et* al., 2008, Goulden and Baulcombe, 1993 and Kohm *et* al., 1993. However, R proteins expression and purification from plant cultures has proved to be challenging. Examples of active protein in the literature are scarce, but promising.

Tameling *et* al., 2002, refolded the CC-NB-ARC portion of I-2 and Mi-1 *in vitro,* after purification from inclusion bodies. The results demonstrated samples of active protein that show ATPase activity.

Ueda *et* al., 2006, expressed a number of constructs of the N R protein from tobacco in *E. coli*. This recombinant proteins had a GST tag attached that was used for its purification on a Glutathione Sepharose™ column. N was characterized as an ATPase, similar to I-2 and Mi-1.

Schmidt *et* al., 2007 expressed M (flax-rust R protein) in *Pichia pastoris* with a N-terminal 9x histidine tag and a deletion of the first 21 amino acids. No

biochemical experiments were performed.

Bernoux *et* al., 2011 determined the crystal structure of L6 (R protein from *Linum usitatissimum*) TIR domain (amino acids 29-229), demonstrating its importance in immune signalling. The recombinant protein was expressed in *E. coli* BL21(DE3) cells.

Maekawa *et* al., 2011 successfully expressed (in *E. coli*) and crystallised the CC domain of MLA (R protein from barley). Full length MLA was also expressed and purified from insect cells and its nucleotide binding properties were tested. Their data show that MLA forms relatively stable complexes with ADP, but not with ATP.

Ve *et* al., 2011 accomplished structure studies from crystals of the TIR domain of L6 (amino acids 29-229, as Bernoux *et* al., 2011), after expression in *E. coli* cells and purification with a hexa-histidine tag, which was subsequently removed.

Williams *et* al., 2011 performed a series of biochemical experiments with various mutant versions of M, which sustain the switch activation model of R proteins. Correct functioning of resistance signalling would involve the exchange of ADP for ATP as the "off" state of R proteins would correspond to the protein bound to an ADP molecule.

In Fenyk *et* al., 2012, NB domains from R1, Rpm1, and PSiP were expressed from *E. coli* cultures and purified with Strep-Tactin Superflow to obtain a solution of native active protein. In this case, all proteins showed a nucleotide phosphatase enzyme activity *in vitro*.

In light of the contrasting biochemistry in different R proteins, further studies should be conducted in order to fully characterize their activity.

1.6 Aims

Fenyk *et* al., 2012 reported a new activity in a group of three NB-LRR proteins. R1, Rpm1 and PSiP were demonstrated to act as nucleotide phosphatases, catalysing the production of nucleosides from nucleotides with a preference for the nucleotide monophosphate as substrate. This differs from the, to date, accepted hypothesis of R proteins acting as strict ATPases (Tameling *et* al., 2002). The nucleotide phosphatase activity is intrinsic to the NB sub-domain, although the role of the ARC sub-domain cannot yet be defined. This biochemistry means that the protein continues hydrolysing the nucleotide until producing a nucleoside, instead of stopping at the diphosphate nucleotide.

A computed structural model for the NB domain of R1 was used to predict important catalytic residues and the effect of mutating them in the protein's activity. (Fenyk *et* al., 2012). There are no R proteins NB-ARC domain crystals in the literature. Only human Apaf-1 (Riedl *et* al., 2005) and CED-4 (Qi *et* al., 2010) have been crystallized and their structures solved. These structures revealed the importance of the locality of the nucleotide bound to the NB-ARC domain. The conformation of Apaf-1 and CED-4 is dependent on the bound nucleotide. This data has been used to create models for R proteins as they share similarities and are members of the NB-ARC family of proteins (Takken and Goverse, 2012). Nevertheless, the information obtained from a model is not comparable to that collected from a crystal structure.

Crystallizing the active domain of a R protein is essential for the fully understanding of the role of R proteins in plant innate immunity. This knowledge would assist in the identification of important residues, which are key for the proteins activity and specificity. These residues might be used, after their identification, as targets for R protein modification. Multiresistant R proteins might be introduced into crop strains. This would reduce costs of crop protection and minimize the use of chemical pesticides, reducing environmental contamination.

The data presented below shows the first steps of a bigger project that

can be followed towards achieving a R protein crystal structure. Expression and purification of a R protein that can be used for biochemical experiments are the aims of this project. Improvement of the techniques developed here may render a way towards the obtaining samples of R protein that can be used for crystallography trials.

2. Materials and Methods

2.1 Most commonly used buffers

2x TBST buffer (see 2.4.5):

    50 mM Tris-HCl pH 8.0

    30 mM NaCl

    0.2 % (v/v) Tween 20

5x STOP buffer (see 2.5.6):

    100 mM Tris-HCl, pH 8.0

    2.5 % SDS

    100 mM EDTA

    10 units μL^{-1} proteinase K

ADPase assay developing buffer (see 2.5.4):

    9:1 isopropanol: 33 % (v/v) aqueous ammonia

ATPase assay developing buffer (see 2.5.3):

    15.5 % (v/v) 33 % (v/v) aqueous ammonia

    15.5 % (v/v) isobutyl-alcohol

    10.5 % (v/v) isobutyl-ethanol

    31.5 % (v/v) 2-etoxyethanol

Bacterial wash buffer (see 2.4.1):

    50 mM Tris-HCl pH 8.5

    1mM EDTA

Binding buffer (see 2.3.6):

    6 M Sodium Perchlorate

    50 mM Tris-HCl pH 8.0

10 mM EDTA

Blocking buffer (see 2.4.5):

2x TBST buffer

1.5 % (w/v) BSA

5 % (w/v) milk powder

Dialysis buffer (see 2.4.13):

50 mM Tris-HCl pH 8.0

15 mM NaCl

Glutathione Sepharose buffers (see 2.4.8):

Wash buffer: 50 mM Tris-HCl pH 8.0

200 mM NaCl

Elution buffer: 50 mM Tris-HCl pH 8.0

10 M reduced glutathione

Inclusion bodies purification (see 2.3.9 and 2.4.10):

Wash buffer: 50 mM Tris-HCl pH 8.0

4 M urea

500 mM NaCl

1 mM EDTA

1 mg / mL deoxycholate

Solubilisation buffer: 50 mM Tris-HCl pH 8.0

4 M urea

10 mM DTT

Ligation buffer (see 2.3.7):

60 mM Tris-HCl pH 7.8

20 mM $MgCl_2$

20 mM DTT

2 mM ATP

10 % (w/v) PEG

Agarose gel loading buffer (see 2.3.5):

    2 % (w/v) orange G

    20 % (w/v) sucrose

Lysis buffer (see 2.4.2):

    50 mM Tris-HCl pH 8.0

    15 mM imidazole

    2 mM DTT

    5 mM $MgCl_2$

    1 mM PMSF

Ni^{+2}-NTA resin buffers (see 2.4.7):

Lysis buffer: 50 mM Tris-HCl pH 8.0

        250 mM NaCl

        20 mM imidazole

Washing buffer A: 50 mM Tris-HCl pH 8.0

        400 mM NaCl

        20 mM $MgCl_2$

        20 mM imidazole

Washing buffer B: 50 mM Tris-HCl pH 8.0

        1.5 M NaCl

        20 mM $MgCl_2$

        20 mM imidazole

Washing buffer C: 50 mM Tris-HCl pH 8.0

        10 mM NaCl

        20 mM $MgCl_2$

        20 mM imidazole

Elution buffer: 50 mM Tris-HCl pH 8.0

        10 mM NaCl

        20 mM Mg Cl_2

        200 mM imidazole

Refolding buffers (see 2.4.11 and 2.4.12; annex 6):

Buffer 1: 50 mM MES pH 6.0

      9.6 mM NaCl

      0.4 mM KCl

      2 mM MgCl$_2$

      2 mM CaCl$_2$

      0.75 M Guanidine HCl

      0.5% Triton X-100

      1 mM DTT

Buffer 2: 50 mM MES pH 6.0

      9.6 mM NaCl

      0.4 mM KCl

      2 mM MgCl$_2$

      2 mM CaCl$_2$

      0.5 M arginine

      0.05% polyethylene glycol 3,550

      1 mM GSH

      0.1 mM GSSH

Buffer 3: 50 mM MES pH 6.0

      9.6 mM NaCl

      0.4 mM KCl

      1 mM EDTA

      0.4 M sucrose

      0.75 M Guanidine-HCl

      0.5% Triton X-100

      0.05% polyethylene glycol 3,550

      1 mM DTT

Buffer 4: 50 mM MES pH 6.0

      240 mM NaCl

      10 mM KCl

      2 mM MgCl$_2$

      2 mM CaCl$_2$

      0.5 M arginine

0.5% Triton X-100

1 mM GSH

0.1 mM GSSH

Buffer 5: 50 mM MES pH 6.0

240 mM NaCl

10 mM KCl

1 mM EDTA

0.4 M sucrose

0.75 M Guanidine-HCl

1 mM DTT

Buffer 6: 50 mM MES pH 6.0

240 mM NaCl

10 mM KCl

1 mM EDTA

0.5 M arginine

0.4 M sucrose

0.5% Triton X-100

0.05% polyethylene glycol 3,550

1 mM GSH

0.1 mM GSSH

Buffer 7: 50 mM MES pH 6.0

240 mM NaCl

10 mM KCl

2 mM $MgCl_2$

2 mM $CaCl_2$

0.75 M Guanidine-HCl

0.05% polyethylene glycol 3,550

1 mM DTT

Buffer 8: 50 mM Tris-Cl pH 8.5

9.6 mM NaCl

0.4 mM KCl

2 mM $MgCl_2$

2 mM $CaCl_2$

0.4 M sucrose

0.5% Triton X-100

0.05% polyethylene glycol 3,550

1 mM GSH

0.1 mM GSSH

Buffer 9: 50 mM Tris-HCl pH 8.5

9.6 mM NaCl

0.4 mM KCl

1 mM EDTA

0.5 M arginine

0.75 M Guanidine HCl

0.05% polyethylene glycol 3,550

1 mM DTT

Buffer 10: 50 mM Tris-HCl pH 8.5

9.6 mM NaCl

0.4 mM KCl

2 mM $MgCl_2$

2 mM $CaCl_2$

0.5 M arginine

0.4 M sucrose

0.75 M Guanidine-HCl

1 mM GSH

0.1 mM GSSH

Buffer 11: 50 mM Tris-HCl pH 8.5

9.6 mM NaCl

0.4 mM KCl

1 mM EDTA

0.5% Triton X-100

1 mM DTT

Buffer 12: 50 mM Tris-HCl pH 8.5

240 mM NaCl

10 mM KCl

1 mM EDTA

0.05% polyethylene glycol 3,550

1 mM GSH

0.1 mM GSSH

Buffer 13: 50 mM Tris-HCl pH 8.5

240 mM NaCl

10 mM KCl

1 mM EDTA

0.5 M arginine

0.75 M Guanidine-HCl

0.5% Triton X-100

1 mM DTT

Buffer 14: 50 mM Tris-HCl pH 8.5

240 mM NaCl

10 mM KCl

2 mM $MgCl_2$

2 mM $CaCl_2$

0.5 M arginine

0.4 M sucrose

0.75 M Guanidine-HCl

0.5% Triton X-100

0.05% polyethylene glycol 3,550

1 mM GSH

0.1 mM GSSH

Buffer 15: 50 mM Tris-HCl pH 8.5

240 mM NaCl

10 mM KCl

2 mM $MgCl_2$

2 mM $CaCl_2$

0.4 M sucrose

1 mM DTT

Running buffer (see 2.4.4):

25 mM Tris-HCl pH 6.8

200 mM glycine

0.1 % (w/v) SDS

SDS loading buffer (see 2.4.4):

    50 mM Tris-HCl pH 6.8

    2 % (w/v) SDS

    0.1 % (w/v) bromophenol blue

    10 % (v/v) glycerol

    100 mM DTT

Strep-tag fusion proteins purification buffers (see 2.4.3):

Buffer W: 100 mM Tris-HCl pH 8.0

           150 mM NaCl

           1 mM EDTA

Elution buffer: 100 mM Tris-HCl pH 8.0

           150 mM NaCl

           1 mM EDTA

           25 mM desthiobiotin

Regeneration buffer: 100 mM Tris-HCl pH 8.0

           150 mM NaCl

           1 mM EDTA

           1 mM HABA

TAE buffer (see 2.3.5):

    40 mM Tris-acetate pH 8.0

    1 mM EDTA

TLC buffer (see 2.4.3 and 2.5.4):

    90 % (v/v) isopropanol

    10 % (v/v) ammonium

Transfer buffer (see 2.4.5):

    20 % (v/v) methanol

    25 mM Tris-HCl pH 8.5

    192 mM glycine

Washing buffer (see 2.4.5):

400 mM NaCl

20 mM Tris-HCl pH 7.5

2 mM EDTA

50 % (v/v) ethanol

2.2. Materials

Chemical	Company	Product code
ϕX174 RF II DNA	New England BioLabs	N3022S
Acetic acid	Sigma	242853
Acetonitrile	Fisher Scientific	A/9627/17
Acrylamide	Sigma	A9926
2, 8- [^{3}H] Adenine	Perkin Elmer	NET063005MC
*2, 8- [^{3}H] Adenine Trisodium Salt	American Radiolabeld Chemicals	0386
Adenosine	Sigma	A9251
Adenosine di-phosphate	Sigma	A2754
Adenosine mono-phosphate	Sigma	A1752
Adenosine tri-phosphate (ATP)	Sigma	A6559
Agarose	Bioline	BIO-41026
Albumin, from bovine serum	Sigma	A7906
Amersham Hyperfilm ECL^{TM}	GE Healthcare®	28-9068-35
Ammonium hydroxide solution	Sigma	221228
Ampicillin sodium salt	Melford	A0104
Antifoam A	Sigma	A-5633
Apyrase from potato	Sigma	A6535
BioTaq^{TM} Red DNA Polymerase	BioLine	BIO-21041
Bovine serum albumin (BSA)	Sigma	C3411
Bradford Reagent	Sigma	B6916
Bromophenol blue	Sigma	B0126
Calcium chloride	Sigma	C1016
3-[(3-Cholamidopropyl) dimethylammonio] -1- propanesulfonate hydrate	Sigma	C9426

(CHAPS)		
Chloramphenicol	Sigma	C0378
Coomasie G-250	Sigma	201391
Cytidine 5'-triphosphate disodium salt	Sigma	C1506
Dimethyl sulfoxide (DMSO)	Sigma	D2650
Dithiothreitol (DTT)	Sigma	43817
DNA marker ladder	Fermentas	SM0311
ECL^{TM} Western Reagent	Amersham	RPN2109
Ethanol	Dep. Stores	-
Ethidium bromide	Sigma	E7637
Ethylenediaminetetraacetic acid (EDTA)	Sigma	E6758
Glucose	Sigma	158968
Glycerol	Sigma	G5516
Glycine	Sigma	241261
Guanidine hydrochloride	Sigma	1001176868
Guanosine 5'-triphosphate sodium salt hydrate	Sigma	G8877
Hydrochloric acid	Sigma	H1758
HyperLadder I	BioLine	BIO-33025
Imidazole	Sigma	15513
Instant blue	Tripel Red	-
Isopropyl beta-D-thiogalactoside (IPTG)	Sigma	I5502
Kanamycin monosulfate	Melford	K0126
L-Arginine	Sigma	101147081
L-glutathione oxidized	Sigma	1001095239
L-glutathione reduced	Sigma	1001214749
Lysogeny broth (LB) medium	Merck	10285.5000
Lysogeny broth (LB) agar	Sigma	L2897
Magnesium chloride	Sigma	M8266
Methanol	Sigma	M1775
2-Mercaptoethanol	BDH	44143
Monoclonal anti-glutathione-S-transferase (GST) antibody produced in rat	Sigma	SAB4200055
Pageruler^{TM} plus pre-stained protein ladder	Fermentas	SM0671
Phosphate buffered saline	Sigma	79382
Polyethylene glycol 8000 (PEG)	Fisher BioReagents	BP233-1
Potassium chloride	Sigma	P9333

2-Propanol	Sigma	443425
Poteinase K	Sigma	P6556
Rbt pAb to 6x His tag®, HRP	abcam	Ab1187-100
Sequi-Blot™Plyvinylidene Fluoride (PVDF) Membrane	Biorad	162-0184
Sodium chloride	Sigma	S7653
Sodium dodecyl sulphate (SDS)	Sigma	L3771
Spectinomycin dihydrochloride pentahydrate	Fluka	85555
Streptomycin sulphate salt	Melford	S-6501
Sucrose	Sigma	P9333
Tetracycline	Sigma	T7660
Tetramethylethylenediamine (TEMED)	Sigma	T9281
TLC precoated sheets PLYGRAM® Sil G	Machery-Nagel	805 013
Tris-HCl	Sigma	93363
Triton X-100	Sigma	T-8787
Trypsine, porcine	Promega	608-274-4330
Tween-20 (Polyoxyethylenesorbitan monolaurate)	Sigma	P1379
Urea	Sigma	U5378
Uridine 5'-triphosphate trisodium salt dihydrate	Sigma	94370

Kit	Company	Product code
QuickFold™ Protein Refolding Kit	AthenaES	0600
Ni-NTA superflow resin	Qiagen	30410
Wizard® Plus Miniprep kit	Promega	A7100
Zero Blunt® TOPO® PCR cloning kit	Invitrogen	K2830-20

Cell lines	Comapny	Product code
E. coli BL21 (DE3)	Novagen	69387
E. coli Mach1 T1	Invitrogen	K2830-20
E. coli DH5α	Invitrogen	12034-013

2.3. Cloning Procedures:

2.3.1 Polymerase chain reaction:

Reactions using *Pfu* DNA polymerase were set up on ice following the manufacturer's protocol. Reactions typically contained 20 mM Tris-HCl pH 8.8, 10 mM KCl, 10 mM $(NH_4)_2SO_4$, 2 mM $MgSO_4$, 1 % (v/v) Triton X-100, 0.1 mg mL^{-1} BSA, 25 pmoles of each primer, 200 µM dNTPs, 250 ng DNA template, and 1 unit *Pfu* DNA polymerase. Polymerase chain reaction (PCR) was typically cycled as listed below.

	Time / minutes	Temperature / °C
Initial denaturation	2	95
Denaturation	0.5	95
Annealing	0.5	55
Elongation	1 per 0.5 kb	73
Final Elongation	10	73

Cycling conditions for Pfu DNA polymerase.

2.3.2 Colony polymerase chain reaction:

Reactions using *Taq* DNA polymerase were set up on ice following the manufacturer's protocol. Reactions typically contained 25 pmoles of each primer, 200 ꙨM dNTP, 1 unit of *Taq* DNA polymerase. The DNA was introduced by touching the colony of interest with a pipette tip and

stirring it into the PCR tube. Polymerase chain reaction was typically cycled as listed below.

	Time/minutes	Temperature/°C
Initial denaturation	2	94
Denaturation	0.5	94
Annealing	0.5	60
Elongation	1	72
Final elongation	2	72

Cycling conditions for Taq DNA polymerase during a colony PCR

2.3.3 Gateway BP clonase II reaction:

75 ng of PCR product and 75 ng of the entry vector pDONR207 were incubated with 2 μg of BP clonase II in a total volume of 5 μL in TAE buffer (40 mM Tris-acetate pH 8.0, 1 mM EDTA). The reaction was incubated at room temperature for one hour and then 2 μg of proteinase K were added. The reaction was vortexed and left for 10 min at 37 ^{o}C. Bacterial cells were transformed with the reaction product (see 2.3.10).

2.3.4 Gateway LR clonase II reaction:

The entry vector containing the PCR fragment was purified from positive colonies from a Gateway BP clonase II reaction (see 2.3.3 and 2.3.11). 75 ng of the product and 75 ng of the destination vector were incubated with 2 μg of BP clonase II in a total volume of 5 μL, in TAE buffer (40 mM Tris-acetate pH 8.0, 1 mM EDTA). The reaction was incubated at room temperature for one hour and then 2 μg of proteinase K were added. The reaction was vortexed and left for 10 min at 37 ^{o}C. Bacterial cells were

transformed with the reaction product (see 2.3.10).

2.3.5 DNA purification from agarose gel:

1.5 % (w/v) or 1 % (w/v) agarose gels were run in TAE buffer (40 mM Tris-acetate, 1 mM EDTA pH 8.0) at 12 V cm^{-1}. DNA sample was mixed at a ratio of 4:1 (sample:buffer) with loading buffer (2 % (w/v) orange G and 20 % (w/v) sucrose in TAE buffer prior to loading. DNA sizes were estimated relative to a 1 kilobase DNA marker ladder. Visualisation of DNA was attained through the in gel presence of ethidium bromide (0.5 µg mL^{-1}) and a UV transilluminator.

2.3.6 Extraction of DNA from agarose gel:

DNA in agarose gels was visualized with a UV transilluminator and the band excised into a 1.5 mL tube. 1 mL of binding (6 M sodium perchlorate, 50 mM Tris-HCl pH 8.0, 10 mM EDTA) was added and left at 37 °C for 30 minutes. 20 µL of 166 mg mL^{-1} silica were added, mixed for 30 minutes at room temperature, centrifuged (12.000 g, 60 sec), and the supernatant discarded. The pellet was resuspended in 125 µL of binding buffer and centrifuged again. The supernatant was discarded and the pellet resuspended in 750 µL of wash buffer (400 mM NaCl, 20 mM Tris-HCl pH 7.5, 2 mM EDTA and 50 % (v/v) ethanol). The sample was centrifuged and the supernatant discarded. The previous step was repeated once more and the pellet left to evaporate the remaining ethanol at room temperature for 5 minutes. 10 µL of ultra pure H$_2$O were then added to the pellet. This was centrifuged once more and the supernatant was transferred to a new tube and stored at -20 °C.

2.3.7 Zero Blunt® TOPO® PCR cloning reaction:

The following reagents were added to a 1.5 mL tube.

pCR®-Blunt II-TOPO® vector	5 ng
Ligation Buffer	5 μL
DNA Insert	> 20 ng
T4 DNA Ligase	3 U

Ligation buffer consisted of 60 mM Tris-HCl pH 7.8, 20 mM $MgCl_2$, 20 mM DTT, 2 mM ATP, and 10 % (w/v) PEG. Reactions were incubated for at least 15 min at room temperature in a final volume of 10 mL.

2.3.8 Estimation of DNA concentration:

Concentrations of DNA in solution were determined by the use of a NanoDrop spectrophotometer (BioLogic). The blank used was pure water. DNA solutions were assumed to be largely free of contaminating proteins if the ratio of absorbance at 260:280 nm was > 1.6.

2.3.9 Restriction enzyme digest:

DNA was digested with restriction enzymes according to the manufacturers instructions. Enzyme concentration was maintained such that it was not greater than 10 % (v/v) of the total reaction volume.

2.3.10 Transformation of chemically competent cells:

25 μL of frozen chemically competent cells were thawed and transferred into ice. DNA was added to thawed cells. The cells were

maintained on ice for 20 minutes before a heat shock in a 42 °C water bath for 30 seconds and 2 minutes in ice. 0.5-1 mL of warm LB medium was added to the cells and the solution was introduced into a 14 mL tube and incubated at 37 °C for 30-60 minutes with shaking. The cells were then centrifuged at 2,500 g for 2 minutes. Most of the supernatant was discarded, leaving 1 mL to resuspend the pellet. This solution was then spread on an LB plate and cultivated at 37 °C overnight.

2.3.11 Purification of plasmid DNA:

Plasmid DNA was purified from 5 mL *E. coli* overnight cultures in LB medium using a commercial miniprep kit according to the manufacturers instructions.

2.3.12 Preparation of competent *E. coli* cells with CaCl$_2$:

5 mL of an overnight culture of *E. coli* grown in the appropriate medium were transferred into 100 mL of LB medium and incubated at 37 °C with agitation until the OD$_{600nm}$ = 0.3-0.6. The cells were then transferred into ice-cold 50 mL tubes and left on ice for 10 minutes. Cells were centrifuged at 2,000 g for 10 minutes at 4 °C. The supernatant was discarded and the pellet mixed with 30 mL of 80 mM MgCl$_2$/20 mM CaCl$_2$. The solution was centrifuged again at 2,000 g for 10 minutes at 4 °C. The supernatant was discarded and the pellet mixed with 2 mL of ice-cold 0.1 M CaCl$_2$ for each 50 mL of original culture. The cells were then used for transformation (see 2.3.10) or aliquoted with 20 % (v/v) glycerol and frozen at -80 °C.

2.3.13 Preparation of bacterial -150 °C frozen stock:

E. coli cells were grown in 5 mL of LB medium containing the

appropriate antibiotics at 37 ℃ overnight. Cells were harvested by centrifugation (3,000 g for 5 minutes at 4 ℃). The supernatant was discarded and the pellet resuspended in 1 mL of LB containing 20 % (v/v) glycerol. The suspension was placed in a labelled cryovial and stored at -150 ℃.

2.4. Protein manipulation:

2.4.1 Expression of recombinant proteins in *E. coli*:

1 L LB medium was inoculated with 70 mL of an overnight *E. coli* starter culture and grown in a 37 ^{o}C temperature controlled shaking incubator at 200 rpm. When cells reached an absorbance value of 0.8-0.9 at 600 nm, IPTG was added to the appropriate concentration. The culture was incubated shaking at 150 rpm for a predesignated time at an appropriate temperature. Bacteria were harvested through centrifugation (12,000 g, 4 ^{o}C, 7 min). The pellet corresponding to 2 L LB was washed with 40 mL bacterial wash buffer (50 mM Tris-HCl pH 8.5, 1mM EDTA), centrifuged (3,000 g, 4 ^{o}C, 25 min) and frozen at -80 ^{o}C until further use.

2.4.2 Lysis of bacteria:

Frozen bacterial pellets (see 2.4.1) were thawed in a 37 ^{o}C water bath. Subsequent steps were performed on ice. The pellet was resuspended in twice its volume of lysis buffer (50 mM Tris-HCl pH 8.0, 15 mM imidazole, 2 mM DTT, 5 mM $MgCl_2$ and 1 mM PMSF). Cells were sonicated in 20 mL batches (2.5 min, 74 W, 2 pulses per second) and centrifuged (75,500 g, 60 min). Crude supernatant containing soluble protein was saved for purification.

2.4.3 Strep-tag fusion protein purification with Strep-Tactin®:

All steps were performed on ice or at 4 $^{\circ}$C. 1 mL of Strep-Tactin ® resin was used for every 30 mL of crude supernatant (see 2.4.2). The resin was pre-equilibrated with 5 mL of buffer W (100 mM Tris-HCl pH 8.0, 150 mM NaCl and 1 mM EDTA) and the crude supernatant was incubated with avidin (a biotin inhibitor from egg white) at room temperature for 10 minutes. The supernatant was left to drain by gravity. Prior to elution of the fusion protein, the column was washed with buffer W, 1.5 M NaCl. Protein was eluted with 3x 0.5 mL of elution buffer (100 mM Tris-HCl pH 8.0, 150 mM NaCl, 1 mM EDTA and 25 mM desthiobiotin). An aliquot of the eluate was analysed by SDS-PAGE gel (see 2.4.4), the remainder was quantified (see 2.4.6), dialysed into dialysis buffer (50 mM Tris-HCl pH 8.0 and 15 mM NaCl), 20% (v/v) glycerol added and stored at -80 $^{\circ}$C until further use. The resin was regenerated with 5 mL of regeneration buffer (100 mM Tris-HCl pH 8.0, 150 mM NaCl, 1 mM EDTA and 1 mM HABA), reequilibrated with 8 mL of buffer W, and stored at 4 $^{\circ}$C with 1 mL of buffer W.

2.4.4 Sodium Dodecyl Sulphate Poly-Acrylamide Gel electrophoresis (SDS-PAGE):

Pre-cast 4-20% gradient SDS-PAGE gels (GE Healthcare) were used in a horizontal electrophoresis system. Samples were mixed 1:2 (v/v) with SDS loading buffer (50 mM Tris-HCl pH 6.8, 2% (w/v) SDS, 0.1% (w/v) bromophenol blue, 10% (v/v) glycerol and 100 mM DTT) and run at 180 V cm^{-1} in running buffer (25 mM Tris-HCl pH 6.8, 200 mM glycine, 0.1% (w/v) SDS). Protein sizes were estimated relative to a protein marker ladder. Gels were stained in Coomassie Instant Blue (Expedeon) and destained in distilled water.

2.4.5 Western blot:

SDS-PAGE gels (see 2.4.4) were transferred onto an activated PDVF membrane (methanol 2 min) for 4 h at 75 V or for 2 h at 100 V and 4 °C in transfer buffer (20 % (v/v) methanol, 25 mM Tris-HCl pH 8.5, 192 mM glycine). Membranes were blocked with blocking buffer (50 mM Tris-HCl pH 8.0, 30 mM NaCl, 0.2 % (v/v) Tween 20, 1.5 % (w/v) BSA and 5 % (w/v) milk powder) for 16 h at 4°C on a shaker at 150 rpm. Membranes were then washed three times with 20 mL of 2x TBST buffer (50 mM Tris-HCl pH 8.0, 30 mM NaCl and 0.2 % (v/v) Tween 20) for 5 min at room temperature with gentle shaking. Membranes were then incubated for an hour in 10 mL of blocking buffer containing the HRP conjugated antibody in a dilution of 1:4,000 (v/v) at room temperature with gentle shaking. The membrane was washed four times with 2x TBST buffer for 10 min at room temperature, with gentle shaking. Membranes were developed using ECL™ reagents and exposed to Hyperfilm ECL™ (GE Healthcare).

2.4.6 Estimating protein concentration:

Spectrophotometer:

The concentration of purified recombinant protein in solution was estimated in an ultraviolet spectrophotometer according to the Beer-Lambert law and an estimated protein extinction coefficient (http://www.biomol.net/en/tools/proteinextinction.htm). The absorbance was measured at 280 nm and the buffer in which the protein was soluble was used as blank.

Bradford:

90 μL of Quick Start™ Bradford were mixed with 10 μL of protein sample and incubated at room temperature for 5 minutes before reading the absorbance of the solution at 595 nm with a spectrophotometer. A standard curve was made using known concentrations of BSA under the same conditions as the sample. Sample absorbance was compared to this curve in order to know the concentration of the sample.

2.4.7 His-tag fusion protein purification with Ni^{+2}-NTA resin:

All steps were performed on ice or at 4 $^{\circ}$C. 1 mL Ni^{+2}-NTA resin (binding capacity of 5-10 mg mL^{-1}) was used for every 30 mL of crude supernatant (see 2.4.2). The resin was preequilibrated with 5 mL of lysis buffer (50 mM Tris-HCl pH 8.0, 250 mM NaCl and 20 mM imidazole). The crude supernatant was incubated with the resin for 2 h, at 4 $^{\circ}$C with gentle rocking before left to drain by gravity. Resin was washed with 15 mL (per 1 mL of Ni^{+2}-NTA resin) wash buffer A (50 mM Tris-HCl pH 8.0, 400 mM NaCl, 20 mM imidazole and 20 mM MgCl$_2$); 15 mL (per 1 mL of Ni^{+2}-NTA resin) wash buffer B (50 mM Tris-HCl pH 8.0, 1.5 M NaCl, 20 mM imidazole and 20 mM MgCl$_2$); and 15 mL (per 1 mL of Ni^{+2}-NTA resin) wash buffer C (50 mM Tris-HCl pH 8.0, 10 mM NaCl, 20 mM imidazole and 20 mM MgCl$_2$). The protein was eluted with 5 mL (per 1 mL of Ni^{+2}-NTA resin) elution buffer (50 mM Tris-HCl pH 8.0, 10 mM NaCl, 200 mM imidazole and 20 mM MgCl$_2$). An aliquot of eluate was saved for analysis by SDS-PAGE (see 2.4.4). Eluate was dialysed into dialysis buffer (50 mM Tris-HCl pH8.0 and 15 mM NaCl), quantified, made up to 20% (v/v) glycerol, and stored at –80 $^{\circ}$C until needed.

2.4.8 GST-tag fusion protein purification with Glutathione Sepharose™:

All steps were performed on ice or at 4 $^{\circ}$C. 250 μL of 50 % (v/v) Glutathione Sepharose slurry (binding capacity of 8 mg mL^{-1}) was used for every 30 mL of crude supernatant (see 2.4.2). The slurry was preequilibrated with 2

mL of PBS previous to the incubation with the crude supernatant at room temperature, for 1 h and with gentle rocking. After incubation, it was left to drain by gravity, washed with 2 mL of PBS and washed with 2 mL of washing buffer (50 mM Tris-HCl pH 8.0 and 200 mM NaCl). Tagged protein was eluted with 4x100 µL of elution buffer (50 mM Tris-HCl pH 8.0 and 10 mM reduced glutathione). Aliquots of the eluates were kept to analyse by SDS-PAGE gel. The remainder was dialysed into dialysis buffer, made up to 20 % (v/v) glycerol, quantified and frozen at -80 $^{\circ}$C until further use.

2.4.9 Determination of urea and NaCl concentrations for purification of inclusion bodies:

Frozen bacterial pellets (see 2.4.1) were thawed in a 37 $^{\circ}$C water bath. Subsequent steps were performed on ice. The pellet was resuspended in twice its volume of lysis buffer (50 mM Tris-HCl pH 8.0, 15 mM imidazole, 2 mM DTT, 5 mM MgCl$_2$ and 1 mM PMSF). Cells were sonicated in 20 mL batches (2.5 min, 74 W, 2 pulses per second) and centrifuged (75,500 g, 60 min). Supernatant was discarded and pellets washed with 5 mL g^{-1} inclusion bodies washing buffer without urea (50 mM Tris-HCl pH 8.0, 500 mM NaCl, 1 mM EDTA, 1 mg mL^{-1} deoxycholate). 100 µL of the solution was added to 7 mL of inclusion bodies washing buffer with different urea (0 M, 2 M, 4 M, 6 M and 8 M urea) and NaCl (0 M, 1 M and 1.5 M NaCl) concentrations. The samples were mixed by vortexing and left at room temperature. After 30 minutes, they were centrifuged (maximum speed, 1 minute) and the supernatant was tested for the presence of soluble denatured protein.

2.4.10 Purification of inclusion bodies after determining the appropriate urea and NaCl concentrations:

Frozen bacterial pellets (see 2.4.1) were thawed in a 37 $^{\circ}$C water bath. Subsequent steps were performed on ice. The pellet was resuspended in

twice its volume of lysis buffer (50 mM Tris-HCl pH 8.0, 15 mM imidazole, 2 mM DTT, 5 mM MgCl$_2$ and 1 mM PMSF). Cells were sonicated in 20 mL batches (2.5 min, 74 W, 2 pulses per second) and centrifuged (75,500 g, 60 min). Supernatant was discarded and pellets washed with 5 mL g^{-1} inclusion bodies washing buffer (50 mM Tris-HCl pH 8.0, 4 M urea, 500 mM NaCl, 1 mM EDTA, 1 mg mL^{-1} deoxycholate), centrifuge at 20,000 g for 15 minutes at 15 $^{\circ}$C. The last two steps were repeated. The pellets were resuspended in 2 mL g^{-1} solubilisation buffer (50 mM Tris-HCl pH 8.0, 4 M urea, 10 mM DTT) and left for 20 minutes at 50 $^{\circ}$C before centrifugation at 20,000 g for 30 minutes at 15 $^{\circ}$C. Supernatant containing denatured protein was saved for refolding and purification of the protein.

2.4.11 Screening for refolding buffers:

After purification of inclusion bodies (see 2.4.10), 15 refolding buffers (Appendix 5) were tested to establish the best condition in which to refold the protein in use. Concentration of purified inclusion bodies was adjusted to 1 mg mL^{-1}. 50 μL of these purified inclusion bodies were added slowly while vortexing to 950 μL of each buffer and to 950 μL of inclusion bodies solubilisation buffer. They were incubated for an hour at 4 $^{\circ}$C or 22 $^{\circ}$C and centrifuged 5 minutes at maximum speed. The supernatant was transferred into a new tube, reserving the pellet in the old tube. Successful refolding was assessed by Western blot (see 2.4.5) of samples from soluble fractions.

2.4.12 Protein refolding after determining the appropriate refolding buffer:

950 μL of freshly made refolding buffer (50 mM Tris-HCl pH 8.5, 9.6 mM NaCl, 0.4 mM KCl, 2 mM MgCl$_2$, 2 mM CaCl$_2$, 0.5 M arginine, 0.4 M sucrose, 0.75 M Guanidine-HCl, 1 mM GSH, 0.1 mM GSSH) were mixed with every 50 μL of denatured protein (see 2.4.9) at a concentration of about 1 mg

mL^{-1}. The solution was vortexed and incubated at 4 ^{o}C for 1 h. The refolded protein was dialysed into dialysis buffer (50 mM Tris-HCl pH 8.0, 15 mM NaCl), concentrated with PEG 8000, quantified and saved for further use.

2.4.13 Dialysis:

Samples were introduced in a dialysis bag that had been previously boiled in distilled water. The dialysis bag was introduced in 1 L dialysis buffer (50 mM Tris-HCl pH 8.0 and 15 mM NaCl unless otherwise specified) with stirring for 1 h 30 minutes at 4 ^{o}C, changing the buffer every 15 minutes.

2.4.14 Concentration with PEG 8000:

Samples in a dialysis bag were covered with PEG 8000 and left at 4 ^{o}C. Every 10 minutes, wet PEG 8000 was substituted by new PEG 8000.

2.4.15 Electroelution:

20 cm long SDS-PAGE gels were run with samples containing denatured protein. Bands corresponding to the correct size of the protein of interest were cut and introduced in a dialysis bag with running buffer to which 4 M urea was added to maintain the protein in a denatured state (avoiding the formation of intermediate refolding states). Bags were then placed in an electrophoresis tank with running buffer to which 4 M urea was also added. A low voltage current was applied during 4 h to elute the protein from the gel band and into the buffer in the dialysis bag. The solution was transferred into a tube and frozen at -20 ^{o}C until further use.

2.5. Biochemistry:

2.5.1 Strict ATPase assay:

Soluble protein (see 2.4.12) was added to a total volume of 5 μL containing 20 mM bis-Tris-Propane pH 7.5, 5 μM ATP and 10 mM MgCl$_2$. Reactions were spiked with 2,8-^{3} H-labeled adenine triphosphate nucleotide for quantitative biochemistry. The reaction was incubated for 1 h at 37 ^{o}C after which, the conversion of ATP into ADP was tested (see 2.5.3).

2.5.2 Nucleotide phosphatase assay:

Soluble protein (see 2.4.12) was added to a total volume of 5 μL containing 20 mM bis-Tris-Propane pH 7.5, 5 μM ADP and 10 mM MgCl$_2$. Reactions were spiked with 2,8-^{3} H-labelled adenine diphosphate nucleotides for quantitative biochemistry. Reactions were incubated for 1 h at 37 ^{o}C, after which, the conversion of ADP into adenosine was tested (see 2.5.4).

2.5.3 Thin layer chromatography for strict ATPase assays:

1 μL of a strict ATPase reaction (see 2.5.1) was spotted onto a silica TLC plate with 0.8 μL of 2 mM ATP and 2 mM ADP spotted on top after drying to act as a marker and carrier. The plates were run in ATPase assay developing buffer (15.5% (v/v) 33% (v/v) aqueous ammonia, 15.5% (v/v) isobutyl-alcohol, 10.5% (v/v) isobutyl-ethanol, 31.5% (v/v) 2-etoxyethanol) for

2 h 30 minutes. After drying, spots were visualized with a TLC scanner at 256 nm.

2.5.4 Thin layer chromatography for nucleotide phosphatase assays:

1 μL of an ADPase reaction (see 2.5.2) was spotted onto a silica TLC plate with 0.8 μL of 10 mM adenosine spotted on top after drying to act as a marker and carrier. The plates were run in ADPase assay developing buffer (9:1 isopropanol:33% (v/v) aqueous ammonia). After drying, spots were visualized at 256 nm and excised for scintillation counting or visualized in a TLC scanner at 256 nm.

2.5.5 Calculation of specific activities:

Strict ATPase or nucleotide phosphatase specific activities were calculated from data obtained after measuring the results of a strict ATPase or a nucleotide phosphatase assay (see 2.5.1 and 2.5.2) with a TLC scanner (see 2.5.3 and 2.5.4). When calculating strict ATPase specific activity, the product measured was ADP. When calculating nucleotide phosphatase specific activity, the product measured was Ado. The equations used are shown below:

product recovered = counts – background

pmoles product = (product recovered / input) * pmoles substrate

pmoles product mg^{-1} min^{-1} = (pmoles product / minutes) / protein concentration (mg mL^{-1})

"Counts": counts obtained from the area where the product appears in the reaction samples analysed.

"Background": counts obtained from the area where the product appears in the negative control.

"Input": total counts obtained from the whole sample.

"Minutes": time that the reaction was incubated, in minutes.

2.5.6 Viral dsDNA nicking:

0.5 μg of viral dsDNA were incubated for 1 h at 37 $^{\circ}$C with 0.43 μg of soluble protein (see 2.4.12). After this, 5x STOP buffer (100 mM Tris-HCl pH 8.0, 2.5 % SDS, 100 mM EDTA, 10 units μL^{-1} proteinase K) was added and the mix incubated for 15 minutes at 37 $^{\circ}$C. The reaction was loaded on an agarose gel (see 2.3.5). Three negative controls were used: 0.5 μg of viral ds-DNA, 0.5 μg of viral dsDNA with STOP buffer and 0.5 μg of viral dsDNA with 1 μg of BSA and STOP buffer. As positive control 1 μg of DNAase I was added to 0.5 μg of viral dsDNA, maintaining the whole process as with the test protein.

3 Results

Resistance proteins in plants play an important role in plant innate immunity (Belkhadir *et* al., 2004, Pan *et* al., 2000, Shen and Schulze-Lefert, 2007, Zipfel, 2008). They are immune receptors that can detect, directly or indirectly, isolate-specific pathogen effectors. Many and diverse studies have been conducted on R proteins (Maekawa *et* al., 2011 and Zhang *et* al., 2010). Some groups have successfully expressed R protein domains and full length proteins (Bernoux *et* al., 2011, Maekawa *et* al., 2011, Schimdt *et* al., 2007, Ve *et* al., 2011, Willliams *et* al., 2011). Nevertheless, only one managed to produce soluble, active protein that was fully biochemically characterized (Fenyk *et* al., 2012). Up to date, an R protein activation model has been accepted in which R proteins are strict ATPases. This is incongruent with findings in Fenyk *et* al., 2012 where it is demonstrated that domains of R1, PSiP and Rpm1 (R proteins from rice, maize and *Arabidopsis*, respectively) are nucleotide phosphatases. Understanding how these proteins function would provide information of great importance for crop protection. In order to achieve this R1 and Rx (an R protein from potato that confers resistance against the Potato Virus X) constructs were used towards the creation of a methodology to obtain soluble, active R proteins as a first step for further investigations on their biochemical activity, structure and, finally, complete understanding of their role in plant innate immunity.

3.1 Expression of Os025g25900 (R1)

A subdomain of an orphan resistance protein from *Oryza sativa ssp.*

japonica Os025g25900 (R1) had been previously expressed as soluble protein (Fenyk *et* al., 2012). The R1 subdomain expressed corresponds to amino acids 197-339, an active nucleotide binding (NB) subdomain (R1-NB). As it was possible to express this resistance protein subdomain, new, bigger domains were created. These constructs included extra C-terminus amino acids (339-521) in the case of R1-NBARC (Appendix 1) and an extra N-terminus subdomain (145-197), in both R1-NB^L and R1-NBARC (Appendix 1). These extra amino acids are thought to have a role in autoregulation of R proteins (Bendahmane *et* al., 2002; Bent, 1996, Hwang and Williamson, 2003; Hwang *et* al., 2000).

3.1.1 Expression constructs

Three strategies were used to generate recombinant plasmids expressing the open reading frames R1-NB^L and R1-NBARC.

3.1.1.1 PCR and Zero Blunt® TOPO® cloning:

DNA corresponding to amino acids 145-521 of R1 (R1-NBARC) was amplified by PCR (see 2.3.1) using primers MJC188 and MJC522 (Appendix 2). The PCR product was ligated into PCRTM-BluntII-TOPO® (see 2.3.7) but no recombinants were obtained despite repeated attempts. Resistance proteins hydrolyse nucleotides (Tameling *et* al., 2002). Residual expression of R1-NBARC could cause the death of the cells and, therefore, no living recombinants would be recovered.

3.1.1.2 Subcloning:

pUC57 containing the complete R1 open reading frame was digested with *XhoI* and *NdeI* (see 2.3.9) and the R1 insert ligated into *XhoI/NdeI* digested

pET-Strep3 (Dixon *et* al., 2009) but no recombinants were recovered despite repeated attempts. As before, in section 3.1.1.1, residual expression of an active R1 domain could cause the death of recombinant cells due to its nucleotide hydrolysing activity (Tameling *et* al., 2002).

3.1.1.3 Gateway:

DNA corresponding to amino acids 145-237 of R1 (R1-NB^L) was amplified by PCR (see 2.4.1) using primers MJC541 and MJC540 (Appendix 2). DNA corresponding to R1-NBARC was amplified using primers MJC535 and MJC540 (Appendix 2). PCR products were cloned into the Gateway entry vector, pDONR207, using BP clonase (see 2.3.3). The constructs were purified and used in a second Gateway reaction (see 2.3.4) where the fragments were introduced in pCola2-DEST (pR1-NB^{L}2, pR1-NBARC2) and pCola3-DEST (pR1-NB^{L}3, pR1-NBARC3), using the LR clonase. *Escherichia coli* BL21 (DE3) strains were satisfactorily transformed (see 2.3.10) carrying the constructs pR1-NB^{L}2, pR1-NB^{L}3, pR1-NBARC2 and pR1-NBARC3 (Appendix 1; Figure 7).
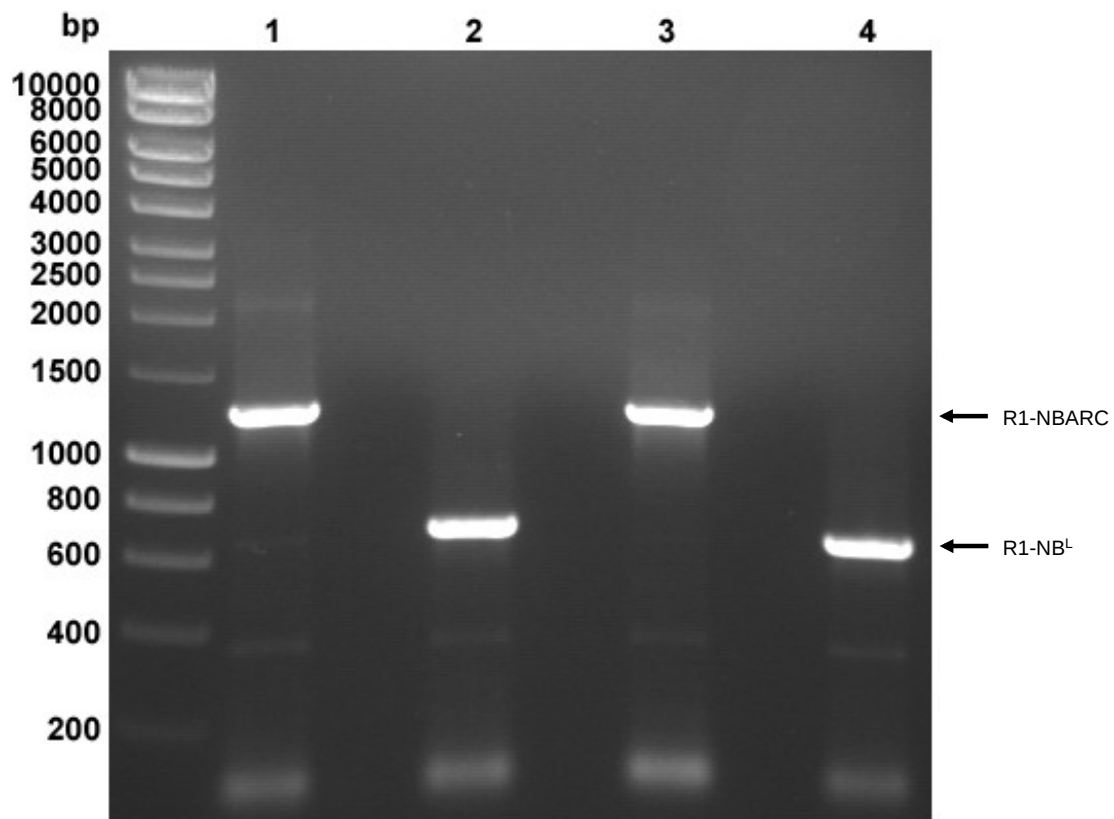
Figure 7 Colony PCR (see 2.3.2) of *E. coli* BL21 (DE3) strains with the expression vectors **1** pR1-NBARC2, **2** pR1-NB^{L}2, **3** pR1-NBARC3 and **4** pR1-NB^{L}3. The primers used were MJC188 and MJC541 (for R1-NB^{L}2 and R1-NB^{L}3; Appendix 2) and MJC188 and MJC535 (for R1-NBARC2 and R1-NBARC3; Appendix 2).

As Figure 7 shows, pR1-NBARC2, pR1-NB^{L}2, pR1-NBARC3 and pR1-NB^{L}3 were successfully introduced into *E. coli* BL21 (DE3) strains, which then were ready to express proteins R1-NBARC and R1-NB^L. The success in these transformations by gateway could be due to the lack of expression of the constructs.

3.1.2 Expression of R1 subdomains as soluble proteins

Proteins corresponding to R1-NB^{L}2, R1-NB^{L}3, R1-NBARC2 and R1-NBARC3 (Appendix 1) carrying a N-terminal hexa-histidine tag and a C-terminal Strep tag were expressed (see 2.4.11) from *E. coli* BL21 (DE3). IPTG was used to induce the expression of these proteins once bacteria grew to an optical density of 0.8 at a wavelength of 600 nm. The temperature, after

inducing protein expression, was either kept at 37 $^{\circ}$C or lowered to 22 $^{\circ}$C.

Despite multiple attempts, no soluble protein was recovered after purification with either Ni^{+2}-NTA resin (see 2.4.7) or Glutathione Sepharose^{TM} (see 2.4.8). In order to test for the expression of protein, Western blots (see 2.4.5) using cell lysate and soluble fraction samples were performed (Figure 8).

✦ Unidentified non-specific band
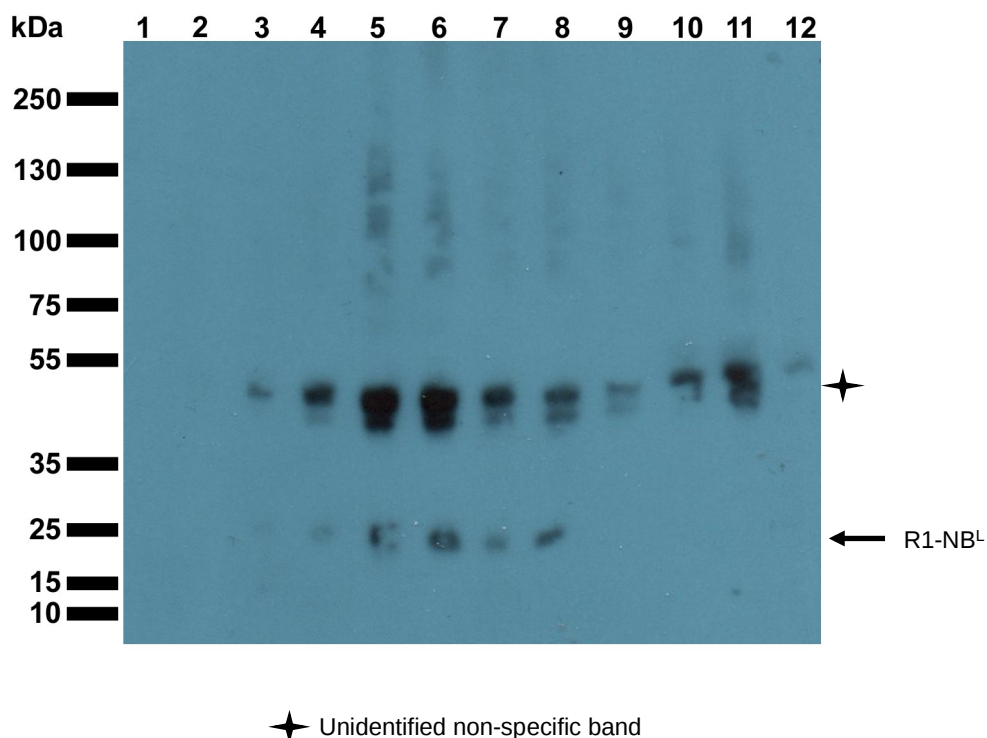
Figure 8 Anti-Strep Western blot (see 2.4.5) with cell lysate samples from *E. coli* BL21 (DE3) R1-NB^{L}2 taken at different times after induction of protein expression with 100 μM IPTG. **1**. 0 h, **2**. 30 minutes, **3**. 1 h, **4**. 1 h 30 minutes, **5**. 2 h, **6**. 2 h 30 minutes, **7**. 3 h, **8**. 3 h 30 minutes, **9**. 4 h, **10**. 4 h 30 minutes, **11**. 5 h, **12**. o/n.

From Figure 8 we can infer the presence of R1-NB^{L}2 (26 kDa) in the cell lysate between 2 h and 3 h and 30 minutes expression (Figure 8, **5-8**), but no protein was ever seen in soluble fraction samples. These results could be due to the protein being expressed, but not refolding properly. Therefore, the use of chaperones was justified as a strategy to overcome this. Chaperones are proteins that enhance other proteins solubility by promoting their correct refolding (Baneyx, 1999, de Marco *et* al., 2007 and Tomoyasu *et* al., 2001). It

is worth pointing out that the non-identified bands that appear in this figure could correspond to a R1-NB^{L}2 dimmer as it has twice its size, its expression is induced by IPTG and it reacts with an anti-Strep specific antibody. Nevertheless, this should be confirmed by mass spectrometry analysis.

3.1.3 Enhancement of R1 subdomains solubility with chaperones

No soluble proteins were recovered from the expression of R1-NB^{L}2, R1-NB^{L}3, R1-NBARC2 and R1-NBARC3 by conventional means. However, protein was present in cell lysates (see 3.1.2) and was hypothesized to be not folding properly. Therefore, the use of chaperones was tested.

Chaperones are proteins that increase other protein's solubility by promoting their correct folding (Baneyx, 1999, de la Fuente *et* al., 2005, de Marco *et* al., 2007 and Tomoyasu *et* al., 2001). This has been demonstrated with different proteins, as seen in de Marco *et* al., 2007 and Tomoyasu *et* al., 2001. In the case of resistance proteins, experiments shown by de la Fuente *et* al., 2005 demonstrate that resistance protein I-2, from tomato, requires the heat shock protein 90 (Hsp90) for its correct refolding and functioning.

E. coli BL21 (DE3) strains were transformed (see 2.3.10) with different chaperone vectors (Appendix 3) containing a series of different chaperone genes including *danK*, *dnaJ* and *groELS* (de Marco *et* al., 2007). Eight different strains were created. These were then transformed (see 2.3.10) with the constructs pR1-NB^{L}2, pR1-NB^{L}3, pR1-NBARC2 and pR1-NBARC3 to create thirty-two strains (Appendix 4).

Positive recombinants (Appendix 4) with different combinations of chaperones and constructs pR1-NB^{L}2, pR1-NB^{L}3, pR1-NBARC2 and pR1-NBARC3 were used in expression tests. 50 mL LB medium was inoculated with 5 mL of an overnight culture and grown in a 37 °C temperature controlled shacking incubator at 200 rpm. When cells reached an absorbance value of 0.8 at 600 nm, IPTG was added to a final concentration of 1 mM. The culture

was incubated by shaking at 150 rpm for 12 hours. Bacteria were harvested (see 2.4.1) and lysed (see 2.4.2). Western blots were performed to test the presence of R1-NB^{L}2, R1-NB^{L}3, R1-NBARC2 and R1-NBARC3. The samples used in Western blots were centrifuged supernatant to test for soluble proteins and cell lysates to test for soluble and insoluble proteins (Figure 9).

+ Unidentified non-specific band
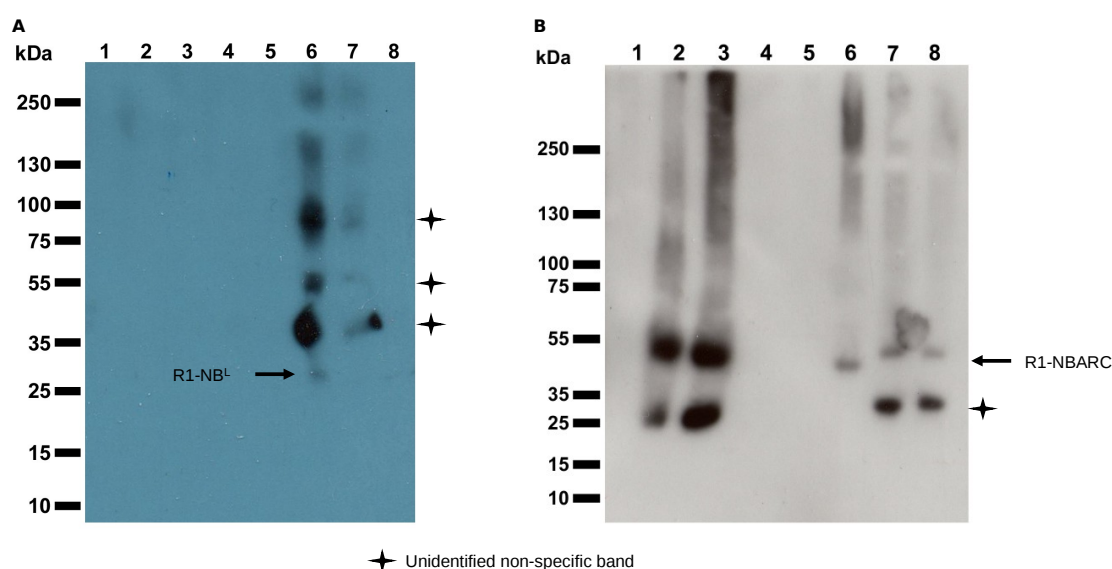
Figure 9 Anti-His (**A**) and anti-Strep (**B**) Western blots (see 2.4.5) with cell lysate samples from *E. coli* BL21 (DE3) chaperone strains with R1 expression constructs. (**A**) **1**. R1-NB^{L}3 I, **2**. R1- NB^{L}3 II, **3**. R1- NB^{L}3 III, **4**. R1- NB^{L}3 IV, **5**. R1- NB^{L}3 V, **6**. R1- NB^{L}3 VI, **7**. R1- NB^{L}3 VII, **8**. R1- NB^{L}3 VIII. (**B**) **1**. R1-NBARC2 I, **2**. R1-NBARC2 II, **3**. R1-NBARC2 III, **4**. R1-NBARC2 IV, **5**. R1-NBARC2 V, **6**. R1-NBARC2 VI, **7**. R1-NBARC2 VII, **8**. R1-NBARC2 VIII.

Figure 9 demonstrates the presence of correct size proteins for R1-NB^{L}3 (**A** weak band in lane 6, 26 kDa) and R1-NBARC2 (**B** 6-8, 48 kDa) in samples of cell lysates obtained after their expression from the different chaperone strains. Chaperone strain VI supported the expression of protein for both R1-NB^{L}3 and R1-NBARC2, therefore strains R1-NB^{L}3 VI and R1-NBARC2 VI were chosen for further analysis.

For both strains, R1-NB^{L}3 VI and R1-NBARC2 VI, an expression test experiment was conducted. Four 50 mL LB medium flasks for each strain were inoculated with 5 mL of an overnight culture and grown in a 37 ^{o}C

temperature controlled shaking incubator at 200 rpm. When cells reached an absorbance value of 0.8 at 600 nm, IPTG was added to two different concentrations: 100 µM and 1 mM. The culture was incubated for 12 hours during which, the temperature was maintained at 37 °C or lowered to 22 °C. Bacteria were harvested (see 2.4.1) and lysed (see 2.4.2). Western blots were performed to test the presence of R1-NB^{L}3 VI and R1-NBARC2 VI. The samples used in Western blots were centrifuged supernatant to test for soluble proteins (Figure 10) and cell lysates to test for soluble and insoluble proteins (Figure 11).
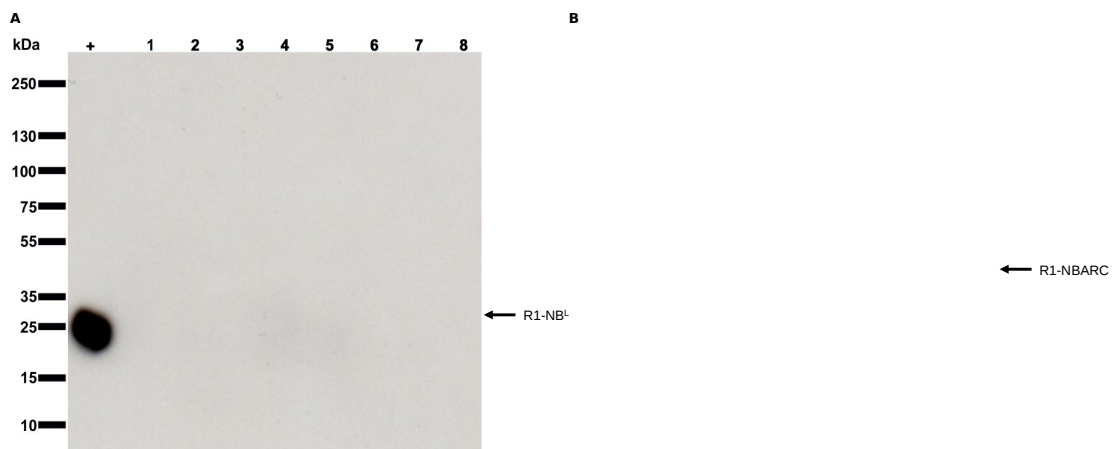

Figure 10 Anti-Strep Western blots (see 2.4.5) with soluble fraction samples from (**A**) R1-NB^{L}3 VI and (**B**) R1-NBARC2 VI expressing protein under different conditions. **+**. F2, GST protein in Arabidopsis (Dixon *et* al., 2009); **1**. 22 °C, 100 µM IPTG, 3 h; **2**. 22 °C, 1 mM IPTG, 3 h; **3**. 22 °C, 100 µM IPTG, o/n; **4**. 22 °C, 1 mM IPTG, o/n; **5**. 37 °C, 100 µM IPTG, 3 h; **6**. 37 °C, 1 mM IPTG, 3 h; **7**. 37 °C, 100 µM IPTG, o/n; **8**. 37 °C, 1 mM IPTG, o/n.

+ Unidentified non-specific band
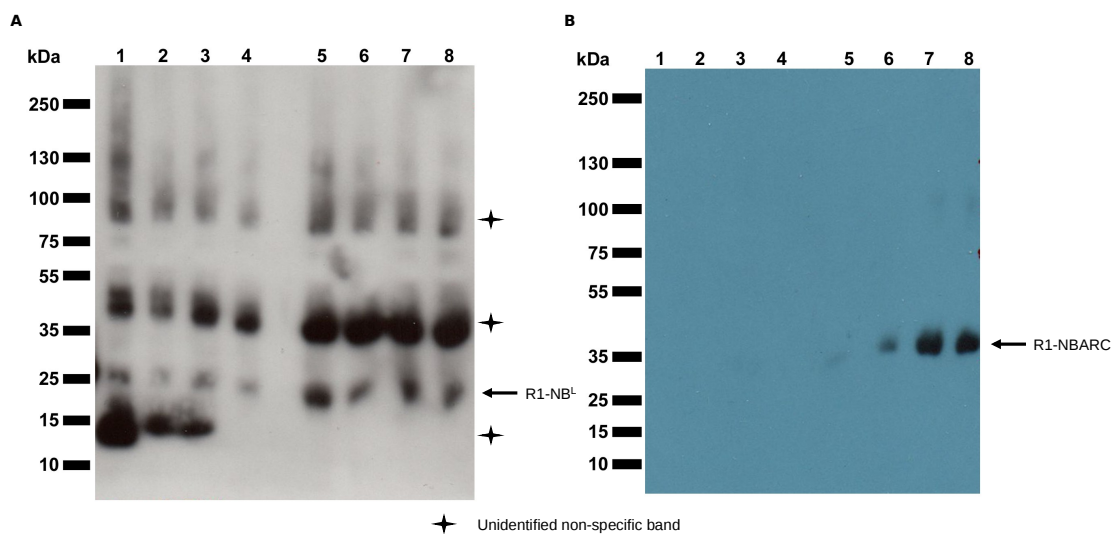
Figure 11 Anti-Strep Western bolts (see 2.4.5) with total fraction samples from (**A**) R1- NB^{L}3 VI and (**B**) R1-NBARC2 VI expressing protein under different conditions.**1**. 22 ^{o}C, 100 μM IPTG, 3 h; **2**. 22 ^{o}C, 1 mM IPTG, 3 h; **3**. 22 ^{o}C, 100 μM IPTG, o/n; **4**. 22 ^{o}C, 1 mM IPTG, o/n; **5**. 37 ^{0}C, 100 μM IPTG, 3 h; **6**. 37 ^{0}C, 1 mM IPTG, 3 h; **7**. 37 ^{0}C, 100 μM IPTG, o/n; **8**. 37 ^{0}C, 1 mM IPTG, o/n.

Comparison of the above Westerns blots (Figure 10 and Figure 11) shows that R1-NB^{L}3 and R1-NBARC2 were being expressed, but were not soluble as both proteins show bands in Westerns blots with samples of cell lysates, but not with soluble fractions. Chaperones do not, therefore, improve the solubility of either protein. As the proteins were being expressed, albeit insoluble, a different approach was implemented to refold insoluble proteins by testing different refolding conditions.

A refolding protocol was used with I-2 (Tameling *et* al., 2002). This resistance protein was expressed in bacteria and accumulated in inclusion bodies. Purification of inclusion bodies, solubilisation of the proteins in the inclusion bodies with high concentrations of urea, and posterior refolding of I-2 resulted in active protein. Following this way of proceeding, a series of refolding conditions (Appendix 5) was tested for R1-NBARC2. This was the construct chosen as it is bigger than R1-NB^L and more closely represents a suitable target for biochemistry.

3.1.4 Refolding of R1-NBARC2

In section 3.1.2 it was shown that R1-NB^L and R1-NBARC are not expressed as soluble proteins in *E. coli* BL21 (DE3) strains although these proteins were present in total lysates (Figure 8). The use of chaperones to improve their solubility did not give soluble protein either (Figure 10). However, R1-NB^L and R1-NBARC were always present in total lysates (Figure 11). As an approach towards refolding insoluble R1-NBARC2, inclusion bodies were purified from *E. coli* BL21 (DE3) strains and the protein was subjected to different refolding conditions (Appendix 5). This protocol has proved to yield active, soluble protein in other experiments (Rudolph and Lilie,

1996).

Inclusion bodies are relatively simple to purify, but the protein must be recovered from the insoluble fraction and refolded into an active protein. To achieve this, the protein first has to be solubilized by denaturation (Rudolph and Lilie, 1996). It is then necessary to test different conditions in order to identify which will provide soluble active protein.

R1-NBARC2 was expressed and the inclusion bodies purified. Different urea and NaCl concentrations were tested (see 2.4.9) to establish the concentration needed in the solubilisation buffer (Figure 12): the highest urea and NaCl concentration that does not solubilize the protein from the inclusion bodies.
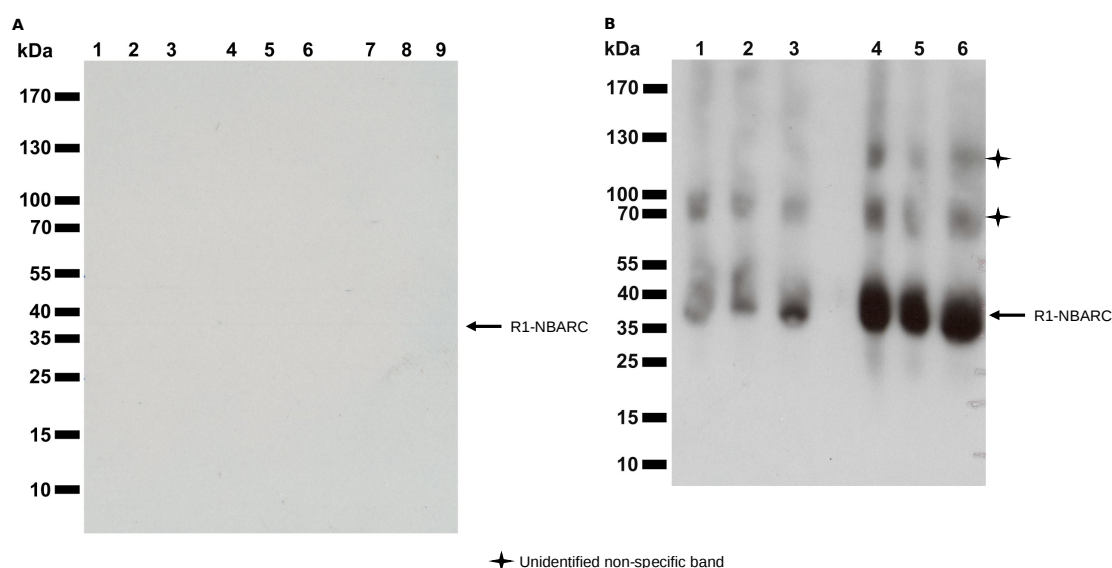
Figure 12 Anti-His Western blots (see 2.4.5) with soluble fraction samples from *E. coli* BL21 (DE3) R1-NBARC2. Different concentrations of urea and NaCl were tested for the purification of inclusion bodies. (**A**) **1**. 0 M urea, 0 M NaCl; **2**. 0 M urea, 1 M NaCl; **3**. 0 M urea, 1.5 M NaCl; **4**. 2 M urea, 0 M NaCl; **5**. 2 M urea, 1 M NaCl; **6**. 2 M urea, 1.5 M NaCl; **7**. 4 M urea, 0 M NaCl; **8**. 4 M urea, 1 M NaCl; **9**. 4 M urea, 1.5 M NaCl. (**B**) **1**. 6 M urea, 0 M NaCl; **2**. 6 M urea, 1 M NaCl; **3**. 6 M urea, 1.5 M NaCl; **4**. 8 M urea, 0 M NaCl; **5**. 8 M urea, 1 M NaCl; **6**. 8 M urea, 1.5 M NaCl.

Results in Figure 12 show that the highest urea and NaCl concentrations

that do not solubilize the protein are 4 M urea and 1.5 M NaCl as no bands can be seen on the SDS-PAGE gel that corresponds to Figure 12 **A**, but are visible on Figure 12, **B**. These are the concentrations used in the solubilisation buffer when performing the refolding experiment for R1-NBARC2.

Once the concentrations of urea and NaCl were determined, a screen of 15 different refolding conditions was performed (see 2.4.11; Appendix 5). The presence of soluble protein in those samples was tested by Western blot (see 2.4.5, Figure 13).
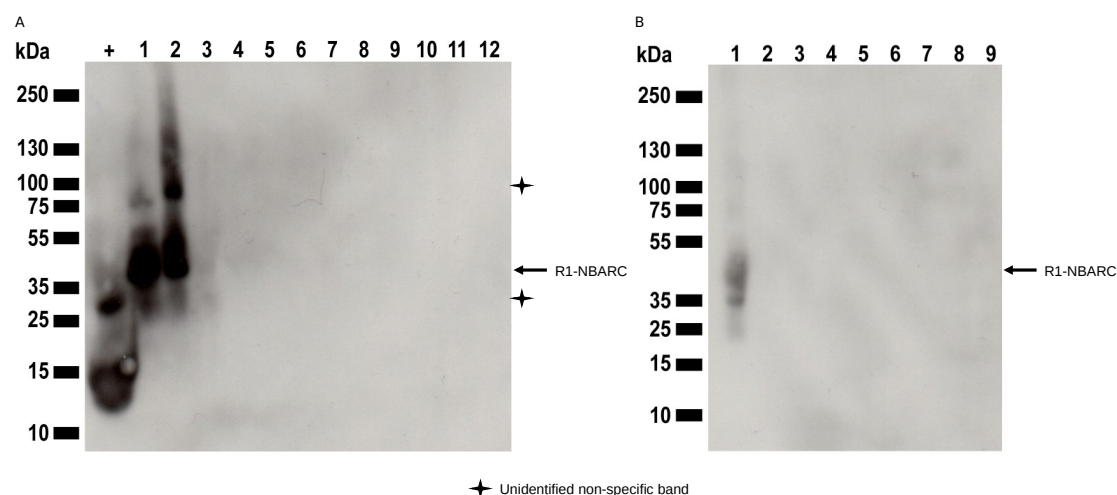
Figure 13 Anti-His Western blots (see 2.4.5) with soluble fraction samples of purified and solubilized inclusion bodies from *E. coli* BL21 (DE3) R1-NBARC2 under different refolding conditions (Appendix 5). (**A**) **+**. Catabolite activator protein (CAP), His tagged protein from *E. coli*, **1**. Purified inclusion bodies, **2**. Solubilized inclusion bodies, **3**. Refolding condition 1 after dialysis, **4**. Refolding condition 8 after dialysis, **5**. Refolding condition 11 after dialysis, **6**. Refolding condition 1, **7**. Refolding condition 2, **8**. Refolding condition 3, **9**. Refolding condition 4, **10**. Refolding condition 5, **11**. Refolding condition 6, **12**. Refolding condition 7. (**B**) **1**. Solubilized inclusion bodies, **2**. Refolding condition 8**, 3**. Refolding condition 9**, 4**. Refolding condition 10**, 5**. Refolding condition 11**, 6.** Refolding condition 12**, 7**. Refolding condition 13, **8**. Refolding condition 14, **9**. Refolding condition 15.

Although there is protein in the purified and solubilized inclusion bodies (Figure 13 **A** 1-2, **B** 1), no protein is present in the soluble fractions after

refolding with each of the different conditions (Figure 13 **A** 6-12, **B** 2-9; Appendix 5). Some samples were dialysed (Figure 13 **A** 3-5) to eliminate a possible negative interaction of salts during Western blotting. Having in mind these results, it is inferred that no soluble protein was obtained with any of the 15 different refolding conditions.

Results from sections 3.1.2, 3.1.3 and 3.1.4 showed that no soluble active protein was ever recovered despite multiple different approaches. No attempts to improve the solubility of proteins R1-NB^L and R1-NBARC were successful. There is evidence of expression of these proteins in cell lysates, although no soluble, active protein could be recovered. Resistance proteins like R1 hydrolyse nucleotides (Tameling *et* al., 2002) and this could be the reason why it is not possible to obtain active proteins from their expression in cells. Other reasons to why these proteins are toxic that cannot be ruled out are that R proteins bind DNA and affect transcription (Choi *et* al., 2001 and Wang *et* al., 2010). Moreover, R proteins could have other unknown activities that result in their toxicity to cells.

Refolding insoluble, inactive protein from expressing bacteria could be an option towards the achievement of recovering soluble, active, toxic proteins. Nevertheless, this approach did not give positive results with R1-NBARC. As resistance proteins have highly conserved structures, the project moved on towards the test of these refolding conditions on Rx (Appendix 5), the potato resistance protein against Potato Virus X (PVX). Rx has been thoroughly studied although it has not yet been produced as a soluble active protein (Bendahmane *et* al., 1995; Goulden *et* al., 1993 and Kohm *et* al., 1993).

3.2 Expression of the Potato Virus X (PVX) resistance gene (Rx)

As no soluble R1 protein was ever recovered despite the use of different approaches (see 3.1), the Rx resistance protein from potato, which infers resistance against Potato Virus X, was used. Two versions of Rx-NBARC were used, wild type and K176R mutant (Rx-NBARC WT and Rx-NBARC

K176R respectively, obtained from Dr. F. L. W. Takken). It has been demonstrated in other resistant proteins (Takken *et* al., 2006) that this type of mutation in the P-loop causes a loss-of-function phenotype.

3.2.1 Protein refolding of Rx:

Amino acids 1-486 of Rx (Rx-NBARC) in the expression vector pGEX-4T-1 were expressed in *E. coli* BL21 (DE3) strains (see 2.4.2). Pellets were lysed (see 2.4.3) and used for purification of inclusion bodies. Two versions of Rx-NBARC were used: the wild type and a K176R mutant (Rx-NBARC WT and Rx-NBARC K176R, respectively).

3.2.1.1 Test of refolding conditions for Rx-NBARC

Different urea and NaCl concentrations were tested (see 2.4.9) to establish the highest concentration that would not solubilize Rx-NBARC. This concentration was established as 4 M urea and no NaCl.

After the concentrations of urea and NaCl were determined, a screening of 15 different refolding conditions was performed (see 2.4.11; Appendix 5). The presence of soluble protein was tested by Western blot (see 2.4.5). Preliminary activity assays were performed in order to identify the condition that allowed recovery of the largest amount of soluble protein in an active conformation.

Resistance proteins in plants are thought to act as ATPases in an "on-off" switch (Bisgrove *et* al., 1994; Takken *et* al., 2006 and Tameling *et* al., 2002). The current model of activation for plant resistance proteins hypothesizes that they attain their active state when an ATP molecule is bound to their NBARC domain. The hydrolysis of this ATP molecule into ADP (strict ATPase activity) would cause a conformational change in the protein, making it enter its inactive state (Takken *et* al., 2006 and Tameling *et* al., 2002). Strict ATPase

activity assays (see 2.5.1) were therefore conducted to monitor Rx for its correctly folded state (Figure 14). However, a recent study (Fenyk *et* al., 2012) demonstrated that the NB subdomain of R1 (orphan resistant protein of Oryza sativa ssp. japonica Os025g25900) has a nucleotide phosphatase activity with preference of substrate as follows: AMP>ADP>ATP. This is the only evidence of this activity in plant resistance proteins to date, but it is also the first time ever a soluble, active resistance protein domain has been expressed and fully biochemically characterized. Following this line of investigation, nucleotide phosphatase activity tests using ADP as substrate (see 2.5.2) were also performed on refolded Rx-NBARC samples (Figure 15).
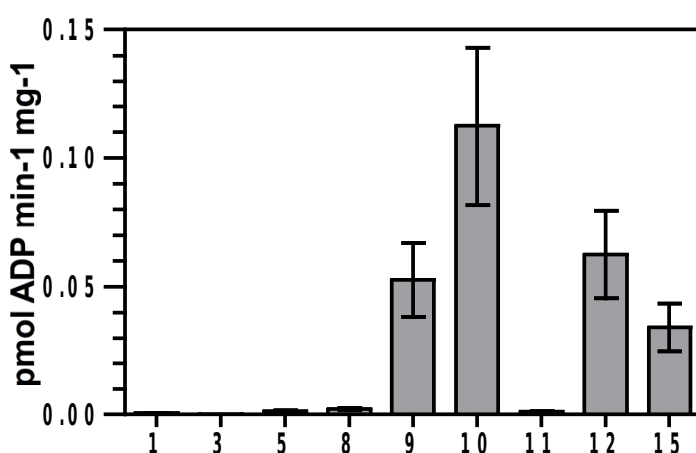
Figure 14 Results from a strict ATPase assay (see 2.5.1) with Rx-NBARC WT under different refolding conditions (Appendix 5). **1**. Refolding condition 1, **3**. Refolding condition 3, **5**. Refolding condition 5, **8**. Refolding condition 8, **9**. Refolding condition 9, **10**. Refolding condition 10, **11**. Refolding condition 11, **12**. Refolding condition 12, **15**. Refolding condition 15. The product searched for was ADP. Data was read with a scintillation counter. Error bars correspond to the standard deviation (n=2).

Strict ATPase reactions performed to create Figure 14 were conducted as explained in 2.5.1, reactions were developed as in 2.5.3 and specific activities were calculated as in 2.5.5.
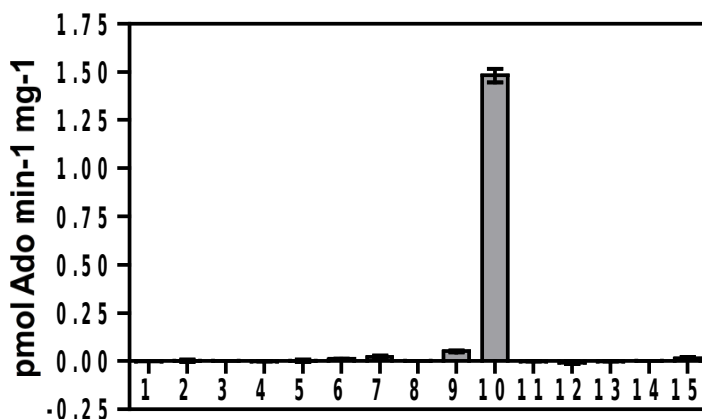
Figure 15 Results from a nucleotide phosphatase assay (see 2.5.2) with ADP as substrate and Rx-NBARC WT under different refolding conditions (Appendix 5). **1**. Refolding condition 1, **2**. Refolding condition 2, **3**. Refolding condition 3, **4**. Refolding condition 4, **5**. Refolding condition 5, **6**. Refolding condition 6, **7**. Refolding condition 7, **8**. Refolding condition 8, **9**. Refolding condition 9, **10**. Refolding condition 10, **11**. Refolding condition 11, **12**. Refolding condition 12, **13**. Refolding condition 13, **14**. Refolding condition 14, **15**. Refolding condition 15. The product searched for was adenosine. Data was read with a scintillation counter. Error bars correspond to the standard deviation (n=2).

The samples used to create Figure 15 were those used in Figure 14. In this case, the spots were developed with a nucleotide phosphatase developing buffer instead of a strict ATPase developing buffer (see 2.5.4) and specific activities were calculated as in 2.5.5. Differences of strict ATPase activity and phosphatase activity using the same protein sample, but varying the refolding conditions might be in those refolding conditions. The protein can not refold properly under all conditions. Some refolding buffers may enhance a correct refolding of Rx-NBARC, while others do not.

From Figures 14 and 15, it can be shown that refolding buffer number 10 (Appendix 5) provides the best conditions for Rx-NBARC WT to refold. It can also be stated that the refolded Rx-NBARC had a higher nucleotide phosphatase activity than strict ATPase activity. Buffers 9 and 10 were then tested with both the wild type and the K176R mutant versions of Rx-NBARC.

3.2.1.2 Comparison of successful refolding conditions for Rx-NBARC

Proteins Rx-NBARC WT and Rx-NBARC K176R were refolded with buffer 9 and buffer 10 (Appendix 5). Their nucleotide phosphatase activities with ADP as substrate were tested through a nucleotide phosphatase activity assay (see 2.5.2, Figure 16).
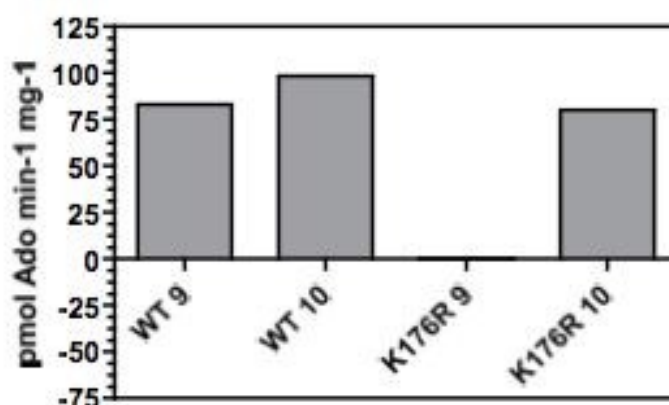
Figure 16 Results from a nucleotide phosphatase activity assay (see 2.5.2) with ADP as substrate and samples of Rx-NBARC WT and Rx-NBARC K176R refolded with buffer 9 and 10. The product searched for was adenosine. Data was read with a scintillation counter.

From Figure 16 it can be inferred that the buffer that yields more active protein for both wild type and mutant Rx-NBARC is buffer 10. This Figure was created with data from preliminary nucleotide phosphatase experiments with refolded samples of Rx-NBARC WT and Rx-NBARC K176R that had not been purified further than an inclusion bodies purification (see 2.4.10). It cannot be used as definitive specific activity data to compare differences between proteins; therefore differences (or lack of them) in activity between wild type and mutant Rx are unreliable. Specific experiments with cleaner samples are shown later (Figure 26 and Figure 36).

<u>3.2.2 Protein purification after refolding</u>

Rx-NBARC WT and Rx-NBARC K176R were purified from inclusion bodies (see 2.4.10), refolded using buffer 10 (see 2.4.12), dialysed (see 2.4.13) and concentrated with PEG 8000 (see 2.4.14). After this process, samples were ready for purification.

Rx-NBARC WT and Rx-NBARC K176R constructs had a glutathione S-transferase (GST) tag on the N-terminus and a hexa-histidine tag on the C-terminus. Each tag was used for purification tests on a Glutathione Sepharose^{TM} purification (see 2.4.8) and a Ni^{+2}-NTA resin (see 2.4.7) after Rx-NBARC WT and Rx-NBARC K176R were refolded (see 2.4.12), dialysed (see 2.4.13) and concentrated (see 2.4.14).

3.2.2.1 Glutathione Sepharose^{TM} purification:

Rx-NBARC constructs had a N-terminal GST tag that was used for purification with a Glutathione Sepharose^{TM} resin after the protein had been refolded, dialysed and concentrated.

Nucleotide phosphatase activity (see 2.5.2 and 2.5.4) was tested in the buffers used during the purification of inclusion bodies, refolding and Glutathione Sepharose^{TM} purification processes (Figure 17).
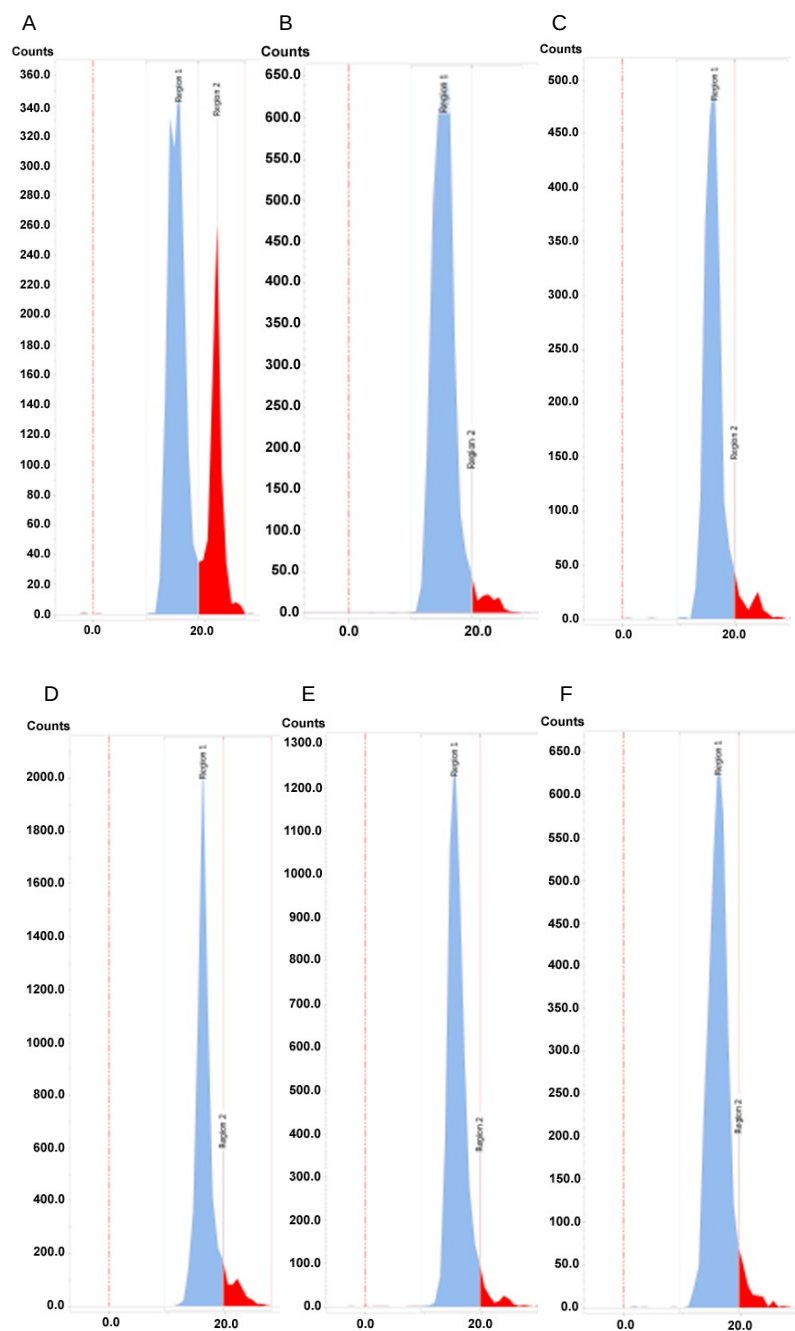
Figure 17 Nucleotide phosphatase activity present in different buffers used during the inclusion bodies purification, refolding and Glutathione Sepharose™ purification processes. ADP was used as substrate and the product searched for was adenosine. Data was read with a TLC scanner. Blue areas correspond to ADP, red to adenosine. (**A**) Positive control: refolded, non-purified Rx-NBARC WT. (**B**) Inclusion bodies washing buffer. (**C**) Refolding buffer 10. (**D**) Dialysis buffer. (**E**) PBS. (**F**) Glutathione Sepharose™ elution buffer.

Figure 17 shows that no nucleotide phosphatase activity is observed in substances in the buffers used for the purification of inclusion bodies, refolding Rx-NBARC, or for Glutathione Sepharose™ purification.

Refolded Rx-NBARC WT and Rx-NBARC K176R (see 2.4.12) were subjected to a Glutathione Sepharose™ purification (see 2.4.8). Nucleotide phosphatase assays (see 2.5.2) were conducted on all samples obtained from these purifications (Figures 18 and 19).
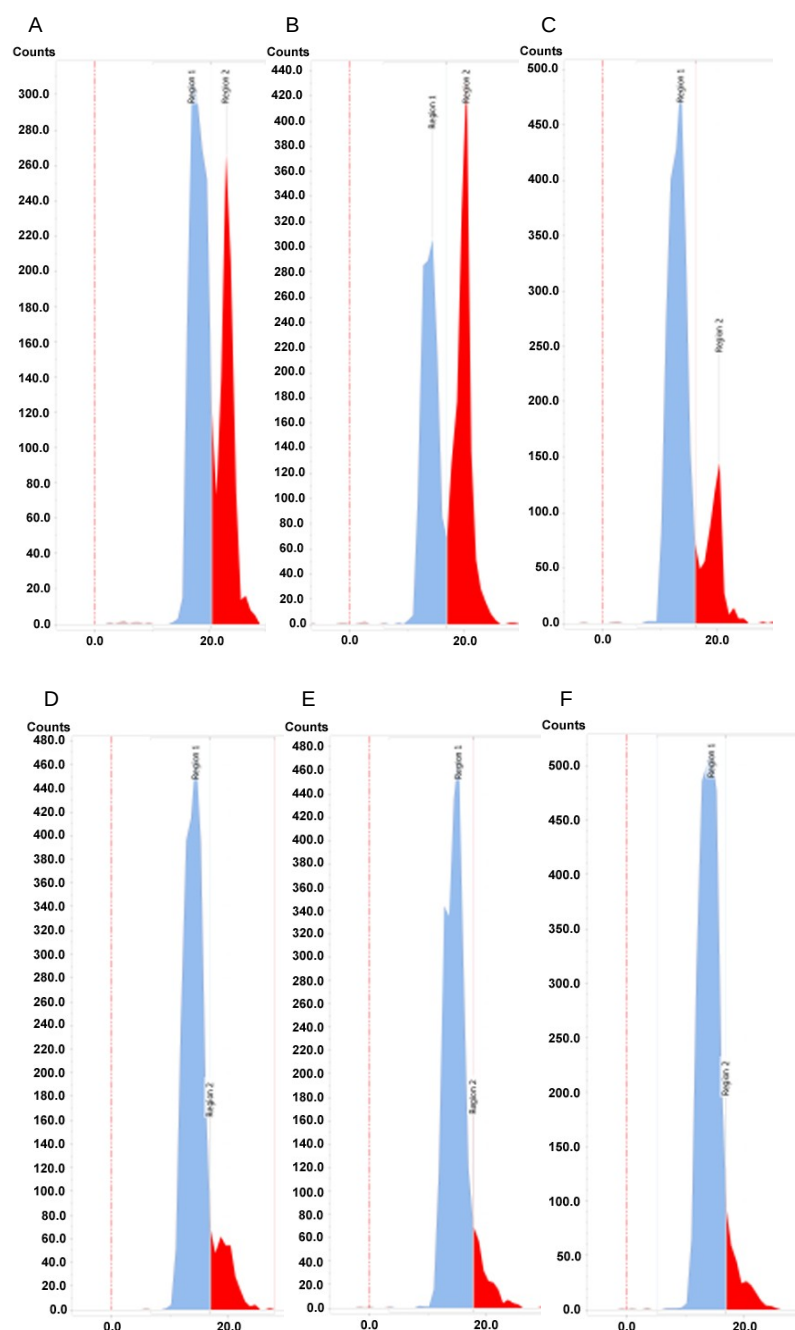
Figure 18 Nucleotide phosphatase assay (see 2.5.2) with ADP as substrate and Rx-NBARC WT samples obtained during a Glutathione Sepharose™ purification (see 2.4.8). Data was read with a TLC scanner. Blue areas correspond to ADP, red to adenosine. (**A**) Positive control, R1-NB (Fenyk *et* al., 2012). (**B**) Flow through. (**C**) Wash one (2 mL PBS). (**D**) Wash two (2 mL washing buffer). (**E**) Eluate one (200 μL of elution buffer). (**F**) Eluate two (200 μL of

elution buffer).
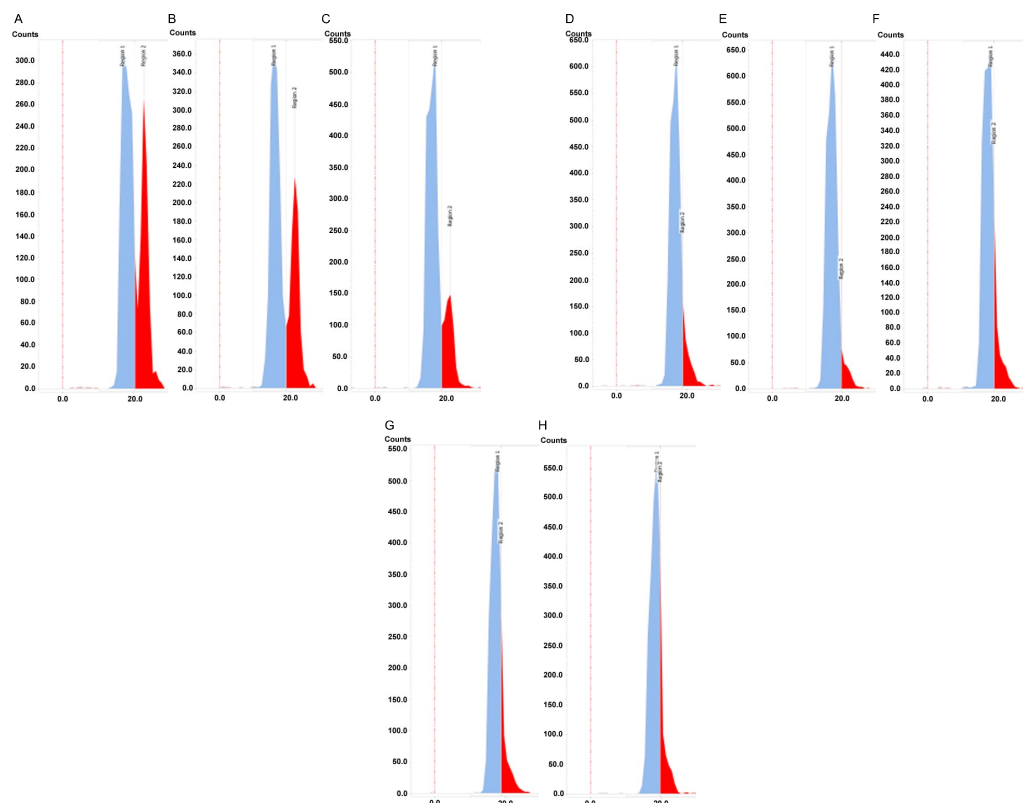
Figure 19 Nucleotide phosphatase assay (see 2.5.2) with ADP used as substrate and Rx-NBARC K176R samples obtained during a Glutathione Sepharose™ purification (see 2.4.8). Data was read with a TLC scanner. Blue areas correspond to ADP, red to adenosine. (**A**) Positive control, Rx-NBARC WT refolded, non-purified. (**B**) Flow through. (**C**) Wash one (2 mL PBS). (**D**) Wash two (2 mL washing buffer). (**E**) Wash three (2 mL PBS). (**F**) Eluate one (150 µL elution buffer). (**G**) Eluate two (150 µL elution buffer). (**H**) Eluate three (150 µL elution buffer).

Nucleotide phosphatase assays (see 2.5.2) performed to create Figures 17 and 18 used ADP as substrate with adenosine analysed as product. Data on Figures 18 and 19 show that nucleotide phosphatase activity was present mainly in the flow through samples. No active phosphatase protein was recovered in eluates. SDS-PAGE gels (see 2.4.4, Figure 20) and Western blots (see 2.4.5, Figure 21) were performed with these samples, but bands corresponding to the correct Rx-NBARC size (75 kDa) were only present in flow throughs, consistent with the data of the activity assays (Figures 18 and

19).
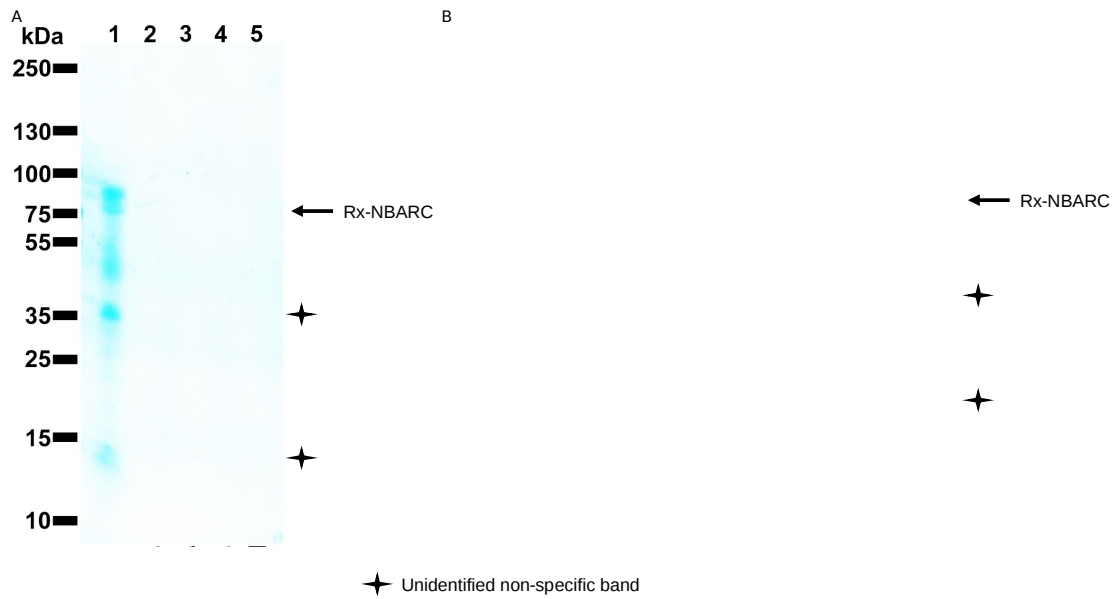
Figure 20 SDS-PAGE gel with samples of (**A**) Rx-NBARC WT and (**B**) Rx-NBARC K176R from a Glutathione Sepharose™ purification (see 2.4.8). (**A**) **1**. Flow through, **2**. Wash one (2 mL PBS), **3**. Wash two (2 mL washing buffer), **4**. Eluate one (200 μL of elution buffer), **5**. Eluate two (200 μL of elution buffer). (**B**) **1**. Refolded, non-purified Rx-NBARC K176R, **2.** Flow through, **3**. Wash one (2 mL PBS), **4**. Wash two (2 mL washing buffer), **5**. Wash three (2 mL PBS), **6.** Eluate one (150 μL of elution buffer), **7**. Eluate two (150 μL of elution buffer), **8**. Eluate three (150 μL of elution buffer).
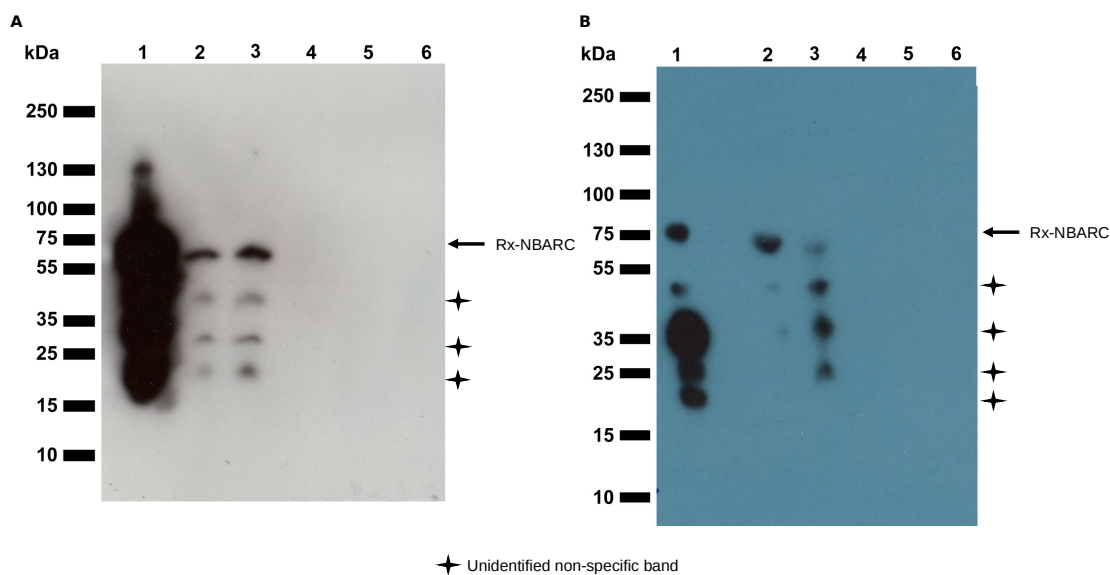
Figure 21 Anti-His (**A**) and anti-GST (**B**) Western blots (see 2.4.5) with samples of (**A**) Rx-NBARC WT and (**B**) Rx-NBARC K176R from a Glutathione Sepharose™ purification (see 2.4.8). (**A**) **+**. CAP, His-tagged protein from *E. coli*, **1**. Refolded, non-purified Rx-NBARC WT, **2**. Flow through, **3**. Wash one (2 mL PBS), **4**. Wash two (2 mL washing buffer), **5**. Wash three (2 mL PBS), **6**. Eluate (150 μL elution buffer). (**B**) **+**. F2, GST-tagged protein (Dixon *et* al., 2004), **1**. Refolded, non-purified Rx-NBARC K176R, **2**. Flow through, **3**. Wash one (2 mL PBS), **4**. Wash two (2 mL washing buffer), **5**. Wash three (2 mL PBS), **6**. Eluate (150 μL elution buffer).

Figures 18-21 demonstrate that no protein was recovered from Glutathione Sepharose™ purifications (see 2.4.8) despite modifying elution and incubation conditions. The reason why Rx-NBARC did not bind to the resin through its GST N-terminus tag might be because the resin was not functioning correctly under the experimental conditions used. A different possibility could be that the buffers used for refolding and dialysing were interfering with the purification process. The third possibility for the GST tag not binding to the glutathione Sepharose™ resin was that it was not refolding properly or it was situated in a position where the binding was obstructed. In order to check these possibilities, a test glutathione Sepharose™ purification (see 2.4.8) was conducted with GST.

Proof of efficiency of the Glutathione Sepharose^{TM} resin:

No Rx-NBARC WT or Rx-NBARC K176R was recovered from eluates and most of it was coming out in the flow through on purification. In order to know if the resin was working or if any of the steps of the experiments were preventing the GST tag in the Rx-NBARC proteins from binding to the resin, the same process was performed with naked GST. Consequently, GST was subjected to the expression, purification and refolding process to which Rx-NBARC had been previously.

GST was expressed from an empty pGEX-6P-1 plasmid (GE Healthcare) in *E. coli* BL21 (DE3). After harvesting, soluble protein from lysates was purified in a Glutathione Sepharose^{TM} resin (see 2.4.8, Figure 22).
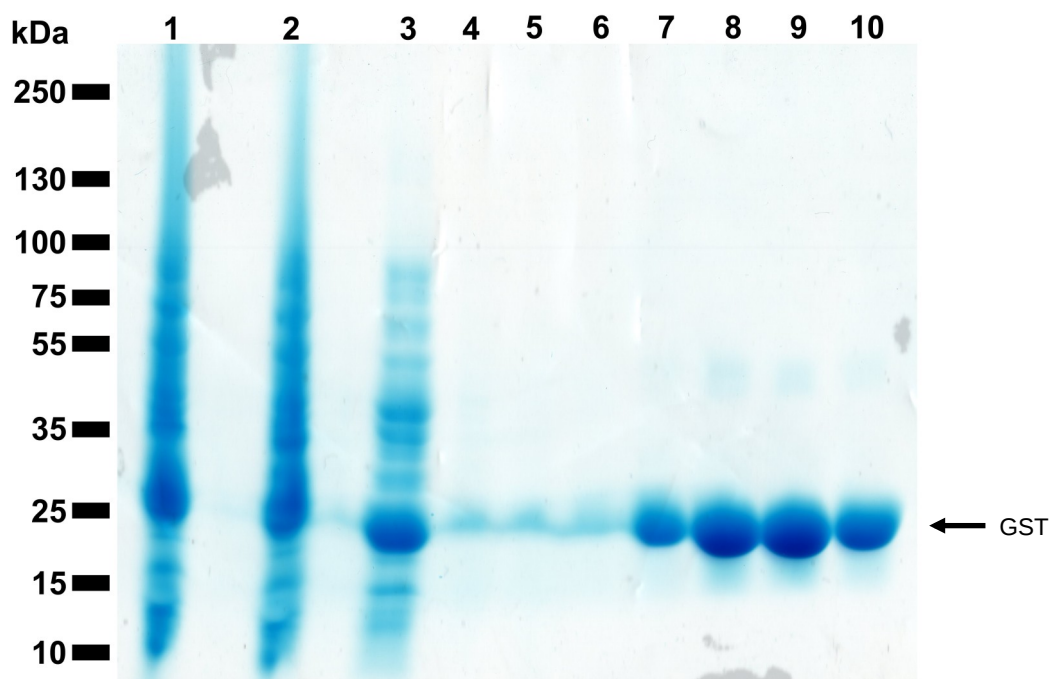
Figure 22 SDS-PAGE gel with samples of GST (26 kDa) from a Glutathione Sepharose^{TM} purification (see 2.4.8). **1**. Pellet after harvesting, **2**. Cell lysate after sonication, **3**. Flow through, **4**. Wash one (2 mL PBS), **5**. Wash two (2 mL washing buffer), **6**. Wash three (2 mL PBS), **7-10**. Eluates (500 μL elution buffer each).

Figure 22 displays that, although some GST was lost on the flow through

and washes, most of it was bound to the Glutathione Sepharose™ resin and was eluted (Figure 22, 7-10). The loss of GST on the first steps of the purification could be due to a saturation of the resin because of the high concentration of GST in the sample.

An aliquot of purified GST was denatured and refolded with refolding buffer 10 (see 2.4.12) as Rx-NBARC proteins were. After this, it was dialysed (see 2.4.13). A second aliquot was denatured and refolded with refolding buffer 10, as Rx-NBARC proteins, but this time, substituting 1 mM GSH and 0.1 mM GSSH for 1 mM DTT. This sample was dialysed too. A third sample was directly dialysed, without being denatured. These three samples were used in three Glutathione Sepharose™ purifications (see 2.4.8) performed at the same time. The presence of protein in the eluates obtained from each of the three purifications was checked with a Bradford experiment (see 2.4.6). The results were positive for the three conditions.

This experiment demonstrates that the Glutathione Sepharose™ resin was in good condition and that the experimental processes before purification were not interfering with purification. The last explanation possible was that either the GST tag was not refolded properly when attached to Rx-NBARC or Rx-NBARC was sterically inhibiting GST binding to the resin. Nevertheless, this was not explained with this experiment and no other trials were conducted. It, therefore, remains as an open question with no answer. Focus was moved towards a different approach so as to purify Rx-NBARC WT and Rx-NBARC K176R using their C-terminal hexa-histidine tag on a Ni^{+2}-NTA resin purification (see 2.4.7)

3.2.2.2 Ni^{+2}-NTA resin purification:

Purification with Glutathione Sepharose™ after refolding, dialysing and concentrating Rx-NBARC constructs did not work: the protein did not bind to the beads and was observed in the flow through. As a different approach, a Ni^{+2}-NTA resin purification (see 2.4.7) was performed with Rx-NBARC WT.

Rx-NBARC constructs have a C-terminal hexa-histidine tag that should make possible their purification using this method. Nevertheless, no better results were obtained from a Ni^{+2}-NTA resin purification than those from a Glutathione Sepharose^{TM}. Nucleotide phosphatase activity (see 2.5.2) was examined in the samples from a Ni^{+2}-NTA purification (see 2.4.7, Figure 23) with Rx-NBARC WT and a Western blot was conducted (see 2.4.5, Figure 24).
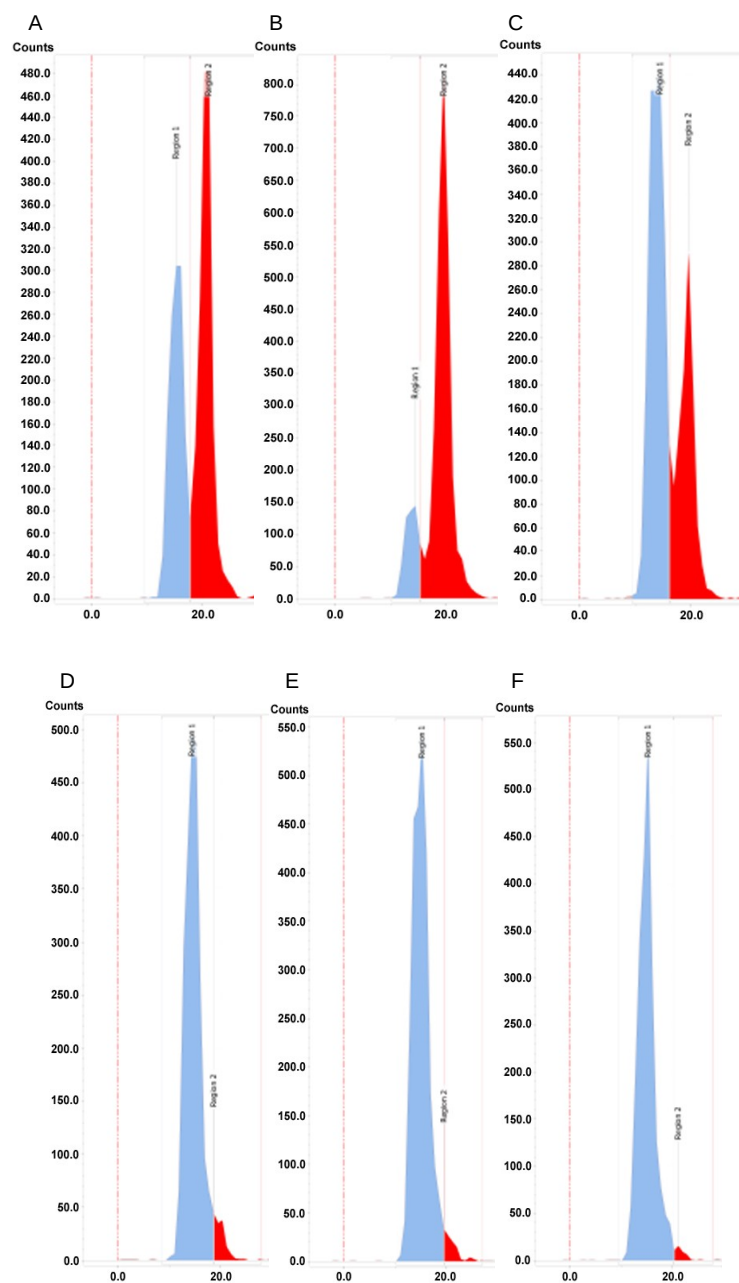
Figure 23 Nucleotide phosphatase assay (see 2.5.2) with Rx-NBARC WT samples obtained during a Ni^{+2}-NTA resin purification (see 2.4.7). Data was read with a TLC scanner. Blue areas correspond to ADP, red to adenosine. (**A**) Positive control: refolded, non-purified Rx-NBARC WT. (**B**) Flow through. (**C**) Wash one (15 mL wash buffer A). (**D**) Wash two (15 mL wash buffer B). (**E**) Wash three (15 mL wash buffer C). (**F**) Eluate (5 mL elution buffer).
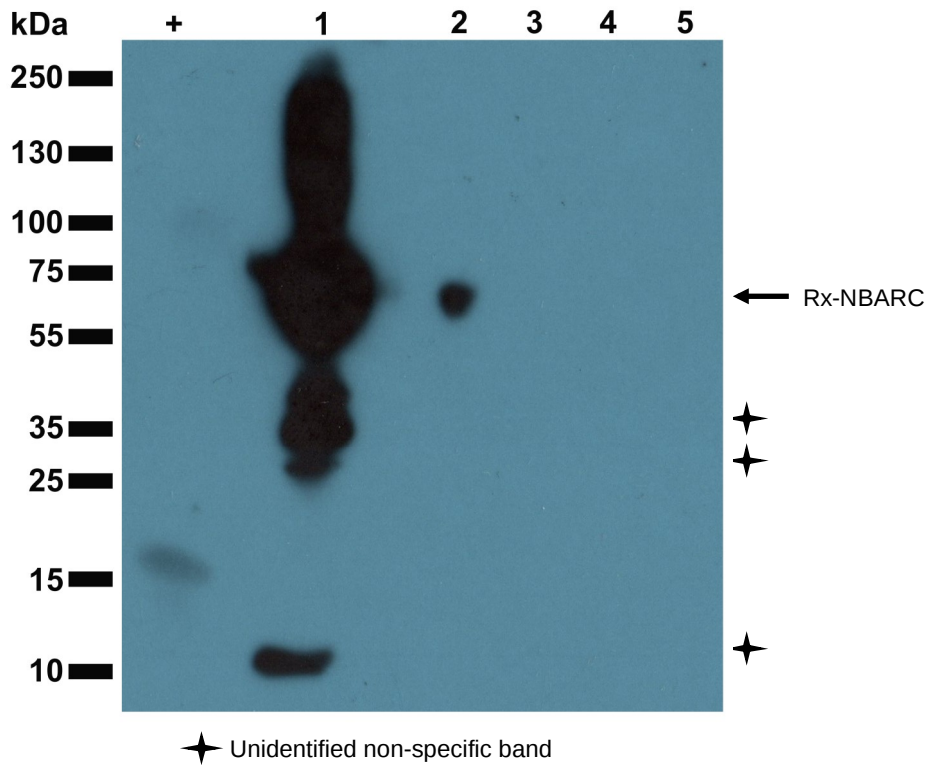
Figure 24 Anti-His Western blot (see 2.4.5) with samples from a Ni-NTA resin purification (see 2.4.7) of Rx-NBARC WT. **+** CAP, His-tagged protein from *E. coli*, **1**. Rx-NBARC WT purified, solubilized inclusion bodies, **2**. Flow through, **3**. Wash one (15 mL wash buffer A), **4**. Wash two (15 mL wash buffer B), **5**. Wash three (15 mL wash buffer C), **6**. Eluate (5 mL elution buffer).

It is evident from Figures 23 and 24 that Rx-NBARC WT was being lost on the flow through and washes. The protein would not bind the Ni^{+2}-NTA resin.

A possible explanation to why Rx-NBARC was not binding to a Glutathione Sepharose^{TM} or a Ni^{+2}-NTA resins could be that the protein was refolding in a way that obstructed the availability of the tags to bind either resin. In order to test this, a Ni^{+2}-NTA resin purification (see 2.4.7) was conducted with Rx-NBARC samples prior the refolding step. It is not necessary to refold a hexa-histidine tag in order for it to bind the resin (Rudolph and Lilie, 1996).

3.2.3 Protein purification before refolding (Ni^{+2}-NTA resin)

The hexa-histidine tag does not have to be refolded in order to perform a correct Ni^{+2}-NTA resin purification (see 2.4.7; Rudolph and Lilie, 1996). As no positive results were obtained from the previous purification trials (see 3.2.1 and 3.2.2), a Ni^{+2}-NTA resin purification was performed with Rx-NBARC WT and Rx-NBARC K176R purified and solubilized inclusion bodies (see 2.4.10), prior to refolding the proteins. The results of this purification are shown in Figure 25.
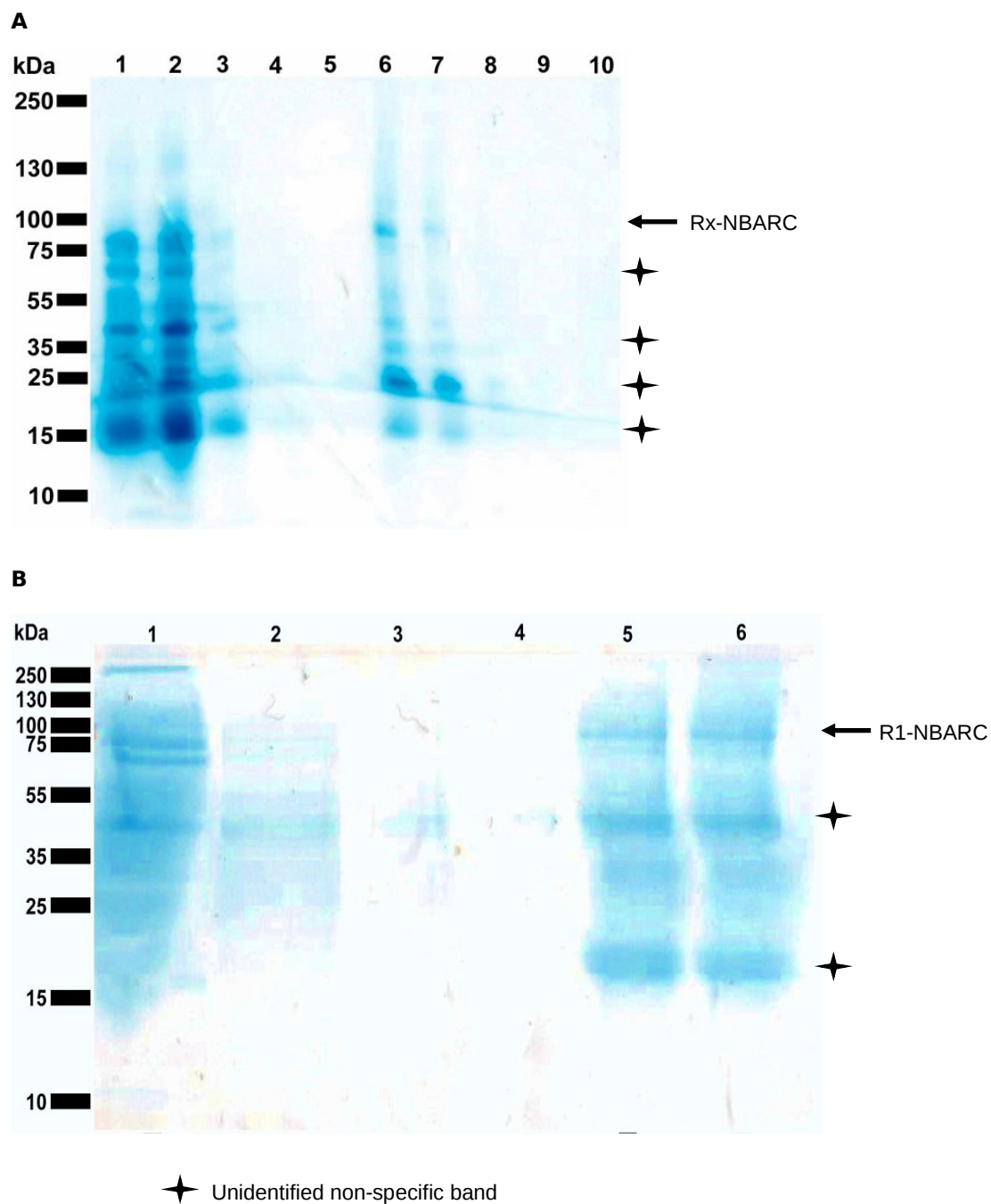
Figure 25 SDS-PAGE gels with samples of (**A**) Rx-NBARC WT and (**B**) Rx-NBARC K176R obtained during a Ni^{+2}-NTA resin purification (see 2.4.7). (**A**) **1**. Rx-NBARC WT purified and solubilized inclusion bodies, **2**. Flow through, **3**. Wash one (15 mL wash buffer A), **4**. Wash two (15 mL wash buffer B), **5**. Wash three (15 mL wash buffer C), **6-10**. Eluates (200 µL elution buffer each). (**B**) **1**. Flow through, **2**. Wash one (15 mL wash buffer A), **3**. Wash two (15 mL wash buffer B), **4.** Wash three (15 mL wash buffer C), **5-6**. Eluates (200 µL elution buffer each).

Samples of Rx-NBARC WT and Rx-NBARC K176R, before refolding, were subject to a Ni^{+2}-NTA purification (see 2.4.10). Eluates were not clean, as shown on the SDS-PAGE gels in Figure 25 (**A** 6-7 and **B** 5-6). Nevertheless, both wild type and K176R mutant were cleaner than samples obtained from inclusion bodies purification (see 2.4.10).

After the Ni^{+2}-NTA purification, eluates were refolded (see 2.4.12), dialysed (see 2.4.13) and concentrated with PEG 8000 (see 2.4.14). Protein concentration of Rx-NBARC WT and Rx-NBARC K176R was calculated by Bradford assay (see 2.4.6). Both samples were made to the same concentration and their nucleotide phosphatase activities were compared (Figure 26). Aliquots were examined by SDS-PAGE gel (see 2.4.4; Figure 27).
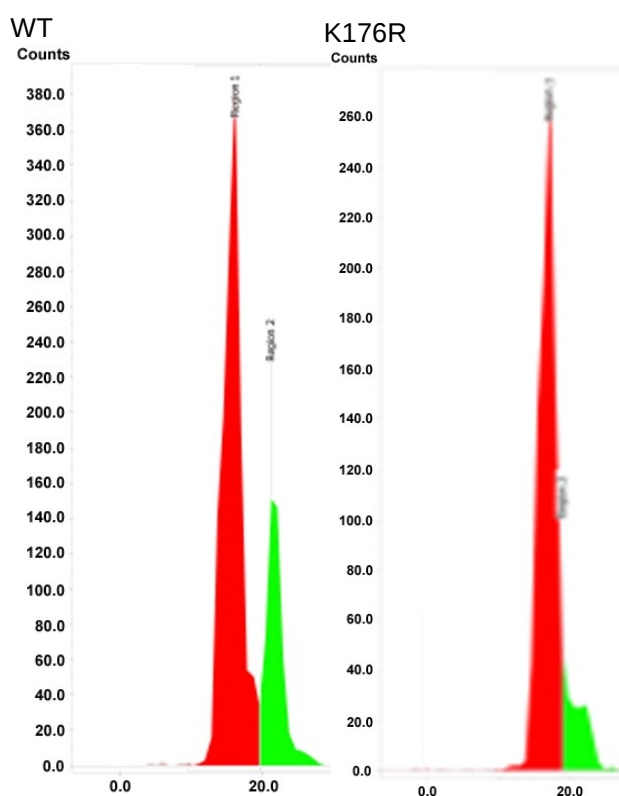
Figure 26 Nucleotide phosphatase assay performed on Rx-NBARC WT and Rx-NBARC K176R samples having been purified with Ni^{+2}-NTA resin (see 2.4.7), refolded (see 2.4.12), dialysed (see 2.4.13) and made the same concentration. Data was read with a TLC scanner. Red areas correspond to ADP, green to adenosine.
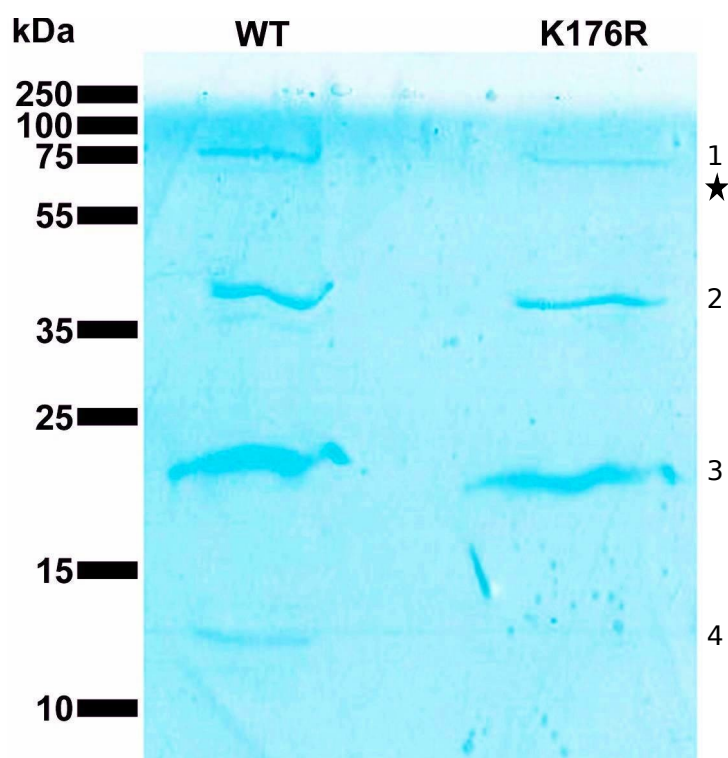
Figure 27 SDS-PAGE gel (see 2.4.4) with samples of Rx-NBARC WT and Rx-NBARC K176R that have been purified with a Ni^{+2}-NTA resin (see 2.4.7), refolded (see 2.4.12) and dialysed (see 2.4.13).

Data on Figure 26 shows that Rx-NBARC WT has a higher specific activity (see 2.5.5) for ADP as substrate in a nucleotide phosphatase assay than Rx-NBARC K176R. These are preliminary nucleotide phosphatase assays, as the samples are not clean. When aliquots of these samples are run on a SDS-PAGE gel (see 2.4.4, Figure 27), four visible bands appear and may correspond to four proteins. These four bands were cut and the SDS-PAGE gel slices corresponding to these bands were analysed by MALDI (Matrix-assisted laser desorption/ionization) mass spectrometry to identify them. The results obtained by these means were compared to the Mascot Search protein database. This confirmed a statistically significant homology of the protein present in band 1 with a GST tagged protein from a glutathione S-transferase cloning vector. As this band is of the correct size of Rx-NBARC, which has a GST tag, it is predicted to be Rx-NBARC. Band 2 corresponds to elongation factor Tu from *E. coli*, of about 44 kDa, which matches the size of

the second band on the SDS-PAGE gel. Band 3 showed homology with different keratin 10 isoforms and with β-lactamases, but as these proteins do not match the molecular weight of band 3 in Figure 27, this protein remains unidentified. Various 30S ribosomal subunit proteins showed homology with the sequence from the protein present in band 4 and they all matched with its size.

3.2.4 Exchange chromatography after a Ni^{+2}-NTA purification and refolding:

Samples of Rx-NBARC WT and Rx-NBARC K176R obtained after a Ni^{+2}-NTA resin purification, refolding, dialysing and concentrating with PEG 8000 (see 3.2.3) were subject to anion exchange chromatography to polish the Rx proteins of contamination (Figure 27). This was unsuccessful, despite multiple attempts: no Rx-NBARC WT or Rx-NBARC K176R proteins were recovered. The samples might have diluted too much during the process of anion exchange chromatography. A new experimental protocol was tested to obtain bigger amounts of clean Rx, as anion exchange proved to dilute too much the samples.

3.2.5 Electroelution:

As the Ni^{+2}-NTA purification was not giving sufficient purified material for in depth analysis, and in order to obtain cleaner Rx-NBARC WT and Rx-NBARC K176R samples, electroelution was tested as an alternative approach. When electroeluting proteins, a sample containing the protein of interest is run on a SDS-PAGE gel which is big enough to clearly separate different size proteins into distinct bands. The area corresponding to the correct size band is cut from the gel and introduced in a dialysis bag. The bag is placed in a tank with a running current. This will cause the protein to elute from the gel slice and into the buffer in the dialysis bag. Denatured protein is accumulated in the buffer inside the dialysis bag (electroeluate) and can be

used for refolding experiments. The samples of Rx-NBARC WT and Rx-NBARC K176R used for electroelution (see 2.4.15) were purified and solubilized inclusion bodies (see 2.4.10). After electroelution (see 2.4.15), electroeluates were subjected to refolding (see 2.4.12), dialysis (see 2.4.13) and concentration with PEG 8000 (see 2.4.14).

Samples of Rx-NBARC WT and Rx-NBARC K176R from purified inclusion bodies (see 2.4.10) were run on 20 cm long SDS-PAGE gels (see 2.4.4). The first gel was stained with Coomassie blue (Figure 28) in order to determine the position of the correct size band (75 kDa) on the gel. Bands corresponding to this size from subsequent gels were cut and used for electroelution (see 2.4.15). The presence of electroeluted protein was checked with an SDS-PAGE gel (see 2.4.4; Figure 29).
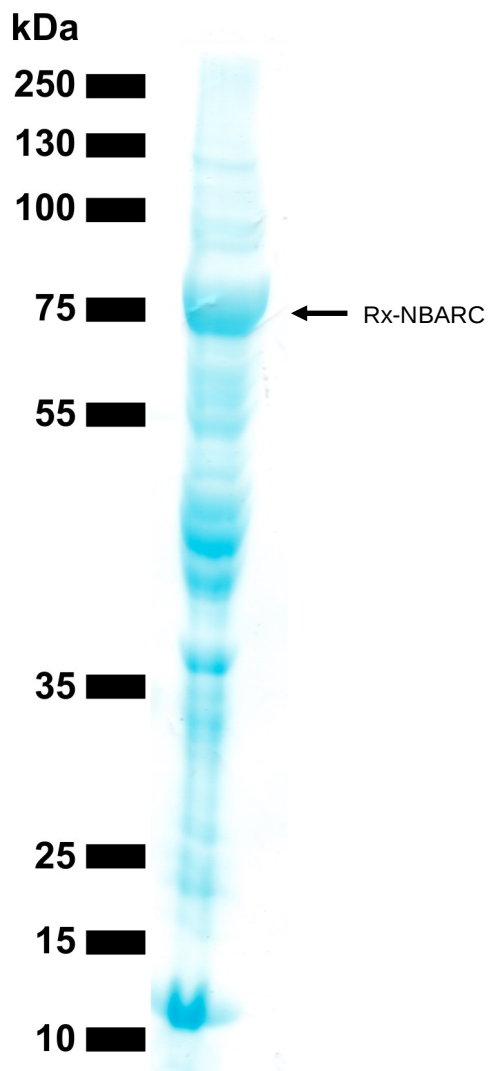
Figure 28 20 cm long SDS-PAGE gel with a sample of purified inclusion bodies from Rx-NBARC WT (75 kDa). The gel was stained with Coomassie blue in order to locate the position of the correct size (75 kDa) band in relation with the prestained protein ladder used.
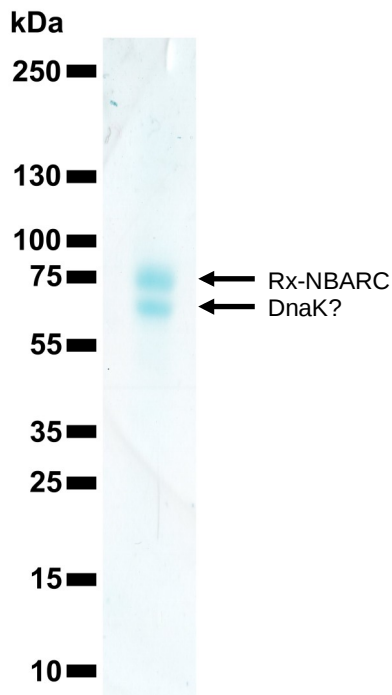
Figure 29 SDS-PAGE gel with a sample of electroeluted Rx-NBARC K176R.

Two bands appear in the SDS-PAGE run with an electroeluate sample of Rx-NBARC K176R (Figure 29). The top one is Rx-NBARC K176R. The lower band is conceivably DnaK. DnaK is an Hsp70-family member chaperone in *E. coli* of 70 kDa. It was purified with R1 and PSiP in Fenyk *et* al., 2012, but this awaits further testing.

After proving the presence of a protein of the correct size in the electroeluted sample (Figure 29), the whole electroeluate (see 2.4.15) was refolded (see 2.4.12), dialysed (see 2.4.13) and concentrated with PEG 8000 (see 2.4.14). The presence of protein at this stage was tested by Bradford (see 2.4.6) and nucleotide phosphatase assays (see 2.5.2).

After a series of electroelutions (see 2.4.15), refolding (see 2.4.12), dialysis (see 2.4.13) and concentrations (see 2.4.14), four samples of Rx-NBARC WT and two samples of Rx-NBARC K176R were obtained. Protein concentrations were established for each sample through a Bradford assay (see 2.4.6). The same amount of protein, 0.43 µg, was used to test the

nucleotide phosphatase activity of each preparation (see 2.5.2) and a comparison of their specific activities was calculated (see 2.5.5; Figure 30 for Rx-NBARC WT and Figure 31 for Rx-NBARC K176R).
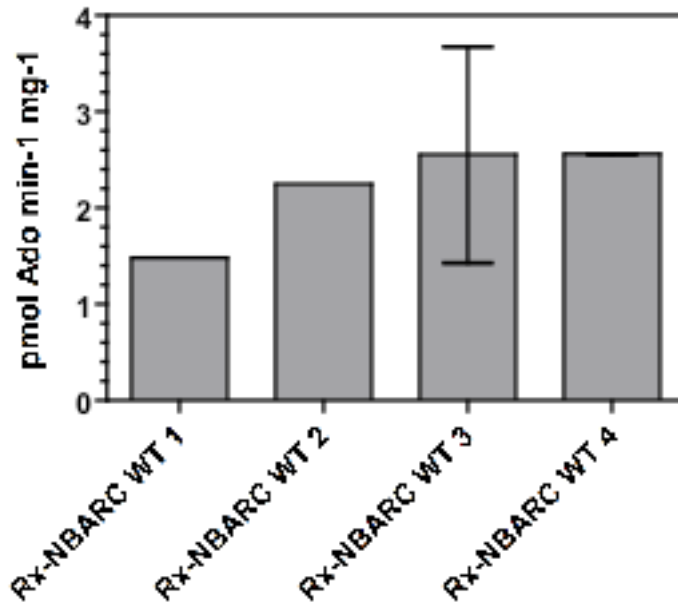
Figure 30 Nucleotide phosphatase specific activity (see 2.5.5) of four different electroeluted and refolded Rx-NBARC WT samples. Error bars correspond to the standard error of the mean (n=3).
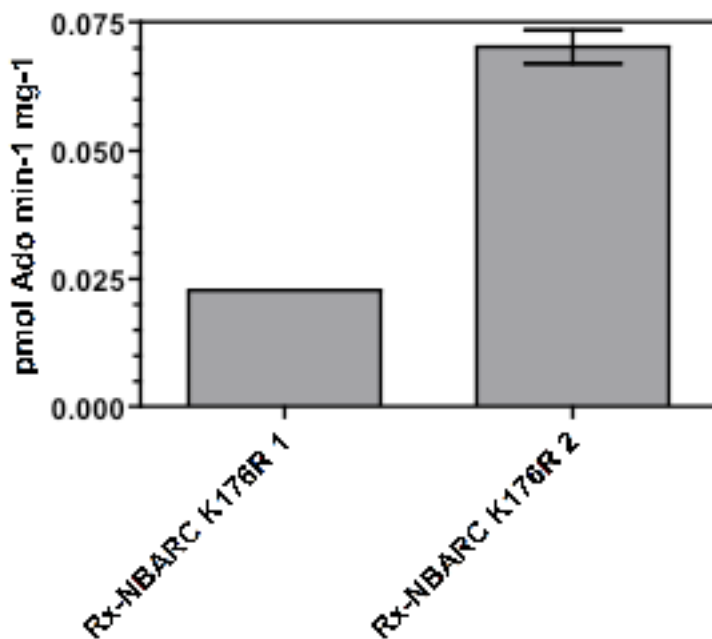
Figure 31 Nucleotide phosphatase specific activity (see 2.5.5) of two different electroeluted and refolded Rx-NBARC K176R samples. Error bars correspond to the standard error of the mean (n=3).

Differences between each sample's specific activity (see 2.5.5; Figures 30 and 31) could be due to inconsistent folding of the protein during the purification process. Also, it could be stated that the K176R mutant version of Rx-NBARC has consistently less nucleotide phosphatase specific activity than the wild type, even though it could be possible that both mutant samples are incorrectly folded. To state with total certainty that the difference in specific activity is only due to the mutation, circular dichroism (CD) experiments should be conducted. CD spectroscopy measures differences in left and right-handed polarized light. Secondary structure in proteins will create a distinct spectrum for its molecule when analysed by CD spectroscopy (Matsuo *et* al., 2005). This data can be used to compare the structure of a protein under different conditions, to study the effect of different mutations in the proteins structure, to compare different proteins or as a first step before resolving a tertiary structure (Lobley *et* al., 2002). It would be possible to identify if Rx-NBARC WT and Rx-NBARC K176R samples are correctly folded, if there are

differences between each sample or if it is the K176R mutation in Rx-NBARC that causes the decrease in specific activity in this protein.

Samples Rx-NBARC WT 4 and Rx-NBARC K176R 2 present the higher specific activity (see 2.5.5) and, were chosen for further biochemistry experiments, unless otherwise specified.

3.2.6 Biochemistry of Rx-NBARC:

Most R proteins have a variable N-terminus, consisting of a coiled-coil (CC) domain or a TIR (homologue of the *Drosophila* Toll and mammalian interleukin-1 receptors) domain. The conserved central domain is predicted to bind nucleotides (NBARC) and there is a variable leucine-rich region (LRR) at the C-terminus (Boller and He, 2009 and Zipfel, 2009). The NBARC domain has a P-loop structure (van Ooijen *et* al., 2008). P-loop NTPases are the most common NTP-binding proteins in the proteome. They are found in all organisms and they form the fifth largest family with the human genome (Gueguen-Chaigon *et* al., 2007).

The current theory in the literature postulates that R proteins are strict ATPases with an "on-off" activation model (Takken *et* al., 2006 and Tameling *et* al., 2002). In this model, the inactive or "off" state corresponds to that of the NBARC domain of the protein interacting with the LRR and C-terminus domains and an ADP molecule (Tameling *et* al., 2002). It is not known what triggers nucleotide exchange in R proteins, but exchange of ADP for an ATP causes a conformational change in the protein and its consequent activation, entering the "on" state. It is the hydrolysis of the ATP molecule that returns an R protein to its inactive, autoinhibited state. Recent results (Fenyk *et* al., 2012) show that R1, an orphan R protein from rice, is a nucleotide phosphatase with a substrate preference of AMP>ADP>ATP and so, strict ATPase is not its main activity. Unpublished data on R1, PSiP, and I-2 has shown that R proteins bind and damage DNA. Different studies (Choi *et* al., 2001 and Wang *et* al., 2010) show there is relation between R protein genes

and DNA binding and damaging. Choi *et* al., 2001 demonstrated the similarity in gene expression induced by DNA-damaging agents and by R proteins in a study performed on pea endocarp tissue. Wang *et* al., 2010 have identified DNA repairing enzymes (BRCA2 and RAD51) in screens for immune related genes. DNA damage could be used as a signal to trigger plant innate immune responses as various studies state that the localization of R proteins in either the nucleus or the cytoplasm is key for their correct immune signalizing (Burch-Smith *et* al., 2007, Cheng *et* al., 2009, Wirthmueller *et* al., 2007 and Zhu *et* al., 2010). Moreover, Rx has been located in the nucleus as well as the cytoplasm (Slootweg *et* al., 2010) and it has been demonstrated that its N-terminus is related with a member of the RanGAP2 family involved in the trafficking through nuclear pores (Tameling *et* al., 2010).

The data presented here represents the initial stage of a larger project to be continued further. Rx-NBARC has been used to test its strict ATPase, nucleotide phosphatase and DNA nicking activities. Toward this end, a series of strict ATPase, nucleotide phosphatase and DNA nicking experiments have been conducted. Rx-NBARC WT and Rx-NBARC K176R samples were used, after being electroeluted and refolded (see 3.2.5).

3.2.6.1 Confirmation of the activity of Rx-NBARC: strict ATPase or nucleotide phosphatase?

As previous results indicate a break from the main line of thought of Rx being a strict ATPase (Fenyk *et* al., 2012), purified Rx-NBARC samples were tested for both strict ATPase and nucleotide phosphatase activity.

Strict ATPase and nucleotide phosphatase assays were run in precoated TLC plates (see 2.5.3 and 2.5.4). The results were read on a TLC scanner where absorbance at 256 nm was measured for each sample. The position of ATP, ADP, AMP and adenosine (Ado) molecules on TLC plates was examined. Once this was established, further ATPase and nucleotide phosphatase activity tests could be conducted and properly analysed.

Where should ATP, ADP, AMP and Ado appear?

When performing nucleotide phosphatase and strict ATPase assays, ATP, ADP, AMP and Ado molecules are separately chromatographed. The position to which these molecules migrate when the reaction is run with nucleotide phosphatase assay developing buffer was known (Fenyk *et* al., 2012), but this was not established when using ATPase assay developing buffer. Therefore, [^{3}H]-ATP, [^{3}H]-ADP, [^{3}H]-AMP, and [^{3}H]-Ado derived from a nucleotide phosphatase assay with R1 (Fenyk *et* al., 2012) were spotted on a TLC plate. ATPase developing buffer was used to separate the molecules as described in 2.5.3 and the plate was read on a TLC scanner at 256 nm (Figure 32).

ATP   **ADP**

AMP   **Ado**

Figure 32 Position where ATP, ADP, AMP and Ado molecules stop on a precoated TLC plate when developed with strict ATPase developing buffer (see 2.5.3). ATP appeared on a window between 20 and 35 mm, ADP between 50 and 70 mm, AMP between 55 and 70 mm and Ado between 65 and 85 mm.

Figure 32 shows that, with this ATPase assay developing buffer, ADP and AMP are not separated. This is not significant for this experiment as it is

possible to separate ATP, ADP/AMP, and Ado this is sufficient to discriminate between a strict ATPase and nucleotide phosphatase activity. A second peak is visible when running [^{3}H]-ATP (Figure 32, ATP, red peak). This peak is evident on mixing ATP is mixed and reaction buffer (see 2.5.1) and could be due to the interaction of ATP with metal, which would cause a change in ATP's charge and, therefore, its migratory properties. No further tests were conducted to confirm this hypothesis, as it has no implications for assays to be performed. Both ATPase and nucleotide phosphatase activity experiments were conducted with Rx-NBARC WT and Rx-NBARC K176R samples.

Is Rx-NBARC a strict ATPase or a nucleotide phosphatase?

Once ATP, ADP/AMP and Ado peaks on TLC plates were identified, strict ATPase (see 2.5.1) and nucleotide phosphatase (see 2.5.2) assays were conducted and analysed with Rx-NBARC samples. Apyrase from potato (*Solanum tuberosum*), an ATPase with ≥ 50 % of base activity ADPase (Handa and Guidotti, 1996) was used as a positive control for ATPase activity. Both Rx-NBARC WT and apyrase were used to test their strict ATPase and nucleotide phosphatase activity. The production of Ado and ADP/AMP was compared for both enzymes (Figure 33).
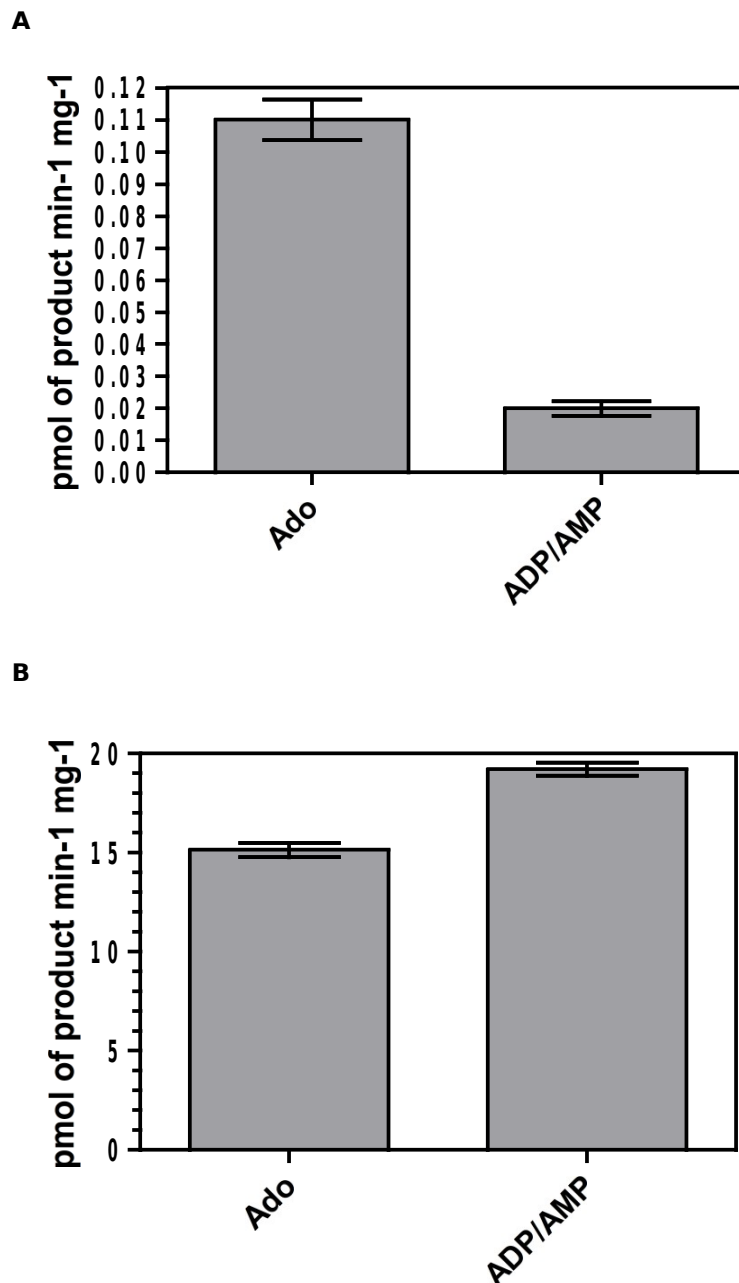
Figure 33 Specific strict ATPase and nucleotide phosphatase activity (see 2.5.5) of (**A**) Rx-NBARC WT (**B)** and apyrase. Strict ATPase assays (see 2.5.1) were conducted with both samples under the same conditions and absorbance at 256 nm was measured for both Ado and ADP/AMP. Error bars correspond to the standard error of the mean (n=3).

ADP/AMP and Ado were measured after an assay (see 2.5.1 and 2.5.3) conducted separately with Rx-NBARC WT (Figure 33, **A**) and apyrase (Figure 33, **B**). This data shows that Rx-NBARC WT cannot be considered a strict

ATPase, but a nucleotide phosphatase. The production of Ado by Rx-NBARC WT is significantly higher compared to the production of ADP/AMP. When compared to apyrase's activity, it is demonstrated that these two enzymes have different activities. In Figure 33, **B**, apyrase shows to produce Ado as well as ADP/AMP. This could be explained with a low substrate affinity for AMP and higher substrate affinity for ATP and ADP. That would be why there is Ado production, while most ADP/AMP molecules are not modified.

From Figure 33, it is clear that apyrase also produced Ado. This enzyme could have a lower affinity for AMP than for ADP and ATP and, therefore, produces Ado while there is still ADP/AMP

Having established that Rx-NBARC is a nucleotide phosphatase and not a strict ATPase, it is now necessary to check the protein's affinity for different substrates and the role of the P-loop in this activity.

3.2.6.2 Rx-NBARC as a nucleotide phosphatase:

As seen from the previous section (3.2.6.1), Rx-NBARC WT is a nucleotide phosphatase and not a strict ATPase. This is in contraposition to the current theory that plant R proteins are strict ATPases. In order to have a better knowledge about the biochemistry of Rx, substrate affinity was tested. Nucleotide phosphatases may have different affinity towards different nucleotides (Fenyk *et* al., 2012). P-loop mutants in other resistance proteins have shown to cause a loss-of-function phenotype (Takken *et* al., 2006) due to a much lower substrate affinity for the substrate in comparison with the wild type. A mutant version of Rx-NBARC that corresponded with this type of P-loop mutation (Rx-NBARC K176R) was used to compare its activity to that of the wild type (Rx-NBARC WT).

Substrate affinity:

Knowing the affinity of Rx for different nucleotides as substrates will help future work towards the understanding of how resistance proteins, as a whole, trigger an innate immune response in plants. Nucleotide phosphatase experiments (see 2.5.2) using ATP, ADP and AMP as substrates were conducted using 16 ng of Rx-NBARC WT in each reaction. Nucleotides were added to a final concentration of 5 μM and reactions were performed under the same conditions (Figure 34).
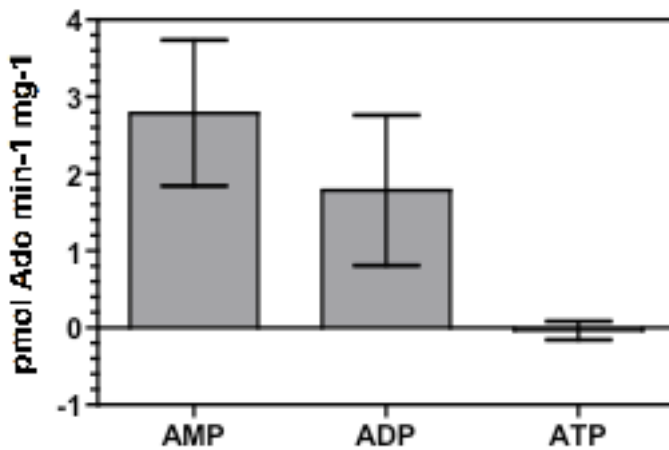
Figure 34 Nucleotide phosphatase specific activity (see 2.5.5) of Rx-NBARC WT using AMP, ADP and ATP as substrates. Error bars correspond to the standard error of the mean (n=3).

Figure 34 shows a difference in affinity of the nucleotide phosphatase activity for ATP, ADP and AMP as substrates. This affinity is as follows: ATP<ADP<AMP. These same results are similar to those reported in Fenyk *et* al., 2012 for R1.

Differences in specific activity between Rx-NBARC WT and Rx-NBARC K176R:

Rx-NBARC K176R presents a mutation in the kinase 1A or P-loop motif of the protein. Equivalent mutations in other resistance proteins have shown to cause a loss-of-function phenotype (Takken *et* al., 2006). P-loop mutants have a lower substrate affinity than that of the wild type R protein. A nucleotide phosphatase assay (see 2.5.2) was performed with both Rx-NBARC WT and Rx-NBARC K176R (Figure 35).
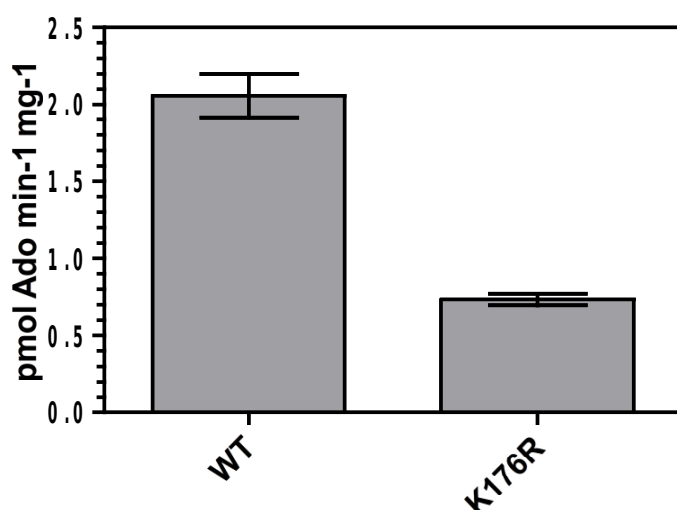
Figure 35 Comparison of nucleotide phosphatase specific activity (see 2.5.5) in Rx-NBARC WT and Rx-NBARC K176R. Error bars correspond to the standard error of the mean (n=3).

Figure 35 was analysed with data from nucleotide phosphatase assays (see 2.5.2) with Rx-NBARC WT and Rx-NBARC K176R. The same concentration of substrate (5 μM ADP) and protein (160 ng) was added to each of the experiments that were incubated for the same time at the same temperature. This figure shows that Rx-NBARC WT has a higher nucleotide phosphatase specific activity than Rx-NBARC K176R.

3.2.6.3 DNA nicking of Rx-NBARC:

Unpublished data from experiments with R1, PSiP, and I-2 has shown that R proteins bind and damage DNA. This could trigger an innate immune resistance response in plants (Choi *et* al., 2001 and Wang *et* al., 2010). Damaging DNA would be used as a way to signal pathogen infection and trigger a response. In order to establish if Rx nicks DNA, viral dsDNA was used in DNA nicking experiments (see 2.5.6) with all Rx-NBARC WT and Rx-NBARC K176R samples (Figure 36, Figure 37).
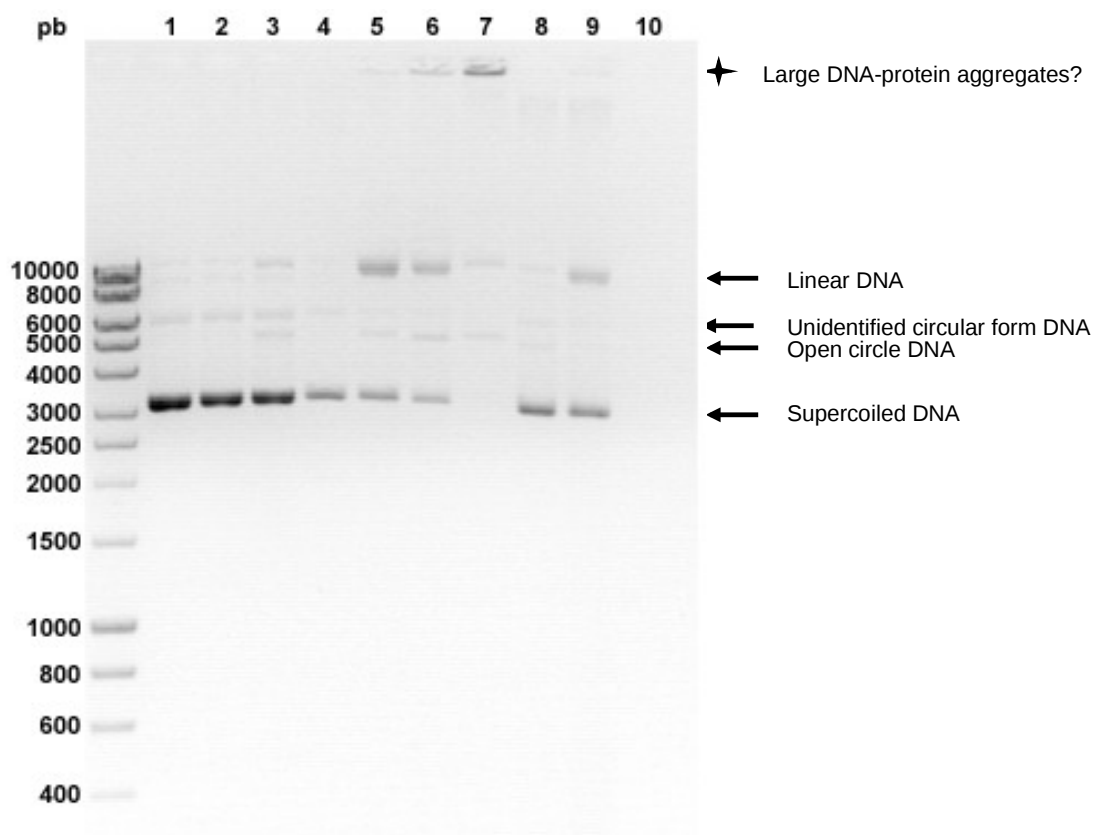
Figure 36 Agarose gel showing the results from a viral dsDNA nicking (see 2.5.6) experiment with Rx-NBARC WT and Rx-NBARC K176R samples. **1**, 0.5 µg viral dsDNA; **2**, 0.5 µg viral dsDNA with STOP buffer; **3**, 0.5 µg viral dsDNA and 1 µg BSA with STOP buffer; **4**, 0.5 µg viral dsDNA and 0.43 ng Rx-NBARC WT 1 with STOP buffer; **5**, 0.5 µg viral dsDNA and 0.43 ng Rx-NBARC WT 2 with STOP buffer; **6**, 0.5 µg viral dsDNA and 0.43 ng Rx-NBARC WT 3 with STOP buffer; **7**, 0.5 µg viral dsDNA and 0.43 ng Rx-NBARC WT 4 with STOP buffer; **8**, 0.5 µg viral dsDNA and 0.43 ng Rx-NBARC K176R 1 with STOP buffer; **9**, 0.5 µg viral dsDNA and 0.43 ng Rx-NBARC K176R 2 with STOP buffer; **10**, 0.5 µg viral dsDNA and 1 µg DNAase

I with STOP buffer.
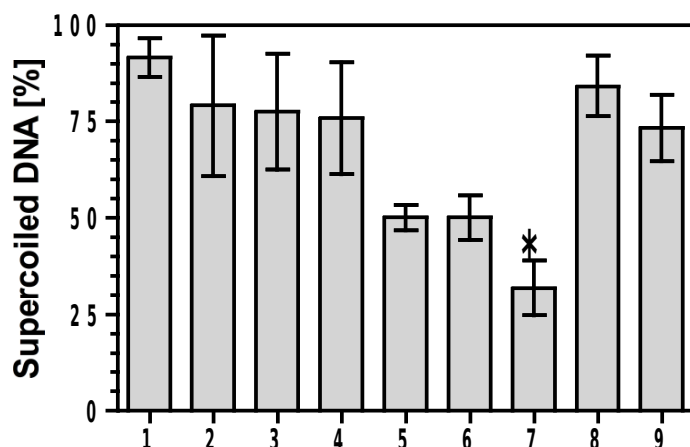
Figure 37 Percentage of supercoiled DNA compared to linear DNA on an agarose gel (Figure 35).Viral dsDNA was used on a DNA nicking assay (see 2.5.6) testing the nicking activity in four samples of Rx-NBARC WT and two samples of Rx-NBARC K176R. **1**, 0.5 μg viral dsDNA; **2**, 0.5 μg viral dsDNA with STOP buffer; **3**, 0.5 μg viral dsDNA and 1 μg BSA with STOP buffer; **4**, 0.5 μg viral dsDNA and 0.43 ng Rx-NBARC WT 1 with STOP buffer; **5**, 0.5 μg viral dsDNA and 0.43 ng Rx-NBARC WT 2 with STOP buffer; **6**, 0.5 μg viral dsDNA and 0.43 ng Rx-NBARC WT 3 with STOP buffer; **7**, 0.5 μg viral dsDNA and 0.43 ng Rx-NBARC WT 4 with STOP buffer; **8**, 0.5 μg viral dsDNA and 0.43 ng Rx-NBARC K176R 1 with STOP buffer; **9**, 0.5 μg viral dsDNA and 0.43 ng Rx-NBARC K176R 2 with STOP buffer. Error bars correspond to the standard error of the mean (n=3).

Data in Figures 36 and 37 demonstrates that Rx-NBARC nicks and, likely binds DNA. It is possible to compare the nucleotide phosphatase and DNA nicking specific activities of each sample (Figures 30 and 37 respectively). This comparison demonstrates that the most active samples in a nucleotide phosphatase assay (see 2.5.2) are the most active on a DNA nicking assay (see 2.5.6) too. It is also noteworthy that both Rx-NBARC K176R samples have low nucleotide phosphatase and DNA nicking activities (Figures 31 and 37, respectively), comparable to that of sample Rx-NBARC WT 1 (Figure 30 and 37). This can be due to the mutation itself or to missfolding problems.

DNA binding of Rx-NBARC:

Data presented in the previous section shows that Rx-NBARC nicks DNA, but does it bind to it too? No specific experiment was conducted in order to clarify if Rx-NBARC binds DNA, but it is possible to hypothesize from what Figure 37 shows. On lanes 5, 6 and 7, not all DNA has entered the gel. It is plausible to hypothesize that this is due to Rx-NBARC interacting with DNA, forming aggregates too big to enter a 1 % agarose gel. The samples on these lanes are also the most active ones, both nicking DNA and as nucleotide phosphatases with ADP as substrate (Figures 37 and 30). Having this in mind, it is conceivable to hypothesize that Rx-NBARC binds DNA. This idea would be in consonance with unpublished data on other R proteins.

Expressing soluble, active R proteins has proved to be very challenging. Transformed cells might experience toxicity due with residual expression of these proteins, as they are nucleotide phosphotases. In this project it is demonstrated that both R1-NBARC (3.1.4) and Rx-NBARC (3.2.1) are accumulated in inclusion bodies, which can be purified. Rx-NBARC samples could be polished of impurities and refolded (3.2.1) to form soluble, active protein used in a series of biochemical assays (3.2.5 and 3.2.6). Data obtained from these experiments demonstrate that Rx-NBARC is not a strict ATPase, but a nucleotide phosphatase (3.2.6.1). This difference from the current theory of R proteins being strict ATPases has been previously seen in experiments conducted on R1 (Fenyk *et* al., 2012). It can also be stated that Rx-NBARC nicks DNA (3.2.6.3). This is in supported with data published in Slootweg *et* al., 2010 and Tameling *et* al., 2010. These two projects demonstrate that Rx's immune signalling activity is related to its nucleocytoplasmic distribution and that Rx's N-terminus domain interacts with a member of RanGAP2 family involved in trafficking through the nuclear pore.

In conjunction, these results can be used in further R proteins analysis. Efforts should be focused towards the obtaining of clean samples of R proteins that could be used in crystallography experiments. Solving a R

protein (or its active domain) structure would be of high importance for the full understanding and knowledge of plant immunity.

4. Conclusion and Future work

4.1 R protein expression and purification

Expressing and purifying R proteins showed to be very challenging. R proteins hydrolyse phosphoester bonds in nucleotides (Fenyk *et* al., 2012, Tameling *et* al., 2006). Residual expression of these proteins, if active, could cause cell death. This might be the explanation as to why obtaining a soluble R protein through bacterial culture is so difficult and why the use of chaperones did not help in obtaining better results. Nevertheless, Ueda *et* al., 2006 succeeded in the expression and purification of active N protein constructs from *E. coli* cultures. In a similar way, Fenyk *et* al., 2012 expressed and purified R1, Rpm1 and PSiP active domains from bacteria cultures. Expression of R1 and PSiP constructs used in this study yielded high protein concentrations. On the other hand, the expression of Rpm1 did not produce a high amount of protein. This contrast might be due to the different specific activities of R1, PSiP, and Rpm1. R1 and PSiP showed a low nucleotide phosphatase specific activity, while Rpm1 had a higher nucleotide phosphatase specific activity. This explanation might be true for experiments conducted on Rx in this project. A possible reason for Rx not expressing as soluble protein might be its high nucleotide phosphatase specific activity.

Bacteria can accumulate toxic proteins in inclusion bodies. Various proteins have been purified from inclusion bodies and been refolded before (Rudolph and Lilie, 1996) resulting in active proteins in solution. Tameling *et* al., 2002 purified two R proteins, I-2 and Mi-1, from inclusion bodies in cultures of *E. coli*. Posterior refolding *in vitro* proved to yield active proteins. A similar protocol is the one described in this project (see 3.2). In this case, an extra purification step was added after the purification of inclusion bodies. Samples obtained are not suitable for crystallography trials, but can be used in biochemistry assays. This methodology, if improved, could be used for R proteins purification and may render a clean sample that can be used towards a NB-ARC crystal structure. Solving a NB-ARC domain structure from R proteins would be key in the progress of an understanding of plant innate immunity.

4.2 Rx-NBARC biochemistry

4.2.1 Rx NB-ARC domain activity

The currently accepted theory of R protein activation proposes R proteins as strict ATPases in an "on-off" switch activation model (Takken and Tameling, 2009). Recent findings by Fenyk *et* al., 2012 on a group of three R proteins differ from this theory. R1 (orphan R protein from rice), PSiP (orphan R protein from maize), and Rpm1 (R protein from *Arabidopsis*) act as nucleotide phosphatases, not strict ATPases. Results with Rx-NBARC proved this R protein to be a nucleotide phosphatase. Two possibilities arise. The first possible explanation is that different R proteins can have different activities. On the other hand, no Rx samples without minor contaminants were produced. Contaminants present in these samples might be responsible for the activity assigned to Rx. Nevertheless, experiments conducted on a loss-of-function P-loop mutant version of Rx (Rx-NBARC K176R) proved to have lower nucleotide phosphatase specific activity, while presenting the same contaminants. Further studies, free of contaminants, of Rx protein should be accomplished with further improvement to methodology.

4.2.2 DNA nicking activity

R proteins have been localized in the cytoplasm and the nucleus of plant cells (Slootweg *et* al., 2010). For complete activation of ETI, various R proteins need to be localized in the nucleus. Burch-Smith *et* al., 2007 demonstrated transport into the nucleus from the cytoplasm was needed for N to properly activate an immune response. Wirthmueller *et* al., 2007 demonstrated this same fact for RPS4, and Zhu *et* al., 2010 for SNC1. The importance of interaction between R proteins and nucleocytoplasmic transporters is proved in Cheng *et* al., 2009. Moreover, the gene expression induced by R proteins activation is similar to that caused by DNA-damaging agents (Choi *et* al., 2001) and Wang *et* al., 2010 identified DNA repairing enzymes that interact with R proteins. It is clear from these data that R proteins' function is related to their localization both in the cytoplasm and the nucleus. DNA damage could be used in the signalling process to trigger

plants innate immunity.

In this project, Rx-NBARC was used in DNA nicking experiments to prove the capability of the protein to damage DNA. However, once a clean sample of R protein is obtained, this activity should be confirmed, as mentioned for before in 4.2.1.

4.3 Future work

Data presented here could be used in future projects where R protein activity and structure is studied. Experiments should be conducted to confirm the correct refolding of the protein. The structure of Rx-NBARC WT and Rx-NBARC K176R in solution should be compared by circular dichroism. This would be key to state that nucleotide phosphatase and DNA nicking activity differences shown by wild type and mutant samples are due to the P-loop mutation and not to inconsistent folding of the proteins in each solution.

The final target of this future project should be solving an R protein structure. This would be key for the understanding of these proteins' function and their role in plant innate immunity. In order to achieve this, clean samples of protein should be obtained and crystallized. The problems to overcome here are not only in the crystallization and structure solving processes, but also in the expression and purification processes. R proteins are expressed and accumulated in inclusion bodies. The purification of these proteins is extremely difficult. To obtain a higher concentration of protein in a clean sample will be the next step forward. A second purification step after electroelution could be an option (anion exchange chromatography, for example).

Once an NB-ARC domain crystal from a R protein is available, important catalytic residues can be proposed as targets for protein modifications that may render R proteins with new activation regulation pathways.

5. References

1. **Aarts, M., Metz, M., Holub, E., Staskawicz, B. J., Daniels, M. J. And Parker, J. E.**, 1998. Different requirements for EDS1 and NDR1 by disease resistance genes define at least two R genes-mediated signalling pathways in *Arabidopsis*. Proceedings of the National Academy of Sciences of the United States of America **95**, 10306-10311.

2. **Ade, J., De Young, B. J., Golstein, C. And Innes, R. W.**, 2007. Indirect activation of a plant nucleotide binding site-leucine-rich repeat protein by a bacterial protease. Proceedings of the National Academy of Sciences of the United States of America **104**, 2531-2536.

3. **Alder, M. N., Rogozin, I. B., Iyer, L. M., Glazko, G. V., Cooper, M. D. And Pancer, Z.**, 2005. Diversity and function of adaptive immune receptors in a jawless vertebrate. Science **310**, 1970-1973.

4. **Allen, R. L., Bittener-Eddy, P. D., Grenville-Briggs, L. J., Metz, J. C., Rehmany, A. P., Rose, L. E. And Beynon, J. L.**, 2004. Host-parasite coevolutionary conflict between *Arabidopsis* and downy mildew. Science **306**, 1957-1960.

5. **Aravind, L., Dixit, V. M. and Koonin, E. V.**, 1999. The domains of death: evolution of the apoptosis machinery. Trends in Biochemical Science **24**, 47-53.

6. **Azevedo, C., Betsuyaku, S., Peart, J., Takahashi, A., Noel, L., Sadanandom, A., Casais, C., Parker, J. And Shirasu, K.**, 2006. Role of SGT1 in resistance protein accumulation in plant immunity. The EMBO Journal **25**, 2007-2016.

7. **Bai, J., Pennill, L. A., Ning, J., Lee, S. W., Ramalingam, J., Webb, C. A., Zhao, B., Sun, Q., Nelson, J. C., Leach, J. E and Hulbert, S.**

H., 2002. Diversity in nucleotide binding site-leucine-rich repeat genes in cereals. Genome Research **12**, 1871-1884.

8. **Baker, B., Zambryski, P., Staskawicz, B. and Dinesh-Kumar, S. P.**, 1997. Signalling in plant-microbe interactions. Science **276**, 726-733.

9. **Baneyx, F.**, 1999. Recombinant protein expression in *Escherichia coli*. Current Opinion in Biotechnology **10**, 411-421.

10. **Baures, I., Candresse, T., Leveau, A., Bendahmane, A. And Sturbois, B.**, 2008. The Rx gene confers resistance to a range of *Potexviruses* in transgenic *Nicotiana* plants. Molecular Plant-Microbe Interactions **21**, 1154-1164.

11. **Bhattacharjee, S., Halane, M. K., Kim, S. H. And Gassmann, W.**, 2011. Pathogen effectors target *Arabidopsis* EDS1 and alter its interactions with immune regulators. Science **334**, 1405-1408.

12. **Bendahmane, A., Kohm, B. A., Dedi, C. and Baulcombe, D. C.**, 1995. The coat protein of potato virus X is a strain-specific elicitor of *Rx*1-mediated virus resistance in potato. The Plant Journal **8**, 933-941.

13. **Bendahmane, A., Kanyuka, K. and Baulcombe, D. C.**, 1999. The Rx gene from potato controls separate virus resistance and cell death responses. The Plant Cell **11**, 781-791.

14. **Bendahmane, A., Querci, M., Kanyuka, K. and Baulcombe, D. C.**, 2000. *Agrobacterium* transient expression system as a tool for the isolation of disease resistance genes: application to the *Rx*2 locus in potato. The Plant Journal **21**, 73-81.

15. **Bendahmane, A., Farnham, G., Moffet, P. and Baulcombe, D. C**, 2002. Constitutive gain-of-function mutants in a nucleotide binding site-luecine rich repeat protein encoded at the *Rx* locus of potato. The Plant Journal **32**, 195-204.

16. **Bent, A. F., Kunkel, B. N., Dahlbeck, D., Brown, K. L., Schmidt, R., Giraudat, J., Leung, J. and Staskawicz, B. J.**, 1994. *RPS2* of *Arabidopsis thaliana*: a leucine-rich repeat class of plant disease resistance genes. Science **265**, 1856-1860.

17. **Bent, A. F.**, 1996. Plant disease resistance genes: function meets structure. The Plant Cell **8**, 1757-1771.

18. **Belkhadir, Y., Subramaniam, R and Dangl, J. L.**, 2004. Plant disease resistance protein signalling: NBS-LRR proteins and their partners. Current Opinion in Plant Biology **7**, 391-399.

19. **Bernoux, M., Ve, T., Williams, S., Warren, C., Hatters, D., Valkov, E., Zhang, X., Ellis, J. G., Kobe, B. And Dodds, P. N.**, 2011. Structural and functional analysis of a plant resistance protein TIR domain reveals interfaces for self-association, signalling, and autoregulation. Cell Host and Microbe **9**, 200-211.

20. **Bisgrove, S. R., Simonich, M. T., Smith, N. M., Sattler, A. and Innes, R. W.**, 1994. A disease resistance gene in Arabidopsis with specificity for two different pathogen avirulence genes. The Plant Cell **6**, 927-933.

21. **Boller, T. and He, S. Y**, 2009. Innate immunity in plants: an arms race between pattern recognition receptors in plants and effectors in microbial pathogens. Science **324**, 742-744.

22. **Burch-Smith, T. M., Schiff, M., Caplan, J. L., Tsao, J., Czymmek, K. and Dinesh-Kumar, S. P.**, 2007. A novel role for the TIR domain in association with pathogen-derived elicitors. PLos Biol **5**, e68.

23. **Catanzariti, A. M., Dodds, P. N., Ve, T., Kobe, B., Ellis, J. G. And Staskawicz, B. J.**, 2010. The AvrM effector from flax rust has a structured C-terminal domain and interacts directly with the M resistance protein. Molecular Plant-Microbe Interactions **23**, 49-57.

24. **Chan, S. L., Mukasa, T., Santelli, E., Low, L. Y. And Pascual, J.**, 2010. The crystal structure of a TIR domain from *Arabidopsis thaliana* reveals a conserved helical region unique to plants. Protein Science **19**, 155-161.

25. **Cheng, Y. T., Germain, H., Wiermer, M., Bi, D., Xu, F., Garcia, A. V., Wirthmueller, L., Despres, C., Parker, J. E., Zhang, Y. and Li, X.**, 2009. Nuclear pore complex component MOS7/Nup88 is required for innate immunity and nuclear accumulation of defence regulators in *Arabidopsis*. The Plant Cell **21**, 2503-2516.

26. **Choi, J. J., Klosterman, S. J. and Hadwiger, L. A.**, 2001. A comparison of the effects of DNA-damaging agents and biotic elicitors on the induction of plant defence genes, nuclear distortion and cell death. Plant Physiology **125**, 752-762.

27. **Collier, S. M. and Moffett, P.**, 2009. NB-LRRs work a "bait and switch" on pathogens. Trends in Plant Science **14**, 1360-1385.

28. **Dangl, J. L. and Jones, J. D. G.**, 2001. Plant pathogens and integrated defence responses to infection. Nature **411**, 826-833.

29. **de la Fuente van Betem, S., Vossen, J. H., de Vries, K. J., van Wees, S., Tameling, W. I. L., Dekker, H. L., de Koster, C. G., Haring, M. A., Takken, F. L. W. and Cornelissen, B. J. C.**, 2005. Heat shock protein 90 and its co-chaperone protein phosphatase 5 interact with distinct regions of the tomato I-2 disease resistance protein. The Plant Journal **43**, 284-298.

30. **de Marco, A.**, 2007. Protocol for preparing proteins with improved solubility by co-expressing with molecular chaperones in *Escherichia coli*. Nature Protocols **2**, 2632-2639.

31. **Dinesh-Kumar, S. P., Tham, W. H. and Baker, B. J.**, 2000. Structure-function analysis of the tobacco mosaic virus resistance gene *N*. Proceedings of the National Academy of Sciences **26**, 14789-14794.

32. **Dixon, D. P., Hawkins, T., Hussey, P. J. and Edwards, R.**, 2009. Enzyme activities and subcellular localization of members of the *Arabidopsis* glutathione transferase superfamily. Journal of Experimental Botany **60**, 1207-1218.

33. **Dodds, P. N., Lawrence, G. J., Catanzariti, A. M., Teh, T., Wang, C. I. A., Ayliffe, M. A., Kobe, B. And Ellis, J. G.**, 2006. Direct protein interaction underlies gene-for-gene specificity and coevolucion of the flax resistance genes and flax rust avirulence genes. Proceedings of the National Academy of Sciences of the United States of America **103**, 8888-8893.

34. **Dodds, P.N.**, 2010. Genome evolution plant pathogens. Science **330**, 1486-1487.

35. **Dodds, P. and Rathjen, J. P.**, 2010. Plant immunity: towards an integrated view of plant-pathogen interactions. Nature Reviews **11**, 539-548.

36. **Ellis, J. G., Lawrence, G. J., Luk, J. E. And Dodds, P. N.**, 1999. Identification of regions in alleles of the flax rust resistance gene *L* that determine differences in the gene-for-gene specificity. The Plant Cell **11**, 495-506.

37. **Fenyk, S., de San Eustaquio Campillo, A., Phol, E., Hussey, P. J. and Cann, M. J**, 2012. A nucleotide phosphatase activity in the nucleotide binding domain of an orphan resistance protein from rice. Journal of Biological Chemistry **287**, 4023-4032.

38. **Goff, S. A., Ricke, D., Lan, T. H., Presting, G., Wang, R., Dunn, M., Glazebrook, J., Sessions, A., Oeller, P., Varma, H., Hadley, D., Hutchinson, D., Martin, C., Katagiri, F., Lange, B. M., Moughamer, T., Xia, Y., Budworth, P., Zhong, J., Miguel, T., Paszkowski, U., Zhang, S., Colbert, M., Sun, W. L., Chen, L., Cooper, B., Park, S., Wood, T. C., Mao, L., Quail, P., Wing, R., Dean, R., Yu, Y., Zharkikh,**

A., Shen, R., Sahasrabudhe, S., Thomas, A., Cannings, R., Gutin, A., Pruss, D., Reid, J., Tavtigian, S., Mitchell, J., Eldredge, G., Scholl, T., Miller, R. M., Bhatnagar, S., Adey, N., Rubano, T., Tusneem, N., Robinson, R., Feldhaus, J., Macalma, T., Oliphant, A. And Briggs, S., 2002. A draft sequence of the rice genome (*Oryza sativa* L. ssp. *japonica*). Science **296**, 92-100.

39. Goulden, M. G. and Baulcombe, D. C., 1993. Functionally homologous host components recognize potato virus X in *Gomphrena globosa* and potato. The Plant Cell **5**, 921-930.

40. Gueguen-Chaigon, V., Chaptal, V., Lariviere, L., Costa, N., Lopes, P., Morera, S. and Nessler, S., 2007. Crystal structure and functional analysis identify the P-loop containing YFH7 of Saccharomyces cerevisiae as an ATP-dependent kinase. Proteins: Structure, Function and Bioinformatics **71**, 804-812.

41. Hajimorad, M. R. and Hill, J. H., 2001. *Rsv1*-mediated resistance against *Soybean mosaic virus*-N is hypersensitive response-independent at inoculation site, but has the potential to initiate a hypersensitive response-like mechanism. Molecular Plant-Microbe Interactions **14**, 587-598.

42. Handa, M. and Guidotti, G., 1996. Purification and cloning of a soluble ATP-diphosphohydrolase (apyrase) from potato tubers (*Solanum tuberosum*). Biochemical and biophysical research communications **218**, 916-923.

43. Heath, M. C., 2000. Hypersensitive response-related death. Plant Molecular Biology **44**, 321-334.

44. Heidrich, K., Wirthmueller, L., Tasset, C., Pouzet, C., Deslandes, L and Parker, J. E., 2011. Arabidopsis EDS1 connects pathogen effector recognition to cell compartment-specific immune responses. Science **334**, 1401-1404.

45. **Hwang, C. F. and Williamson, V. M.**, 2003. Leucine-rich repeat-mediated intramolecular interactions in nematode recognition and cell death signalling by the tomato resistance protein Mi. The Plant Journal **34**, 585-593.

46. **Hwang, C. F., Bhakta, A. V., Truesdell, G. M., Pudlo, W. M. and Williamson, V. M.**, 2000. Evidence for a role of the N terminus and leucine-rich repeat region of the *Mi* gene regulation on localized cell death. The Plant Cell **12**, 1319-1329.

47. **Jones, J. D. G. and Dangl, J. L.**, 2006. The plant immune system. Nature Reviews **444**, 323-329.

48. **Kim, M. G., Kim, S. Y., Kim, W. Y., Mackey, D. and Lee, S. Y.**, 2008. Responses of *Arabidopsis thaliana* to challenge by *Pseudomonas syringae*. Molecules and Cells **25**, 323-331.

49. **Kobe, B. and Deisenhofer, J.**, 1994. The leucine-rich repeat: a versatile binding motif. Trends In Biochemical Sciences **19** 415-421.

50. **Kohm, B. A., Goulden, M. G., Gilbert, J. E., Kavanagh, T. A. and Baulcombe, D. C.**, 1993. A potato virus X resistance gene mediates an induced, nonspecific resistance in protoplasts. The Plant Cell **5**, 913-920.

51. **Leipe, D. D., Koonin, E. V. and Aravind, L.**, 2004. STAND, a class of P-loop NTPases including animal and plant regulators of programmed cell death: multiple, complex domain architectures, unusual phyletic patterns, and evolution by horizontal gene transfer. Journal of Molecular Biology **343**, 1-28.

52. **Lobley, A., Whitmore, L. and Wallace, B. A.**, 2002. DICHROWEB: an interactive website for the analysis of protein secondary structure from circular dichroism spectra. Bioinformatics **18**, 211-212.

53. **Lukasik, E. And Takken, F. L. W.**, 2009. STANDing strong, resistance

proteins instigators of plant defence. Current Opinion in Plant Biology **12**, 427-436.

54. **Lukasik-Shreepaathy, E., Vossen, J. H., Tameling, W. I. L., de Vroomen, M. J., Cornelissen, B. J. C. and Takken, F. L. W.**, 2012. Protein-protein interactions as a proxy to monitor conformational changes and activation states of the tomato resistance protein I-2. Journal of Experimental Botany **63**, 3047-3060.

55. **Maekawa, T., Cheng, W., Spiridon, L. N., Toller, A., Lukasik, E., Saijo, Y., Liu, P., Shen, Q. H., Micluta, M. A., Somssich, I. E., Takken, F. L. W., Petrescu, A. J., Chai, J. And Schulze-Lefert, P.**, 2011. Coiled-coil domain-dependent homodimerization of intracellular barley immune receptors defines a minimal functional module for triggering cell death. Cell Host and Microbe **9**, 187-199.

56. **Matsuo, K., Yonehara, R. and Gekko, K.**, 2005. Improved estimation of the secondary structures of proteins by vacuum-ultraviolet circular dichroism spectroscopy. Journal of Biochemistry **138**, 79-88

57. **Meyers, B. C., Dickerman, A. W., Michelmore, R. W., Sivaramakrishnan, S., Sobral, B. W. And Young, N. D.**, 1999. Plant disease resistance genes encode members of an ancient and diverse protein family within the nucleotide-binding superfamily. The Plant Journal **20**, 317-332.

58. **Meyers, B. C., Kozik, A., Griego, A., Kuang, H. And Michelmore, R. W.**, 2003. Genome-wide analysis of NBS-LRR-encoding genes in *Arabidopsis*. The Plant Cell **15**, 809-834.

59. **Michelmore, R. W. and Meyers, B. C.**, 1998. Clusters of resistance genes in plants evolve by divergent selection and a birth-and-death process. Genome Research **8**, 1113-1130.

60. **Monaghan, J. and Li, X.**, 2008. R protein activation: another player revealed. Cell Host and Microbe **3**, 9-10.

61. **Moutinho, A., Hussey, P. J., Trewavas, A. J. And Malho, R.**, 2001. cAMP acts as a second messenger in pollen tube growth and reorientation. Proceedings of National American Sciences **98**, 10481-10486.

62. **Pan, Q., Liu, Y. S., Budai-Hadrian, O., Sela, M., Carmel-Goren, L., Zamir, D. and Fluhr, R.**, 2000. Comparative genetics of nucleotide binding site-leucine rich repeat resistance gene homologues in the genome of two dicotyledons: tomato and *Arabidopsis*. Genetics society of America **155**, 309-322.

63. **Rairdan, G. J. and Moffet, P.**, 2006. Distinct domains in the ARC region of the potato resistance protein Rx mediate LRR binding and inhibition of activation. The Plant Cell **18**, 2082-2093.

64. **Rairdan, G. J., Collier, S. M., Sacco, M. A., Baldwin, T. T., Boettrich, T. And Moffet, P.**, 2008. The coiled-coil and nucleotide binding domains of the potato Rx resistance protein function in pathogen recognition and signalling. The Plant Cell **20**, 739-751.

65. **Riedl, S. J., Li, W., Chao, Y., Schwarzenbacher, R. and Shi, Y.**, 2005. Structure of the apoptotic protease-activating factor 1 bound to ADP. Nature **434**, 926-933.

66. **Rudolph, R. and Lilie, H.**, 1996. In vitro folding of inclusion body proteins. FASEB Journal **10**, 49-56.

67. **Schmidt, S. A., Williams, S. J., Wang, C. A., Sornaraj, P., James, B., Kobe, B., Dodds, P. N., Ellis, J. G. And Anderson, P. A.**, 2007. Purification of the M flax-rust resistance protein expressed in *Pichia pastoris*. The Plant Journal **50**, 1107-1117.

68. **Seeholzer, S., Tsuchimatsu, T., Jordan, T., Bieri, S., Pajonk, S., Yang, W., Jahoor, A., Shimizu, K. K., Keller, B. And Schulze-Lefert, P.**, 2010. Diversity of the Mla powdery mildew resistance locus from cultivated barley reveals sites of positive selection. Molecular Plant-

Microbe Interactions **23**, 497-509.

69. **Sela, H., Spiridon, L. N., Petrescu, A. J., Akerman, M., Mandel-Gutreaund, Y., Nevo, E., Loutre, C., Keller, B., Sculman, A. H. And Fahima, T.**, 2012. Ancient diversity of splicing motifs and protein surfaces in the wild emmer wheat (*Triticum dicoccoides*) LR10 coiled coil (CC) and leucine-rich repeat (LRR) domains. Molecular Plant Pathology **13**, 276-287.

70. **Shen, Q. H., Saijo, Y., Mauch, S., Biskup, C., Bieri, S., Keller, B., Seki, H., Ulker, B., Somssich, I. E. and Schulze-Lefert, P.**, 2007. Nuclear activity of MLA immune receptors links isolate-specific and basal disease-resistance responses. Science **315**, 1098-1103.

71. **Shirasu, K. and Schulze-Lefert, P.**, 2000. Regulators of cell death in disease resistance. Plant Molecular Biology **44**, 371-385.

72. **Slootweg, E., Roosien, J., Spiridon, L. N., Petrescu, A. J., Tameling, W., Joosten, M., Pomp, R., van Schaik, C., Dees, R., Borst, J. W., Smant, G., Schots, A., Bakker, J. and Goverse, A.**, 2010. Nucleocytoplasmic distribution is required for activation of resistance by potato NB-LRR receptor Rx1 and is balanced by its functional domains. The Plant Cell **22**, 4195-4215.

73. **Staskawicz, B. J., Ausbel, F. M., Baker, B. J., Ellis, J. G. And Jones, J. D.**, 1995. Molecular genetics of plant disease resistance. Science **268**, 661-667.

74. **Takken, F. L. W., Albercht, M. and Tameling, W. I. L.**, 2006. Resistance proteins: molecular switches of plant defence. Current Opinion in Plant Biology **9**, 383-390.

75. **Takken, F. L. W. and Tameling, W. I. L.**, 2009. To nibble at plant resistance proteins. Science **324**, 744-746.

76. **Takken, F. L. W. and Goverse, A.**, 2012. How to build a pathogen

detector: structural basis of NB-LRR function. Current Opinion in Plant Biology **15**, 375-384.

77. **Tameling, W. I. L, Elzinga, S. D. J., Darmin, P. S., Vossen, J. H., Takken, F. L. W., Haring, M. A. and Cornelissen, B. J. C.**, 2002. The tomato R gene products I-2 and Mi-1 are functional ATP binding proteins with ATPase activity. The Plant Cell **14**, 2929-2939.

78. **Tameling, W. I. L., Vossen, J. H., Albrecht, M., Lengauer, T., Berden, J. A., Haring, M. A., Cornelissen, B. J. C and Takken, R. L. W.**, 2006. Mutations in the NB-ARC domain of I-2 that impair ATP hydrolysis cause autoactivation. American Society of Plant Biologists **140**, 1233-1245.

79. **Tameling, W. I. L., Nooijen, C., Ludwig, N., Boter, M., Slootweg, E., Goverse, A., Shirasu, K. and Joosten, M. H. A. J.**, 2010, RanGAP2 mediates nucleocytoplasmic partitioning of the NB-LRR immune receptor Rx in the *Solanaceae*, thereby dictating Rx function. The Plant Cell **22**, 4176-4194.

80. **Tao, Y., Yuan, F., Leister, R. T., Ausubel, F. M. and Katagiri, F.**, 2000. Mutational analysis of the *Arabidopsis* nucleotide binding site-leucine-rich repeat resistance gene RPS2.The Plant Cell **12**, 2541-2554.

81. **Tao, Y., Xie, Z., Chen, W., Glazebrook, J., Chang, H. S., Han, B., Zhu, T., Zou, G. and Katagiri, F.**, 2003. Quantitative nature of *Arabidopsis* responses during compatible and incompatible interactions with the bacterial pathogen *Pseudomonas syringae*. The Plant Cell **15**, 317-330.

82. **Tomoyasu, T., Mogk, A., Langen, H., Goloubinoff, P. and Bukau, B.**, 2001. Genetic dissection of the roles of chaperones and proteases in protein folding and degradation in the *Escherichia coli* cytosol. Molecular Microbiology **40**, 397-413.

83. **Traut, T. W.**, 1994. The functions and consensus motifs of nine types of peptides segments that form different types of nucleotide-binding sites. European Journal of Biochemistry **229**, 9-19.

84. **van Ooijen, G., Mayr, G., Kasiem, M. M. A., Albercht, M., Cornelissen, B. J. C. and Takken, F. L. W.**, 2008. Structure-function analysis of the NB-ARC domain of plant disease resistance proteins. Journal of Experimental Botany **59**, 1383-1397.

85. **Ve, T., Williams, S. J., Stamp, A., Valkov, E., Dodds, P. N., Anderson, P. A and Kobe, B.** 2011. Acta Crystallographica **F67**, 1603-1607.

86. **Weaver, L. M., Swiderski, M. R., Jonathan, Y. L and Jones, D. G.**, 2006. The *Arabidopsis thaliana* TIR-NB-LRR R-protein, RPP1A; protein localization and constitutive activation of defence by truncated alleles in tobacco and *Arabidopsis*. The Plant Journal **47**, 829-840.

87. **Wiermer, M., Feys, B. J. And Parker, J. E.**, 2005. Plant immunity:the EDS1 regulatory node. Current Opinion in Plant Biology **8**, 383-389.

88. **Williams, S. J., Sornaraj, P., deCourcy-Ireland, E., Menz, R. I., Kobe, B., Ellis, J. G., Dodds, P. N. And Anderson, P. A.**, 2011. An autoactive mutant of the M flax rust resistance protein has a preference for binding ATP, whereas wild-type M protein binds ADP. Molecular Plant-Microbe Interaction **24**, 897-906.

89. **Wirthmueller, L., Zhang, Y., Jones, J. D. G. and Parker, J. E.**, 2007. Nuclear accumulation of the *Arabidopsis* immune receptor RPS4 is necessary for triggering EDS1-dependent defence. Current Biology **17**, 2023-2029.

90. **Yan, N., Chai, J., Lee, E. S., Gu, L., Liu, Q., He, J., Wu, J. W., Kokel, D., Li, H., Hao, Q., Xue, D. and Shi, Y.**, 2005. Structure of the CED-4-CED-9 complex provides insights into programmed cell death in *Caenorhabditis elegans*. Nature **437**, 831-837.

91. **Zhang, J. and Zhou, J. M.**, 2010. Plant immunity triggered by microbial molecular signatures. Molecular Plant **3**, 783-793.

92. **Zhu, Z., Xu, F., Zhang, Y., Cheng, Y. T., Wiermer, M., Li, X. and Zhang, Y.**, 2010. Arabidopsis resistance protein SNC1 activates immune responses through association with a transcriptional corepressor. PNAS **107**, 13960-13965.

93. **Zipfel, C.**, 2008. Pattern-recognition receptors in plant innate immunity. Current Opinion in Immunology **20**, 10-16.

6. Appendices

6.1. Appendix 1: expression vectors

Construct	Insert	Vector
R1-NB^{L}2	R1$_{145-237}$	pCola2-DEST
R1-NBARC2	R1$_{145-521}$	pCola2-DEST
R1-NB^{L}3	R1$_{145-237}$	pCola3-DEST
R1-NBARC3	R1$_{145-521}$	pCola3-DEST
Rx-NBARC WT	Rx$_{1-486}$	pGEX-4T-1
Rx-NBARC K176R	Rx$^{K176R}_{1-486}$	pGEX-4T-1

6.2. Appendix 2: primers

Primer	Sequence of nucleotides	Gene
MJC188	GTA AAA CGA CGG CCA G	M13 forward sequencing primer
MJC522	GGC CTC GAG GGA CAG ACG TTG CTG ACC	LOC_Os02g25900
MJC535	GGC ACC ACT TTG TAC AAG AAA GCT GGG TCG GAC AGA CGT TGC TGA CC	LOC_Os02g25900
MJC540	Ggc ACA AGT TTG TAC AAA AAA GCA GGC TCG GCA GGC TCA CTG CAC AGC G	LOC_Os02g25900
MJC541	GGC ACC ACT TTG TAC AAG AAA GCT GGG TCG TCC ATT TTA TCC ACG CG	LOC_Os02g25900

6.3. Appendix 3: chaperone vectors

Chaperones	Plasmid	Reference
Lac Iq, Gro ESL	pBB528, pBB541	De Marco *et* al., 2007 and Tomoyasu *et* al., 2001
DnaK, DnaJ, Gro ESL low concentration, GrpE, ClpB	pBB550, pBB540	De Marco *et* al., 2007 and Tomoyasu *et* al., 2001
DnaK, DnaJ, GrpE, ClpB	pBB535, pBB540	De Marco *et* al., 2007 and Tomoyasu *et* al., 2001
DnaK, DnaJ, GrpE	pBB535, pBB530	De Marco *et* al., 2007 and Tomoyasu *et* al., 2001
DnaK, DnaJ, Gro ESL high concentration, GrpE, ClpB	pBB542, pBB540	De Marco *et* al., 2007 and Tomoyasu *et* al., 2001
DnaK, DnaJ. GroESL high concentration	pBB542	De Marco *et* al., 2007
DnaK, Dna J, Gro ESL low concentration	pBB550	De Marco *et* al., 2007
Ibp AB	pBB572	De Marco *et* al., 2007

6.4. Appendix 4: chaperone strains

Name	Construct	Chaperones
R1-NB^L2 I	R1-NB^L2	Lac Iq, Gro ESL
R1-NB^L2 II	R1-NB^L2	DnaK, DnaJ, Gro ESL low concentration, GrpE, ClpB
R1-NB^L2 III	R1-NB^L2	DnaK, DnaJ, GrpE, ClpB
R1-NB^L2 IV	R1-NB^L2	DnaK, DnaJ, GrpE

R1-NB^{L}2 V	R1-NB^{L}2	DnaK, DnaJ, Gro ESL high concentration, GrpE, ClpB
R1-NB^{L}2 VI	R1-NB^{L}2	DnaK, DnaJ. GroESL high oncentration
R1-NB^{L}2 VII	R1-NB^{L}2	DnaK, Dna J, Gro ESL low concentration
R1-NB^{L}2 VIII	R1-NB^{L}2	Ibp AB
R1-NB^{L}3 I	R1-NB^{L}3	Lac Iq, Gro ESL
R1-NB^{L}3 II	R1-NB^{L}3	DnaK, DnaJ, Gro ESL low concentration, GrpE, ClpB
R1-NB^{L}3 III	R1-NB^{L}3	DnaK, DnaJ, GrpE, ClpB
R1-NB^{L}3 IV	R1-NB^{L}3	DnaK, DnaJ, GrpE
R1-NB^{L}3 V	R1-NB^{L}3	DnaK, DnaJ, Gro ESL high concentration, GrpE, ClpB
R1-NB^{L}3 VI	R1-NB^{L}3	DnaK, DnaJ. GroESL high oncentration
R1-NB^{L}3 VII	R1-NB^{L}3	DnaK, Dna J, Gro ESL low concentration
R1-NB^{L}3 VIII	R1-NB^{L}3	Ibp AB
R1-NBARC2 I	R1-NBARC2	Lac Iq, Gro ESL
R1-NBARC2 II	R1-NBARC2	DnaK, DnaJ, Gro ESL low concentration, GrpE, ClpB
R1-NBARC2 III	R1-NBARC2	DnaK, DnaJ, GrpE, ClpB
R1-NBARC2 IV	R1-NBARC2	DnaK, DnaJ, GrpE
R1-NBARC2 V	R1-NBARC2	DnaK, DnaJ, Gro ESL high concentration, GrpE, ClpB
R1-NBARC2 VI	R1-NBARC2	DnaK, DnaJ. GroESL high oncentration
R1-NBARC2 VII	R1-NBARC2	DnaK, Dna J, Gro ESL low concentration
R1-NBARC2 VIII	R1-NBARC2	Ibp AB
R1-NBARC3 I	R1-NBARC3	Lac Iq, Gro ESL
R1-NBARC3 II	R1-NBARC3	DnaK, DnaJ, Gro ESL low concentration, GrpE, ClpB

R1-NBARC3 III	R1-NBARC3	DnaK, DnaJ, GrpE, ClpB
R1-NBARC3 IV	R1-NBARC3	DnaK, DnaJ, GrpE
R1-NBARC3 V	R1-NBARC3	DnaK, DnaJ, Gro ESL high concentration, GrpE, ClpB
R1-NBARC3 VI	R1-NBARC3	DnaK, DnaJ. GroESL high oncentration
R1-NBARC3 VII	R1-NBARC3	DnaK, Dna J, Gro ESL low concentration
R1-NBARC3 VIII	R1-NBARC3	Ibp AB

6.5. Appendix 5: refolding buffers

	50 mM MES, pH 6.0	50 mM Tris-HCl, pH 8.5	9.6 mM NaCl	240 mM NaCl	0.4 mM KCl	10 mM KCl	2mM $MgCl_2$	2 mM $CaCl_2$	0.75 M Guanidine-HCl	0.5 M arginine	0.4 M sucrose	1 mM EDTA	0.05% PEG 3500	0.5% Triton X-100	1mM DTT	1 mM GSH	0.1 mM GSSH
Buffer 1	X		X		X		X	X	X					X	X		
Buffer 2	X		X		X		X	X		X			X			X	X
Buffer 3	X		X		X				X		X	X	X	X	X		
Buffer 4	X			X		X	X	X		X				X		X	X
Buffer 5	X				X	X			X		X	X			X		
Buffer 6	X			X		X				X	X	X	X	X		X	X
Buffer 7	X			X		X	X	X	X				X		X		
Buffer 8		X	X		X		X	X			X		X	X		X	X
Buffer 9		X	X		X				X	X			X		X		
Buffer 10		X	X		X		X	X	X	X	X					X	X
Buffer 11		X	X		X								X	X	X		
Buffer 12		X		X	X							X	X			X	X
Buffer 13		X		X	X				X	X		X		X	X		
Buffer 14		X		X		X	X	X	X	X	X		X	X		X	X
Buffer 15		X		X		X	X				X				X		